TEXAS INSTRUMENTS

ADS8920B
ADS8922B
ADS8924B

SBAS729B – JUNE 2016 – REVISED AUGUST 2017

# ADS892xB 16-Bit, High-Speed SAR ADCs With Integrated Reference Buffer, and Enhanced Performance Features

## 1 Features

- Resolution: 16-Bits
- High Sample Rate With No Latency Output:
  - ADS8920B: 1-MSPS
  - ADS8922B: 500-kSPS
  - ADS8924B: 250-kSPS
- Integrated LDO Enables Single-Supply Operation
- Low Power Reference Buffer with No Droop
- Excellent AC and DC Performance:
  - SNR: 96.8-dB, THD: –125-dB
  - INL: ±0.25-LSB
  - DNL: ±0.2-LSB, 16-Bit No-Missing-Codes
- Wide Input Range:
  - Unipolar Differential Input Range: $\pm V_{REF}$
  - $V_{REF}$ Input Range: 2.5-V to 5-V
- Single-Supply, Low-Power Operation
- Enhanced-SPI Digital Interface
  - Interface SCLK: 18-MHz at 1-MSPS
  - Configurable Data Parity Output
- Extended Temperature Range: –40°C to +125°C
- Small Footprint: 4-mm × 4-mm VQFN

## 2 Applications

- Test and Measurement
- Medical Imaging
- High-Precision, High-Speed Data Acquisition

## 3 Description

The ADS8920B, ADS8922B, and ADS8924B (ADS892xB) belong to a family of pin-to-pin compatible, high-speed, single-channel, high-precision, 16-bit successive approximation register (SAR) based analog-to-digital convertors (ADCs) with an integrated reference buffer and integrated low-dropout regulator (LDO). The device family includes the ADS890xB (20-bit) and ADS891xB (18-bit) resolution variants.

The ADS89xxB boost analog performance while maintaining high-resolution data transfer by using TI's Enhanced-SPI feature. Enhanced-SPI enables the ADS89xxB to achieve high throughput at lower clock speeds, thereby simplifying the board layout and lowering system cost. Enhanced-SPI also simplifies clocking-in of data, thereby making this device ideal for applications involving FPGAs, DSPs. The ADS89xxB is compatible with a standard SPI Interface.

The ADS89xxB has an internal data parity feature that can be appended to the ADC data output. ADC data validation by the host, using parity bits, improves system reliability.

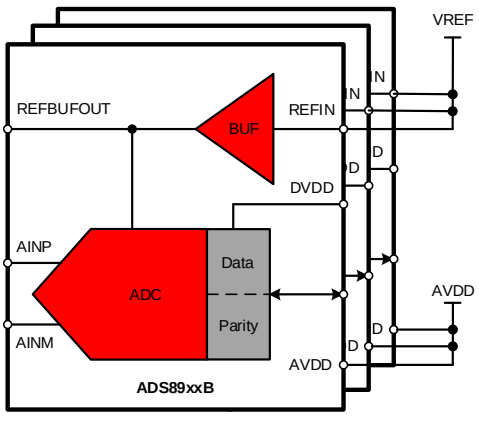
**SPI Interface Clock at 1 MSPS**

| DEVICE RESOLUTION | 3-WIRE SPI | 3-WIRE ENHANCED SPI |
|---|---|---|
| 20 bits | 70 MHz | 22 MHz |
| 18 bits | 58 MHz | 20 MHz |
| 16 bits | 52 MHz | 18 MHz |

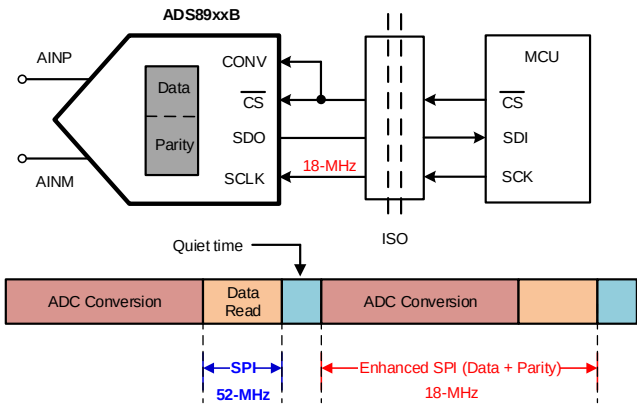
(1) For all features of the enhanced SPI, see the *Interface Module* section.

**Ease of System Design With ADS89xxB Integrated Features**

Multi-ADC System with Single Supply and Reference




Lowest Clock Speeds at 1-MSPS using 3-Wire Enhanced-SPI




An IMPORTANT NOTICE at the end of this data sheet addresses availability, warranty, changes, use in safety-critical applications, intellectual property matters and other important disclaimers. PRODUCTION DATA.

## Table of Contents

1 Features ... 1
2 Applications ... 1
3 Description ... 1
4 Revision History ... 2
5 Pin Configuration and Functions ... 3
6 Specifications ... 5
6.1 Absolute Maximum Ratings ... 5
6.2 ESD Ratings ... 5
6.3 Recommended Operating Conditions ... 5
6.4 Thermal Information ... 5
6.5 Electrical Characteristics ... 6
6.6 Timing Requirements ... 8
6.7 Switching Characteristics ... 9
6.8 Typical Characteristics ... 13
7 Detailed Description ... 18
7.1 Overview ... 18
7.2 Functional Block Diagram ... 18
7.3 Feature Description ... 19
7.4 Device Functional Modes ... 25
7.5 Programming ... 27
7.6 Register Maps ... 51
8 Application and Implementation ... 57
8.1 Application Information ... 57
8.2 Typical Application ... 59
9 Power-Supply Recommendations ... 64
10 Layout ... 65
10.1 Layout Guidelines ... 65
10.2 Layout Example ... 66
11 Device and Documentation Support ... 67
11.1 Documentation Support ... 67
11.2 Related Links ... 67
11.3 Receiving Notification of Documentation Updates 67
11.4 Community Resources ... 67
11.5 Trademarks ... 68
11.6 Electrostatic Discharge Caution ... 68
11.7 Glossary ... 68
12 Mechanical, Packaging, and Orderable Information ... 68

## 4 Revision History

NOTE: Page numbers for previous revisions may differ from page numbers in the current version.

**Changes from Revision A (July 2016) to Revision B** — **Page**

- Changed *Device Information* table into *SPI Interface Clock at 1 MSPS* table ... 1
- Changed front-page diagram ... 1
- Changed REFBUFOUT pin description from "Reference buffer output, ADC reference input" to "Internal reference buffer output, external reference input" ... 3
- Changed $DV_{DD}$ range in condition line of Electrical Characteristics from 2.35 V to 3.6 V to 1.65 V to 5.5 V ... 6
- Changed maximum value for $DV_{DD}$ range in *Electrical Characteristics*, *Timing Requirements*, and *Switching Characteristics* from 3.6 V to 5.5 V ... 6
- Added $T_A$ = 25°C to reference buffer offset voltage test condition in *Electrical Characteristics* table ... 6
- Changed input offset thermal drift typ value from 10 to 1 ... 6
- Added $f_{IN}$ = 2 kHz test condition to SFDR in *Electrical Characteristics* table ... 7
- Added descriptive text and one figure to the *Reference Buffer Module* section ... 19
- Deleted text from first note element regarding data transfer activity in zone 2 ... 34
- Added new option bullet for multiSPI digital interface module in *Data Transfer Protocols* section ... 34
- Deleted "For the ADS892xB, limit the value of $R_{FLT}$ to a maximum of 2.5-Ω in order to avoid any significant degradation in linearity performance. " from the last paragraph of the *Charge Kickback Filter* section ... 58
- Changed *Data Acquisition (DAQ) Circuit for Lowest Distortion and Noise Performance...* section for clarity ... 59
- Added more design parameters to *Design Parameters* table ... 59
- Added two new application curves ... 60
- Added new typical application subsection ... 61

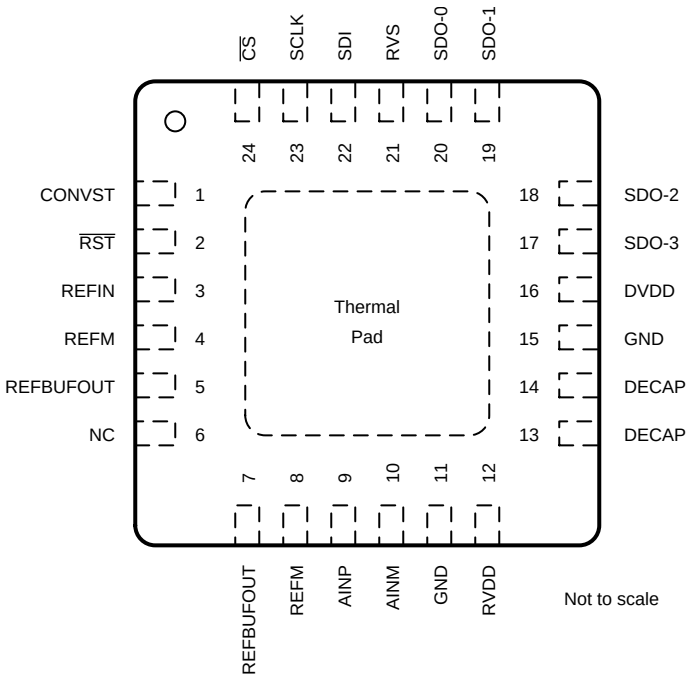
**Changes from Original (June 2016) to Revision A** — **Page**

- Changed from product preview to production data ... 1
- Changed $DV_{DD}$ specified throughput value in the *Recommended Operating Conditions* from 3.6 V to 5.5 V ... 5


Copyright © 2016–2017, Texas Instruments Incorporated

# 5 Pin Configuration and Functions

**RGE Package**
**24-Pin VQFN**
**Top View**




**Pin Functions**

| PIN | | FUNCTION | DESCRIPTION |
|---|---|---|---|
| NAME | NO. | | |
| AINM | 10 | Analog input | Negative analog input |
| AINP | 9 | Analog input | Positive analog input |
| $\overline{CS}$ | 24 | Digital input | Chip-select input pin; active low<br>The device takes control of the data bus when $\overline{CS}$ is low.<br>The SDO-x pins go to Hi-Z when $\overline{CS}$ is high. |
| CONVST | 1 | Digital input | Conversion start input pin.<br>A CONVST rising edge brings the device from ACQ state to CNV state. |
| DECAP | 13, 14 | Power supply | Place decoupling capacitor here for internal power supply. Short pin 13 and 14 together. |
| DVDD | 16 | Power supply | Interface power supply pin |
| GND | 11, 15 | Power supply | Ground |
| NC | 6 | No connection | Float these pins; no external connection. |
| REFBUFOUT | 5, 7 | Analog input/output | Internal reference buffer output, external reference input. Short pin 5 and 7 together. |
| REFIN | 3 | Analog input | Reference voltage input |
| REFM | 4, 8 | Analog input | Reference ground potential |
| $\overline{RST}$ | 2 | Digital input | Asynchronous reset input pin.<br>A low pulse on the $\overline{RST}$ pin resets the device. All register bits return to the default state. |
| RVDD | 12 | Power supply | Analog power supply pin. |
| RVS | 21 | Digital output | Multifunction output pin.<br>With $\overline{CS}$ held high, RVS reflects the status of the internal ADCST signal.<br>With $\overline{CS}$ low, the status of RVS depends on the output protocol selection. |
| SCLK | 23 | Digital input | Clock input pin for the serial interface.<br>All system-synchronous data transfer protocols are timed with respect to the SCLK signal. |
| SDI | 22 | Digital input | Serial data input pin.<br>This pin is used to feed data or commands into the device. |

Copyright © 2016–2017, Texas Instruments Incorporated

## Pin Functions (continued)

| PIN | | FUNCTION | DESCRIPTION |
|---|---|---|---|
| NAME | NO. | | |
| SDO-0 | 20 | Digital output | Serial communication pin: data output 0 |
| SDO-1 | 19 | Digital output | Serial communication pin: data output 1 |
| SDO-2 | 18 | Digital output | Serial communication pin: data output 2 |
| SDO-3 | 17 | Digital output | Serial communication pin: data output 3 |
| Thermal pad | | Supply | Exposed thermal pad; connect to GND. |


Copyright © 2016–2017, Texas Instruments Incorporated

# 6 Specifications

## 6.1 Absolute Maximum Ratings

over operating free-air temperature range (unless otherwise noted)(1)

| | MIN | MAX | UNIT |
|---|---|---|---|
| RVDD to GND | –0.3 | 7 | V |
| DVDD to GND | –0.3 | 7 | V |
| REFIN to REFM | –0.3 | $RV_{DD}$ + 0.3 | V |
| REFM to GND | –0.1 | 0.1 | V |
| Analog Input (AINP, AINM) to GND | –0.3 | $V_{REF}$ + 0.3 | V |
| Digital input ($\overline{RST}$, CONVST, $\overline{CS}$, SCLK, SDI) to GND | –0.3 | $DV_{DD}$ + 0.3 | V |
| Digital output (READY, SDO-0, SDO-1, SDO-2, SDO-3) to GND | –0.3 | $DV_{DD}$ + 0.3 | V |
| Analog Input (AINP, AINM) to RVDD and GND | –130 | 130 | mA |
| Operating free-air temperature, $T_A$ | –40 | 125 | °C |
| Storage temperature, $T_{stg}$ | –65 | 150 | °C |

(1) Stresses beyond those listed under *Absolute Maximum Ratings* may cause permanent damage to the device. These are stress ratings only, which do not imply functional operation of the device at these or any other conditions beyond those indicated under *Recommended Operating Conditions*. Exposure to absolute-maximum-rated conditions for extended periods may affect device reliability.

## 6.2 ESD Ratings

| | | | VALUE | UNIT |
|---|---|---|---|---|
| $V_{(ESD)}$ | Electrostatic discharge | Human-body model (HBM), per ANSI/ESDA/JEDEC JS-001(1) | ±2000 | V |
| | | Charged-device model (CDM), per JEDEC specification JESD22-C101(2) | ±500 | |

(1) JEDEC document JEP155 states that 500-V HBM allows safe manufacturing with a standard ESD control process.
(2) JEDEC document JEP157 states that 250-V CDM allows safe manufacturing with a standard ESD control process.

## 6.3 Recommended Operating Conditions

over operating free-air temperature range (unless otherwise noted)

| | | | MIN | NOM | MAX | UNIT |
|---|---|---|---|---|---|---|
| $RV_{DD}$ | Analog supply voltage (RVDD to AGND) | | 3 | 5 | 5.5 | V |
| $DV_{DD}$ | Digital supply voltage (DVDD to AGND) | Operating | 1.65 | 3 | 5.5 | V |
| | | Specified throughput | 2.35 | 3 | 5.5 | |
| $V_{REF}$ | Reference input voltage on REFIN | | 2.5 | | $RV_{DD}$ – 0.3 | V |
| $C_{REFBUF}$ | External ceramic decoupling capacitor | | 10 | | | µF |
| $R_{ESR}$ | External series resistor | | 0 | | 1.3 | Ω |
| $T_A$ | Specified free-air operating temperature | | –40 | 25 | 125 | °C |

## 6.4 Thermal Information

| THERMAL METRIC(1) | | ADS892xB RGE (VQFN) 24 PINS | UNITS |
|---|---|---|---|
| $R_{\theta JA}$ | Junction-to-ambient thermal resistance | 31.9 | °C/W |
| $R_{\theta JC(top)}$ | Junction-to-case (top) thermal resistance | 29.9 | °C/W |
| $R_{\theta JB}$ | Junction-to-board thermal resistance | 8.9 | °C/W |
| $\psi_{JT}$ | Junction-to-top characterization parameter | 0.3 | °C/W |
| $\psi_{JB}$ | Junction-to-board characterization parameter | 8.9 | °C/W |
| $R_{\theta JC(bot)}$ | Junction-to-case (bottom) thermal resistance | 2.0 | °C/W |

(1) For more information about traditional and new thermal metrics, see the *Semiconductor and IC Package Thermal Metrics* application report.

Copyright © 2016–2017, Texas Instruments Incorporated

## 6.5 Electrical Characteristics

At $RV_{DD}$ = 5.5 V, $DV_{DD}$ = 1.65 V to 5.5 V, $V_{REF}$ = 5 V, and maximum throughput (unless otherwise noted).
Minimum and maximum values at $T_A$ = –40°C to +125°C; typical values at $T_A$ = 25°C.

| PARAMETER | | TEST CONDITIONS | MIN | TYP | MAX | UNIT |
|---|---|---|---|---|---|---|
| **ANALOG INPUT** | | | | | | |
| FSR | Full-scale input range (AINP – AINM) | | $-V_{REF}$ | | $V_{REF}$ | V |
| $V_{IN}$ | Absolute input voltage (AINP and AINM to REFM) | | 0 | | $V_{REF}$ | V |
| $V_{CM}$ | Common-mode voltage (AINP + AINM) / 2 | | ($V_{REF}$ / 2) – 0.1 | $V_{REF}$ / 2 | ($V_{REF}$ / 2) + 0.1 | V |
| $C_{IN}$ | Input capacitance | Sample mode | | 60 | | pF |
| | | Hold mode | | 4 | | pF |
| **VOLTAGE REFERENCE INPUT (REFIN)** | | | | | | |
| $I_{REF}$ | Reference input current | $V_{REF}$ = 5 V | | 0.1 | 1 | µA |
| $C_{REF}$ | Internal capacitance | | | 10 | | pF |
| **REFERENCE BUFFER OUTPUT (REFBUFOUT)** | | | | | | |
| $V_{(RO)}$ | Reference buffer offset voltage ($V_{REFBUFOUT} – V_{REF}$) | With EN_MARG = 0b(1), $T_A$ = 25°C(2) | –250 | | 250 | µV |
| $C_{REFBUF}$ | External ceramic decoupling capacitor | | 10 | | | µF |
| $R_{ESR}$ | External series resistor | | 0 | | 1.3 | Ω |
| $I_{SHRT}$ | Short-circuit current | | | 30 | | mA |
| | Margining range | With EN_MARG = 1b(1) | | ±4.5 | | mV |
| | Margining resolution | With EN_MARG = 1b(1) | | 280 | | µV |
| **DC ACCURACY(3) ($C_{REFBUF}$ = 10 µF, $R_{ESR}$ = 0 Ω)** | | | | | | |
| | Resolution | | | 16 | | Bits |
| NMC | No missing codes | | 16 | | | Bits |
| INL | Integral nonlinearity(4) | | -0.5 | ±0.3 | 0.5 | LSB(5) |
| DNL | Differential nonlinearity(4) | | -0.5 | ±0.2 | 0.5 | LSB(5) |
| $E_{(IO)}$ | Input offset error(4) | $T_A$ = 25°C(2) | -3 | ±0.5 | 3 | LSB(5) |
| | | $T_A$ = –40°C to +125°C(2) | -5 | ±3 | 5 | |
| $dV_{OS}/dT$ | Input offset thermal drift(2) | | | 1 | | µV/°C |
| $G_E$ | Gain error(4) | EN_MARG = 0b(1)(6) | -0.03 | ±0.005 | 0.03 | %FSR |
| $dG_E/dT$ | Gain error thermal drift | EN_MARG = 0b(1)(6) | | 3.6 | | ppm/°C |
| TNS | Transition noise | | | 0.5 | | LSB(5) |
| | First output code deviation for burst-mode data acquisition | See *Reference Buffer Module* | –3 | | 3 | TNS |
| CMRR | Common-mode rejection ratio | dc to 20 kHz | | 80 | | dB |
| **SAMPLING DYNAMICS** | | | | | | |
| | Aperture delay | | | 4 | | ns |
| $t_{j\text{-rms}}$ | Aperture jitter | | | 2 | | ps RMS |
| $f_{3\text{-DB(small)}}$ | Small-signal bandwidth | | | 23 | | MHz |

(1) See the REF_MRG Register.
(2) For selected $V_{REF}$, see the OFST_CAL Register.
(3) While operating with internal reference buffer and LDO.
(4) See Figure 8, Figure 9, Figure 14, and Figure 15 for statistical distribution data for DNL, INL, offset, and gain error parameters.
(5) LSB = least-significant bit. 1 LSB at 16-bit resolution is approximately 15 ppm.
(6) Includes internal reference buffer errors and drifts.


Copyright © 2016–2017, Texas Instruments Incorporated

## Electrical Characteristics (continued)

At $RV_{DD}$ = 5.5 V, $DV_{DD}$ = 1.65 V to 5.5 V, $V_{REF}$ = 5 V, and maximum throughput (unless otherwise noted). Minimum and maximum values at $T_A$ = –40°C to +125°C; typical values at $T_A$ = 25°C.

| PARAMETER | | TEST CONDITIONS | MIN | TYP | MAX | UNIT |
|---|---|---|---|---|---|---|
| **AC ACCURACY(3)(7) ($C_{REFBUF}$ = 10 µF, $R_{ESR}$ = 0 Ω)** | | | | | | |
| SINAD | Signal-to-noise + distortion | $f_{IN}$ = 2 kHz | 95.7 | 95.9 | | dB |
| SNR | Signal-to-noise ratio | $f_{IN}$ = 2 kHz | 96 | 96.8 | | dB |
| | | $f_{IN}$ = 100 kHz | | 95 | | |
| THD | Total harmonic distortion | $f_{IN}$ = 2 kHz | | –125 | | dB |
| | | $f_{IN}$ = 100 kHz | | –110 | | |
| SFDR | Spurious-free dynamic range | $f_{IN}$ = 2 kHz | | 125 | | dB |
| **LDO OUTPUT (DECAP)** | | | | | | |
| $V_{LDO}$ | LDO output voltage (DECAP pins) | | | 2.85 | | V |
| $C_{LDO}$ | External ceramic capacitor on DECAP pins | | 1 | | | µF |
| $t_{PU_LDO}$ | LDO power-up time | $C_{LDO}$ = 1 µF, $RV_{DD} > V_{LDO}$ | | 1 | | ms |
| $I_{SHRT-LDO}$ | Short-circuit current | | | 100 | | mA |
| **DIGITAL INPUTS** | | | | | | |
| $V_{IH}$ | High-level input voltage | 1.65 V < $DV_{DD}$ < 2.3 V | 0.8 $DV_{DD}$ | | $DV_{DD}$ + 0.3 | V |
| | | 2.3 V < $DV_{DD}$ < 5.5 V | 0.7 $DV_{DD}$ | | $DV_{DD}$ + 0.3 | |
| $V_{IL}$ | Low-level input voltage | 1.65 V < $DV_{DD}$ < 2.3 V | –0.3 | | 0.2 $DV_{DD}$ | V |
| | | 2.3 V < $DV_{DD}$ < 5.5 V | –0.3 | | 0.3 $DV_{DD}$ | |
| | Input current | | | ±0.01 | 0.1 | µA |
| **DIGITAL OUTPUTS** | | | | | | |
| $V_{OH}$ | High-level output voltage | $I_{OH}$ = 500-µA source | 0.8 $DV_{DD}$ | | $DV_{DD}$ | V |
| $V_{OL}$ | Low-level output voltage | $I_{OH}$ = 500-µA sink | 0 | | 0.2 $DV_{DD}$ | V |
| **POWER SUPPLY** | | | | | | |
| $I_{RVDD}$ | Analog supply current | ADS8920B at $RV_{DD}$ = 5 V, 1-MSPS | | 4.2 | 5.3 | mA |
| | | ADS8922B at $RV_{DD}$ = 5 V, 500-KSPS | | 3.2 | 4 | mA |
| | | ADS8924B at $RV_{DD}$ = 5 V, 250-KSPS | | 2.8 | 3.5 | mA |
| | | Static, no conversion | | 970 | | µA |
| | | Static, PD_ADC = 1b(8) | | 900 | | µA |
| | | Static, PD_REFBUF = 1b(8) | | 120 | | µA |
| | | Static, PD_ADC = 1b and PD_REFBUF = 1b(8) | | 40 | | µA |
| $I_{DVDD}$ | Digital supply current | $DV_{DD}$ = 3 V, $C_{LOAD}$ = 10 pF, no conversion | | 1 | | µA |
| $P_{RVDD}$ | Power dissipation | ADS8920B at $RV_{DD}$ = 5 V, 1-MSPS | | 21 | 26.5 | mW |
| | | ADS8922B at $RV_{DD}$ = 5 V, 500-KSPS | | 16 | 20 | |
| | | ADS8924B at $RV_{DD}$ = 5 V, 250-KSPS | | 14 | 17.5 | |

(7) For $V_{IN}$ = –0.1 dBFS.
(8) See the PD_CNTL Register.

Copyright © 2016–2017, Texas Instruments Incorporated

## 6.6 Timing Requirements

| | | | MIN | TYP | MAX | UNIT | TIMING DIAGRAM |
|---|---|---|---|---|---|---|---|
| **CONVERSION CYCLE** | | | | | | | |
| $f_{cycle}$ | Sampling frequency | ADS8920B | | | 1000 | kHz | Figure 1 |
| | | ADS8922B | | | 500 | | |
| | | ADS8924B | | | 250 | | |
| $t_{cycle}$ | ADC cycle-time period | ADS8920B | 1 | | | µs | |
| | | ADS8922B | 2 | | | | |
| | | ADS8924B | 4 | | | | |
| $t_{wh_CONVST}$ | Pulse duration: CONVST high | | 30 | | | ns | |
| $t_{wl_CONVST}$ | Pulse duration: CONVST low | | 30 | | | ns | |
| $t_{acq}$ | Acquisition time | | 300 | | | ns | |
| $t_{qt_acq}$ | Quiet acquisition time | | 30 | | | ns | Figure 46, see Data Transfer Protocols |
| $t_{d_cnvcap}$ | Quiet aperture time | | 20 | | | ns | |
| **ASYNCHRONOUS RESET, AND LOW POWER MODES** | | | | | | | |
| $t_{wl_RST}$ | Pulse duration: $\overline{RST}$ low | | 100 | | | ns | Figure 2 |
| **SPI-COMPATIBLE SERIAL INTERFACE** | | | | | | | |
| $f_{CLK}$ | Serial clock frequency | 2.35 V ≤ $DV_{DD}$ ≤ 5.5 V, $T_A$ = –40°C to +125°C, $V_{IH}$ > 0.7 $DV_{DD}$, $V_{IL}$ < 0.3 $DV_{DD}$ | | | 70 | MHz | Figure 3 |
| | | 1.65 V ≤ $DV_{DD}$ < 2.35 V, $T_A$ = –40°C to +125°C, $V_{IH}$ > 0.8 $DV_{DD}$, $V_{IL}$ < 0.2 $DV_{DD}$ | | | 20 | | |
| | | 1.65 V ≤ $DV_{DD}$ < 2.35 V, $T_A$ = 0°C to +60°C, $V_{IH}$ > 0.8 $DV_{DD}$, $V_{IL}$ < 0.2 $DV_{DD}$ | | | 57 | | |
| | | 1.65 V ≤ $DV_{DD}$ < 2.35 V, $T_A$ = –40°C to +125°C, $V_{IH}$ > 0.9 $DV_{DD}$, $V_{IL}$ < 0.1 $DV_{DD}$ | | | 68 | | |
| $t_{CLK}$ | Serial clock time period | | $1/f_{CLK}$ | | | ns | Figure 3 |
| $t_{ph_CK}$ | SCLK high time | | 0.45 | | 0.55 | $t_{CLK}$ | Figure 3 |
| $t_{pl_CK}$ | SCLK low time | | 0.45 | | 0.55 | $t_{CLK}$ | |
| $t_{su_CSCK}$ | Setup time: $\overline{CS}$ falling to the first SCLK capture edge | | 12 | | | ns | |
| $t_{su_CKDI}$ | Setup time: SDI data valid to the SCLK capture edge | | 1.5 | | | ns | |
| $t_{ht_CKDI}$ | Hold time: SCLK capture edge to (previous) data valid on SDI | | 1 | | | ns | |
| $t_{ht_CKCS}$ | Delay time: last SCLK falling to $\overline{CS}$ rising | | 7 | | | ns | |
| **SOURCE-SYNCHRONOUS SERIAL INTERFACE (External Clock)(1)** | | | | | | | |
| $f_{CLK}$ | Serial clock frequency | SDR (DATA_RATE = 0b), 2.35 V ≤ $DV_{DD}$ ≤ 5.5 V | | | 70 | MHz | Figure 4, see Data Transfer Protocols |
| | | DDR (DATA_RATE = 1b), 2.35 V ≤ $DV_{DD}$ ≤ 5.5 V | | | 35 | | |
| $t_{CLK}$ | Serial clock time period | | $1/f_{CLK}$ | | | ns | |

(1) The external clock option is not recommended when operating with $DV_{DD}$ < 2.35 V. See Table 9.


Copyright © 2016–2017, Texas Instruments Incorporated

## 6.7 Switching Characteristics

At $RV_{DD}$ = 5.5 V, $DV_{DD}$ = 1.65 V to 5.5 V, $V_{REF}$ = 5 V, and maximum throughput (unless otherwise noted). Minimum and maximum values at $T_A$ = –40°C to +125°C; typical values at $T_A$ = 25°C.

| PARAMETER | | | MIN | TYP | MAX | UNIT | TIMING DIAGRAM |
|---|---|---|---|---|---|---|---|
| **CONVERSION CYCLE** | | | | | | | |
| $t_{conv}$ | Conversion time | ADS8920B | 580 | | 640 | ns | Figure 1 |
| | | ADS8922B | 1100 | | 1200 | | |
| | | ADS8924B | 2400 | | 2500 | | |
| **ASYNCHRONOUS RESET, AND LOW POWER MODES** | | | | | | | |
| $t_{d_rst}$ | Delay time: $\overline{RST}$ rising to RVS rising | | | | 3 | ms | Figure 2 |
| $t_{PU_ADC}$ | Power-up time for converter module | | 1 | | | ms | See PD_CNTL Register |
| $t_{PU_REFBUF}$ | Power-up time for internal reference buffer, $C_{REFBUF}$ = 10 µF | | 10 | | | ms | |
| $t_{PU_Device}$ | Power-up time for device | $C_{LDO}$ = 1 µF, $C_{REFBUF}$ = 10 µF | 10 | | | ms | |
| **SPI-COMPATIBLE SERIAL INTERFACE** | | | | | | | |
| $t_{den_CSDO}$ | Delay time: $\overline{CS}$ falling to data enable | | | | 9 | ns | Figure 3 |
| $t_{dz_CSDO}$ | Delay time: $\overline{CS}$ rising to SDO going to Hi-Z | | | | 10 | ns | |
| $t_{d_CKDO}$ | Delay time: SCLK launch edge to (next) data valid on SDO | | | | 13 | ns | |
| $t_{d_CSRDY_f}$ | Delay time: $\overline{CS}$ falling to RVS falling | | | | 12 | ns | Figure 4 |
| $t_{d_CSRDY_r}$ | Delay time: $\overline{CS}$ rising to RVS rising | After NOP operation | | | 30 | ns | Figure 4 |
| | | After WR or RD operation | | | 120 | | |
| **SOURCE-SYNCHRONOUS SERIAL INTERFACE (External Clock)**(1) | | | | | | | |
| $t_{d_CKSTR_r}$ | Delay time: SCLK launch edge to RVS rising | | | | 13 | ns | Figure 4 |
| $t_{d_CKSTR_f}$ | Delay time: SCLK launch edge to RVS falling | | | | 13 | ns | |
| $t_{off_STRDO_f}$ | Time offset: RVS falling to (next) data valid on SDO | | -2 | | 2 | ns | |
| $t_{off_STRDO_r}$ | Time offset: RVS rising to (next) data valid on SDO | | -2 | | 2 | ns | |
| $t_{ph_STR}$ | Strobe output high time, 2.35 V ≤ $DV_{DD}$ ≤ 5.5 V | | 0.45 | | 0.55 | $t_{STR}$ | |
| $t_{pl_STR}$ | Strobe output low time, 2.35 V ≤ $DV_{DD}$ ≤ 5.5 V | | 0.45 | | 0.55 | $t_{STR}$ | |
| **SOURCE-SYNCHRONOUS SERIAL INTERFACE (Internal Clock)** | | | | | | | |
| $t_{d_CSSTR}$ | Delay time: $\overline{CS}$ falling to RVS rising | | 15 | | 50 | ns | Figure 5 |
| $t_{STR}$ | Strobe output time period | INTCLK option | | 15 | | ns | |
| | | INTCLK / 2 option | | 30 | | | |
| | | INTCLK / 4 option | | 60 | | | |
| $t_{ph_STR}$ | Strobe output high time | | 0.45 | | 0.55 | $t_{STR}$ | |
| $t_{pl_STR}$ | Strobe output low time | | 0.45 | | 0.55 | $t_{STR}$ | |

(1) The external clock option is not recommended when operating with $DV_{DD}$ < 2.35 V. See Table 9.

Copyright © 2016–2017, Texas Instruments Incorporated

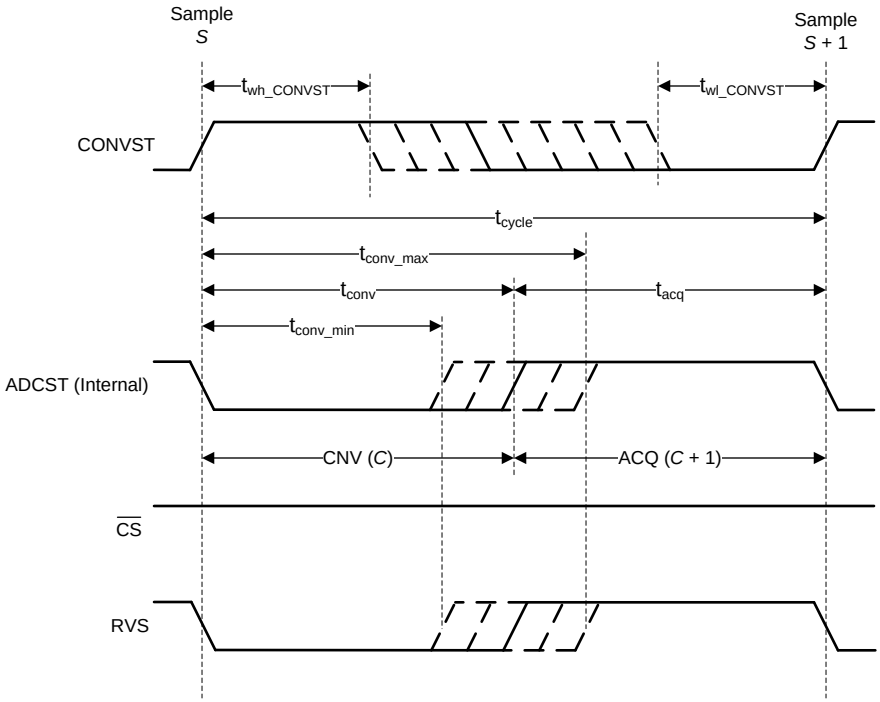



**Figure 1. Conversion Cycle Timing**

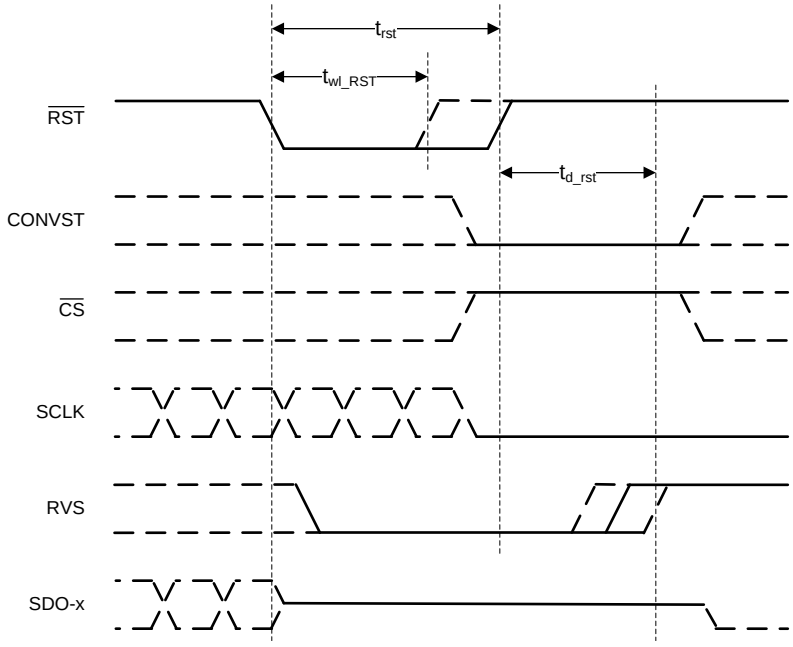
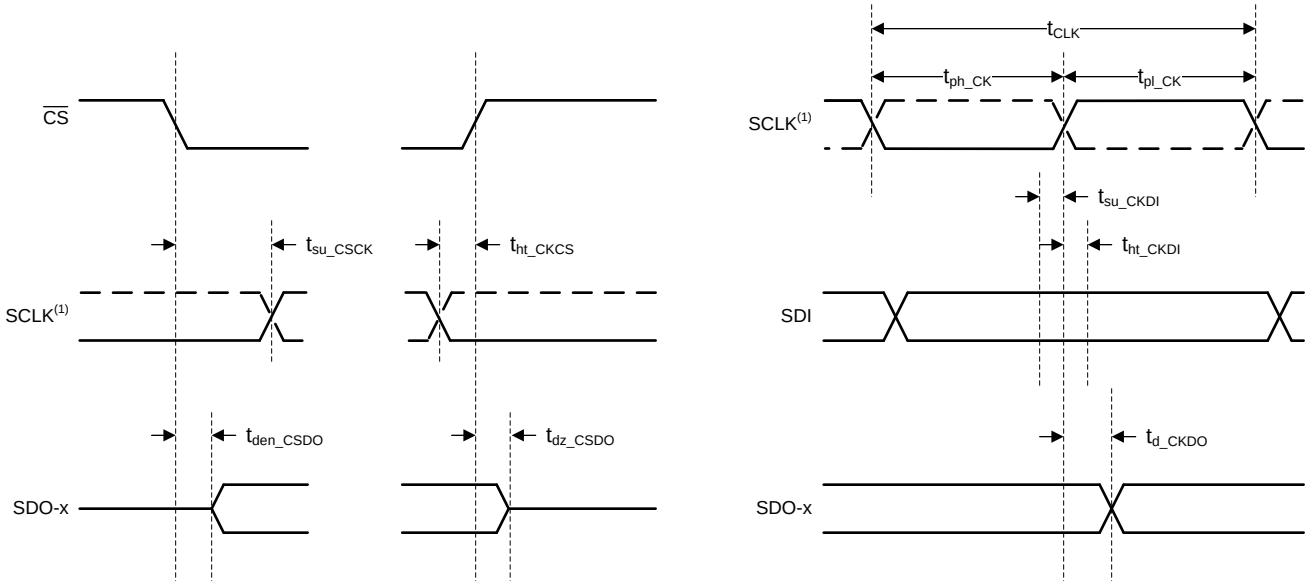



**Figure 2. Asynchronous Reset Timing**


Copyright © 2016–2017, Texas Instruments Incorporated




(1) The SCLK polarity, launch edge, and capture edge depend on the SPI protocol selected.

**Figure 3. SPI-Compatible Serial Interface Timing**

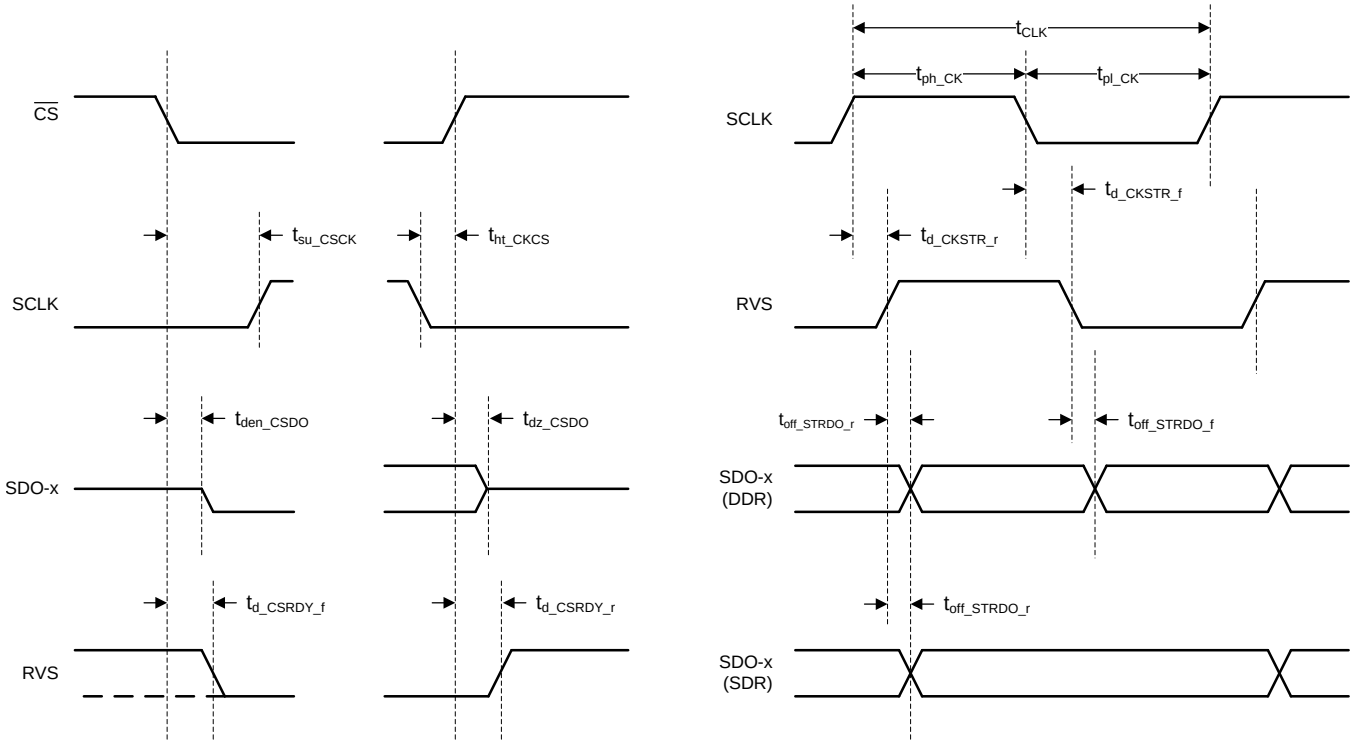



**Figure 4. Source-Synchronous Serial Interface Timing (External Clock)**

Copyright © 2016–2017, Texas Instruments Incorporated

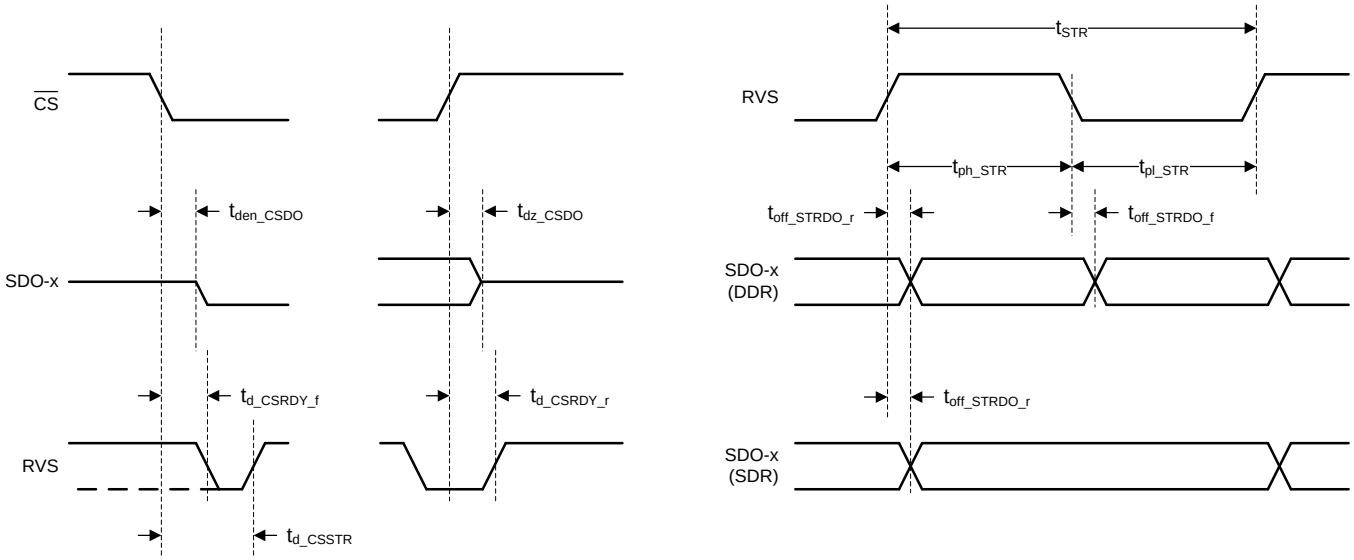
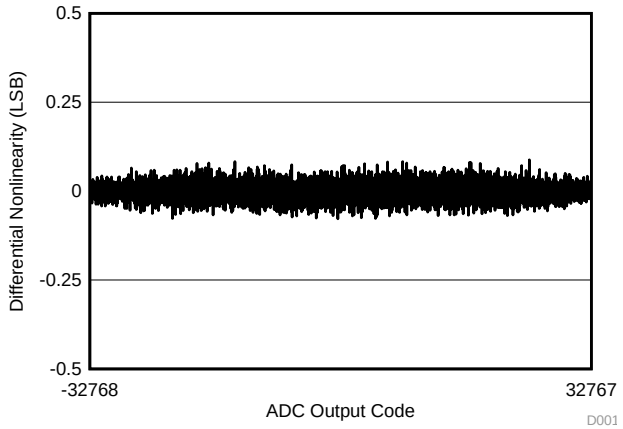



**Figure 5. Source-Synchronous Serial Interface Timing (Internal Clock)**


Copyright © 2016–2017, Texas Instruments Incorporated

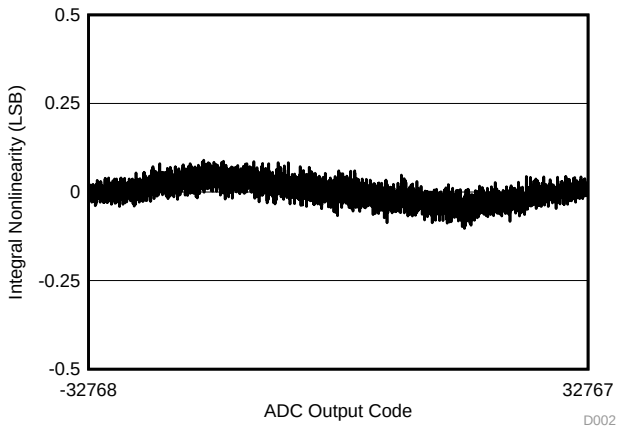
## 6.8 Typical Characteristics

at $T_A$ = 25°C, $RV_{DD}$ = 5.5 V, $DV_{DD}$ = 3 V, $V_{REF}$ = 5 V, and maximum-rated throughput (unless otherwise noted)



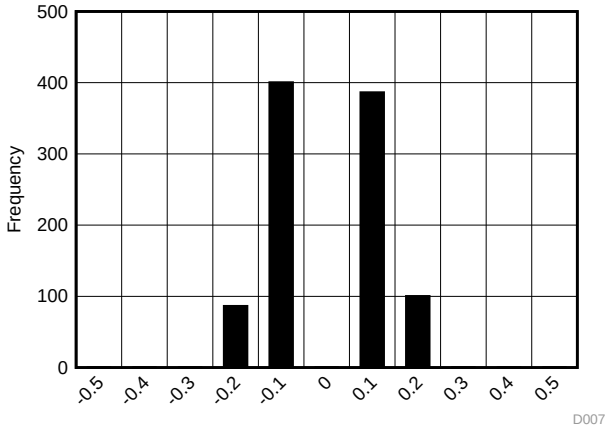

Typical DNL = ±0.2 LSB

**Figure 6. Typical DNL**



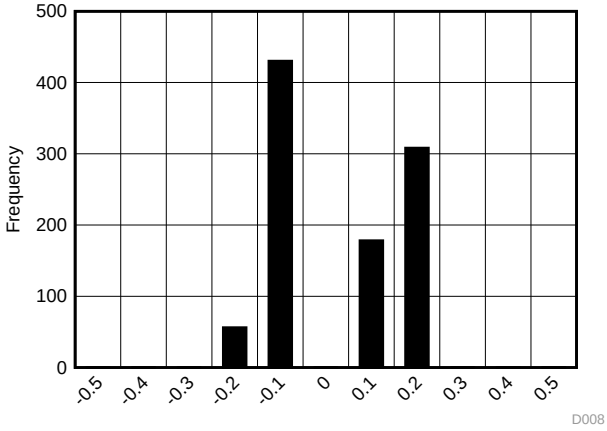

Typical INL = ±0.3 LSB

**Figure 7. Typical INL**




1000 devices

**Figure 8. Typical DNL Distribution**




1000 devices

**Figure 9. Typical INL Distribution**

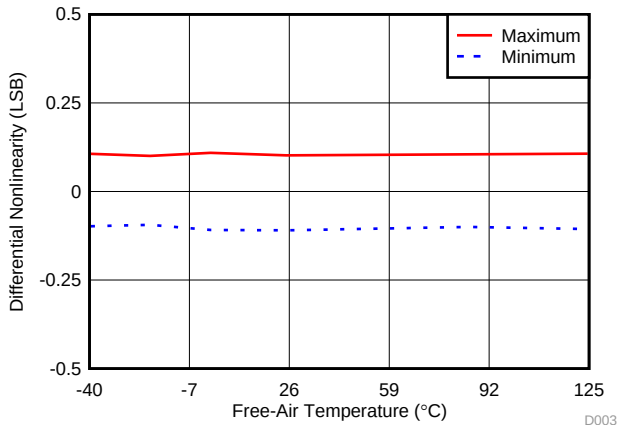



**Figure 10. DNL vs Temperature**

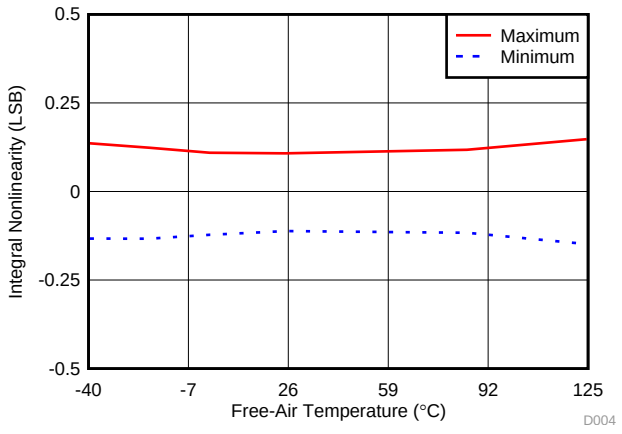



**Figure 11. INL vs Temperature**

## Typical Characteristics (continued)

at $T_A$ = 25°C, $RV_{DD}$ = 5.5 V, $DV_{DD}$ = 3 V, $V_{REF}$ = 5 V, and maximum-rated throughput (unless otherwise noted)

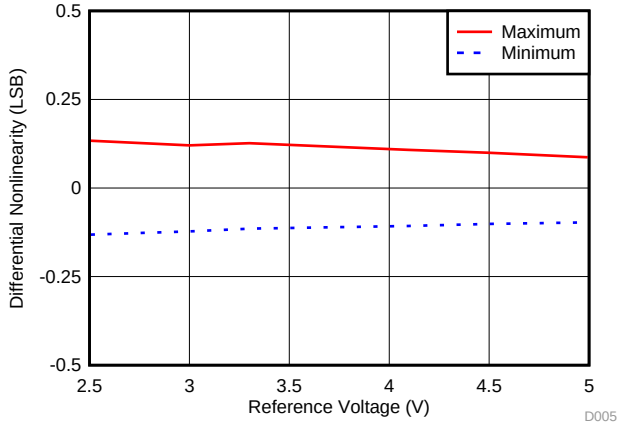



**Figure 12. DNL vs Reference Voltage**

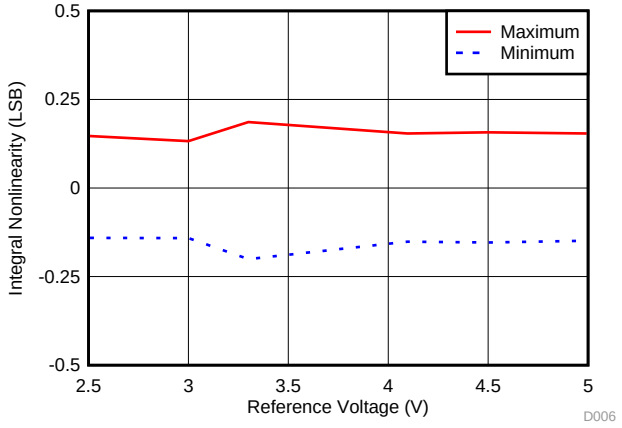



**Figure 13. INL vs Reference Voltage**

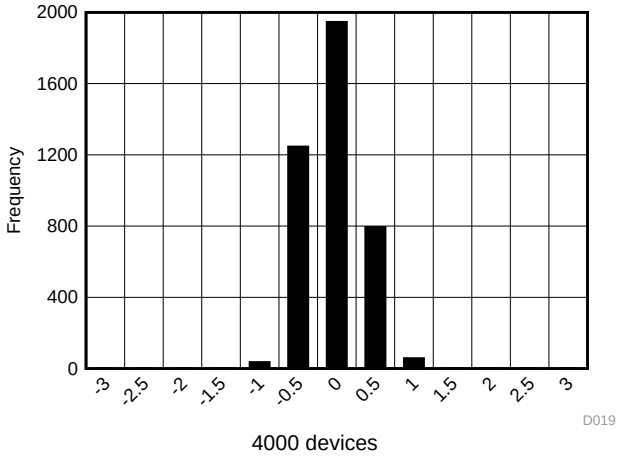



**Figure 14. Typical Offset Distribution**

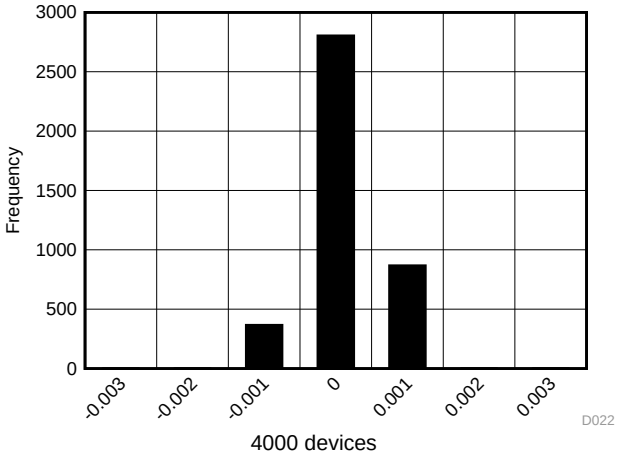



**Figure 15. Typical Gain Error Distribution**

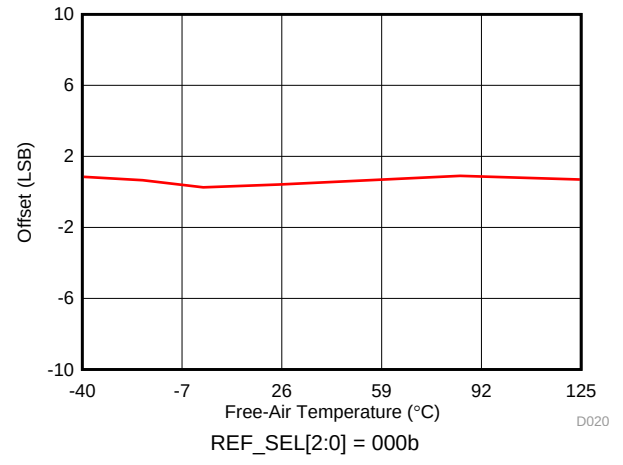



**Figure 16. Offset vs Temperature**

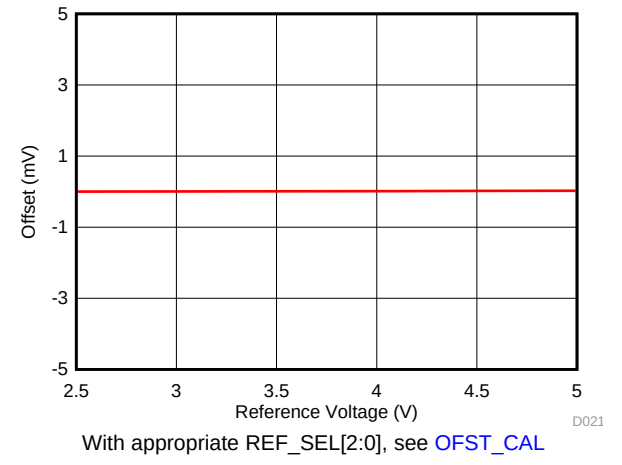
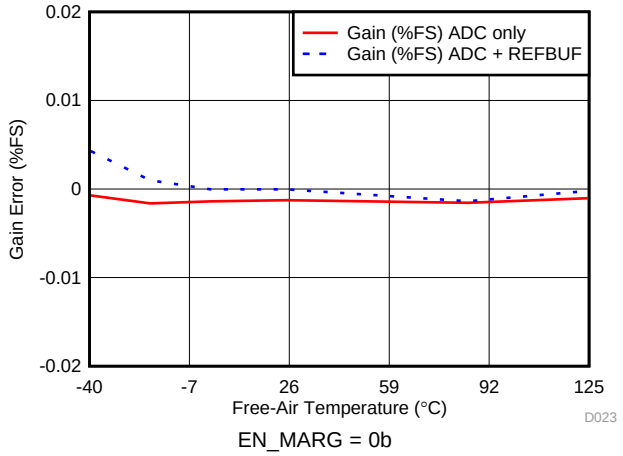



**Figure 17. Offset vs Reference Voltage**


Copyright © 2016–2017, Texas Instruments Incorporated

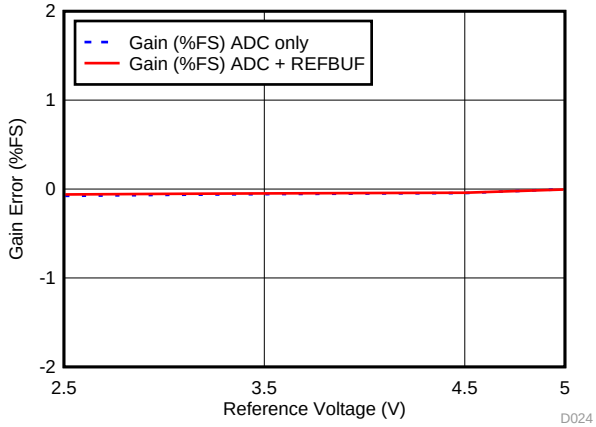
## Typical Characteristics (continued)

at $T_A$ = 25°C, $RV_{DD}$ = 5.5 V, $DV_{DD}$ = 3 V, $V_{REF}$ = 5 V, and maximum-rated throughput (unless otherwise noted)



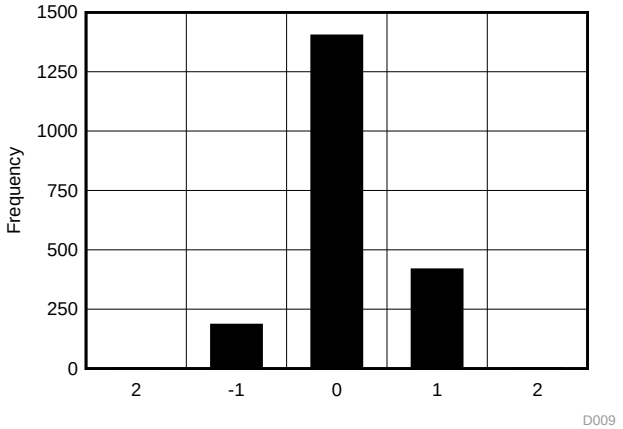

EN_MARG = 0b

**Figure 18. Gain Error vs Temperature**



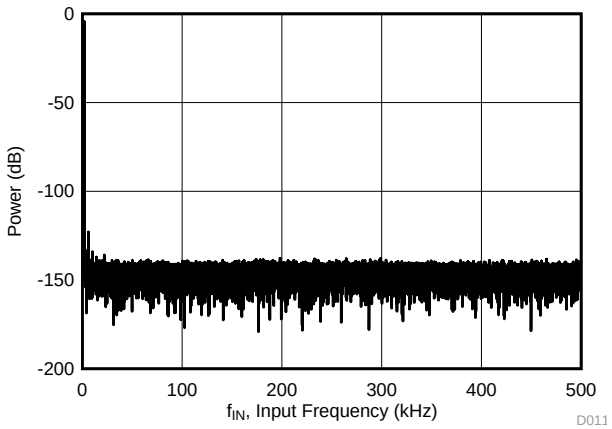

EN_MARG = 0b

**Figure 19. Gain Error vs Reference Voltage**



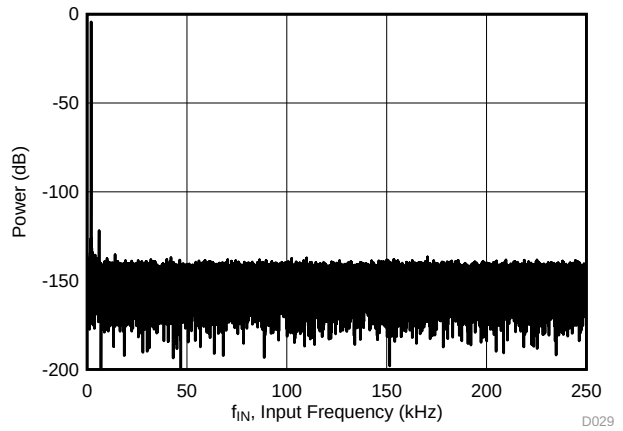

Standard Deviation = 0.47 LSB

**Figure 20. DC Input Histogram**



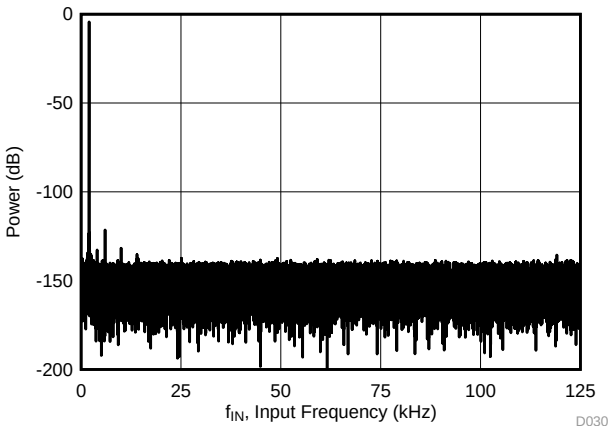

$f_{IN}$ = 2 kHz SNR = 96.8 dB THD = –125 dB

**Figure 21. Typical FFT - ADS8920B**




$f_{IN}$ = 2 kHz SNR = 96.8 dB THD = –125 dB

**Figure 22. Typical FFT - ADS8922B**




$f_{IN}$ = 2 kHz SNR = 96.8 dB THD = –125 dB

**Figure 23. Typical FFT - ADS8924B**

Copyright © 2016–2017, Texas Instruments Incorporated

## Typical Characteristics (continued)

at $T_A$ = 25°C, $RV_{DD}$ = 5.5 V, $DV_{DD}$ = 3 V, $V_{REF}$ = 5 V, and maximum-rated throughput (unless otherwise noted)

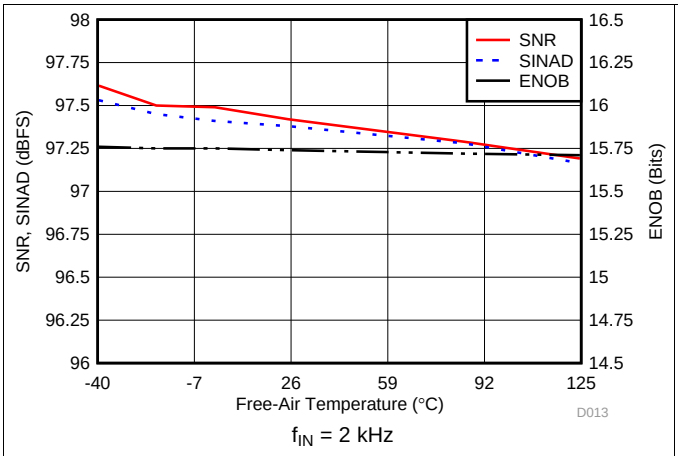



**Figure 24. Noise Performance vs Temperature**

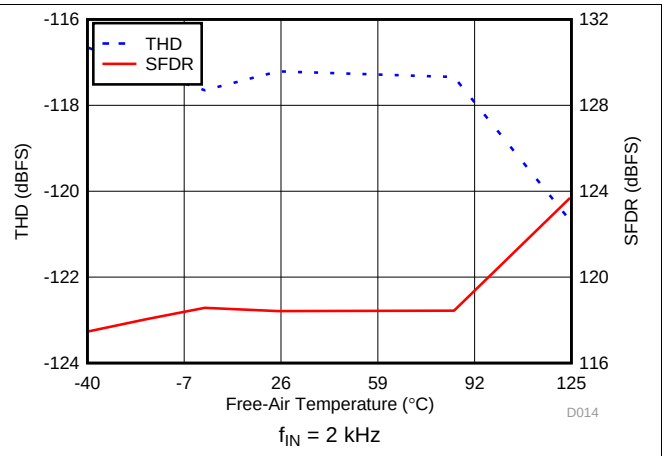



**Figure 25. Distortion Performance vs Temperature**

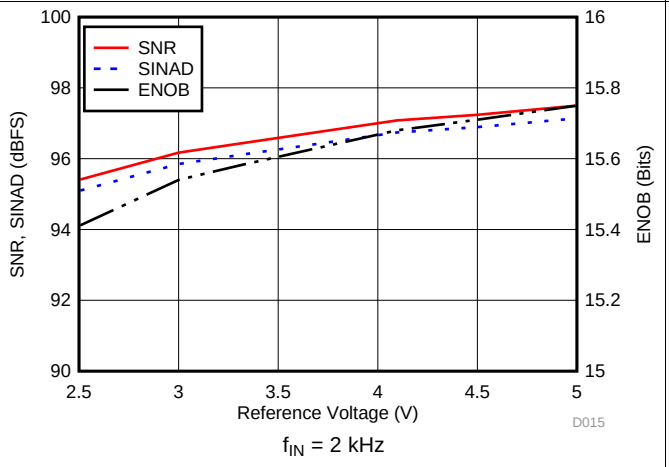



**Figure 26. Noise Performance vs Reference Voltage**

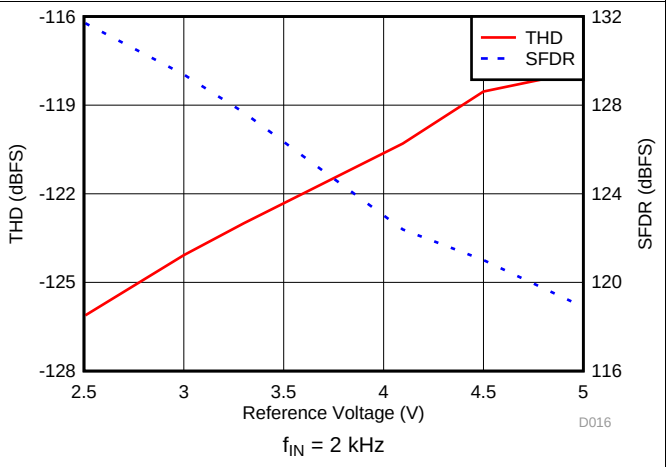



**Figure 27. Distortion Performance vs Reference Voltage**

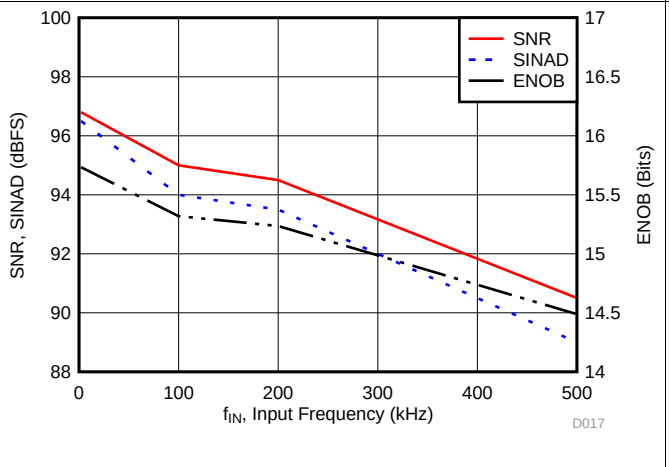



**Figure 28. Noise Performance vs Input Frequency**

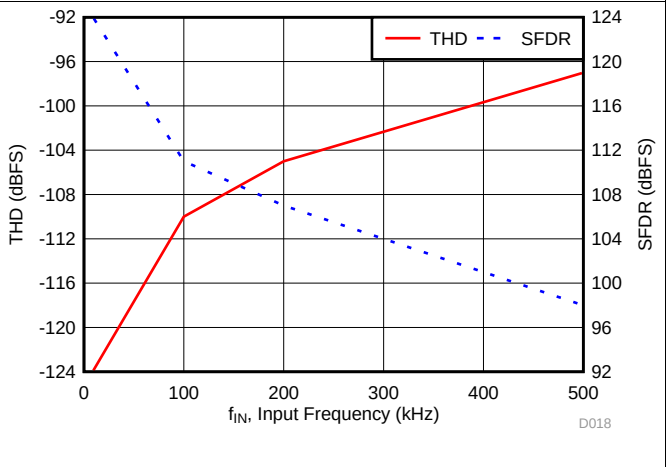



**Figure 29. Distortion Performance vs Input Frequency**


Copyright © 2016–2017, Texas Instruments Incorporated

## Typical Characteristics (continued)

at $T_A$ = 25°C, $RV_{DD}$ = 5.5 V, $DV_{DD}$ = 3 V, $V_{REF}$ = 5 V, and maximum-rated throughput (unless otherwise noted)

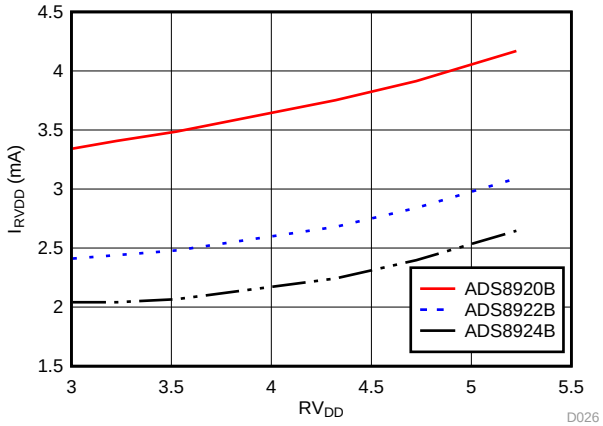



**Figure 30. Analog Supply Current vs Supply Voltage**

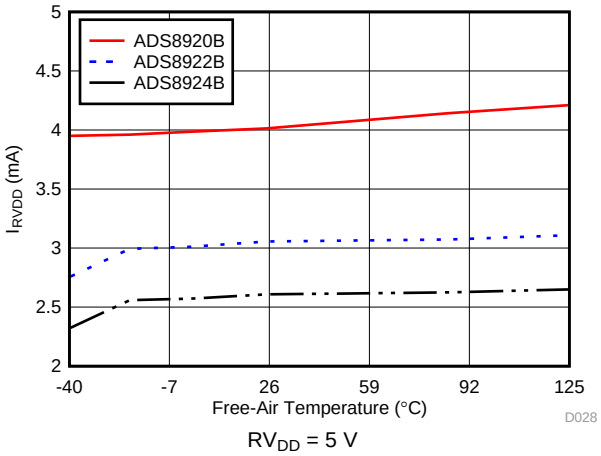



**Figure 31. Analog Supply Current vs Temperature**

# 7 Detailed Description

## 7.1 Overview

The ADS892xB is a family of high-speed, successive approximation register (SAR), analog-to-digital converters (ADC) based on a charge redistribution architecture. These compact devices integrate a reference buffer and LDO, and feature high performance at a high throughput rate with low power consumption.

This device family supports unipolar, fully differential, analog input signals. The integrated reference buffer supports the burst mode of data acquisition for external reference voltages in the range 2.5 V to 5 V, and offers a wide selection of input ranges without additional input scaling.

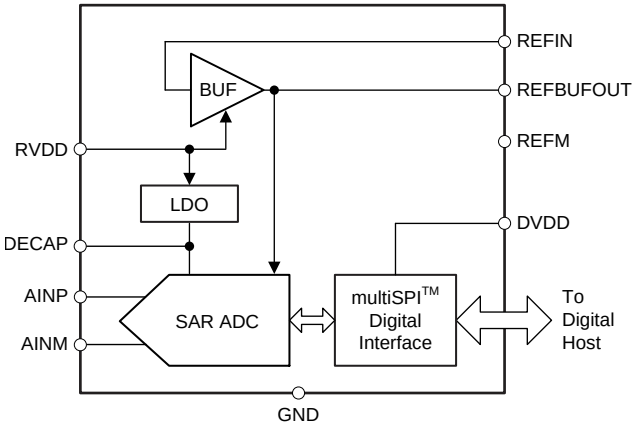
When a conversion is initiated, the differential input between the AINP and AINM pins is sampled on the internal capacitor array. The device uses an internal clock to perform conversions. During the conversion process, both analog inputs are disconnected from the internal circuit. At the end of conversion process, the device reconnects the sampling capacitors to the AINP and AINM pins and enters an acquisition phase.

The integrated LDO allows the device to operate on a single supply, $RV_{DD}$. The device consumes only 21 mW, 16 mW, or 14 mW of power when operating at the rated maximum throughput of 1 MSPS, 500 kSPS, or 250 kSPS, respectively, with the internal reference buffer and LDO enabled.

The enhanced multiSPI digital interface is backward-compatible with traditional SPI protocol. Configurable features simplify board layout, timing, and firmware, and support high throughput at lower clock speeds, thus allowing an easy interface with a variety of microcontrollers, DSPs, and FPGAs.

The ADS892xB enables test and measurement, medical, and industrial applications to achieve fast, low-noise, low-distortion, low-power data acquisition in small form factors.

## 7.2 Functional Block Diagram





Copyright © 2016–2017, Texas Instruments Incorporated

## 7.3 Feature Description

From a functional perspective, the device comprises four modules: the low-dropout regulator (LDO), the reference buffer (BUF), the converter (SAR ADC), and the interface (multiSPI digital interface), as shown in the *Functional Block Diagram* section.

The LDO module is powered by the $RV_{DD}$ supply, and generates the bias voltage for internal circuit blocks of the device. The reference buffer module buffers the external reference voltage source from the dynamic, capacitive switching load present on the reference pins during the conversion process. The converter module samples and converts the analog input into an equivalent digital output code. The interface module facilitates communication and data transfer between the device and the host controller.

### 7.3.1 LDO Module

To enable single-supply operation, the device features an internal low-dropout regulator (LDO). The LDO is powered by the $RV_{DD}$ supply, and the output is available on the two DECAP pins. This LDO output powers the critical analog blocks within the device, and must not be used for any other external purposes.

Short the two DECAP pins together, and decouple with the GND pin by placing a 1-µF, X7R-grade, ceramic capacitor with a 10-V rating, as shown in Figure 32. There is no upper limit on the value of the decoupling capacitor; however, a larger decoupling capacitor results in a longer power-up time for the device. See the *Layout* section for layout recommendations.

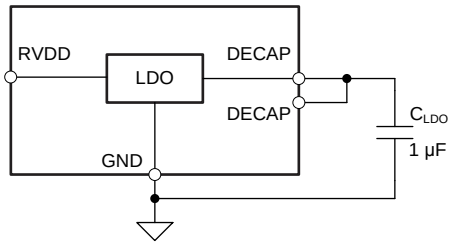



**Figure 32. Internal LDO Connections**

### 7.3.2 Reference Buffer Module

On the CONVST rising edge, the device moves from ACQ state to CONV state, and the internal capacitors are switched to the REFBUFOUT pins as per the successive approximation algorithm. Most of the switching charge required during the conversion process is provided by external decoupling capacitor $C_{REFBUF}$. If the charge lost from the $C_{REFBUF}$ is not replenished before the next CONVST rising edge, the voltage on REFBUFOUT pins is less than $V_{REFBUFOUT}$. The subsequent conversion occurs with this different reference voltage, and causes a proportional error in the output code. The internal reference buffer of the device maintains the voltage on REFBUFOUT pins within 0.5-LSB of $V_{REFBUFOUT}$. All the performance characteristics of the device are specified with the internal reference buffer and specified values of $C_{REFBUF}$ and $R_{ESR}$.

In burst-mode of operation, the device stays in ACQ state for a long duration of time and then performs a burst of conversions. During the acquisition state (ACQ), the sampling capacitor ($C_S$) is connected to the differential input pins and no charge is drawn from the REFBUFOUT pins. However, during the very first conversion cycle, there is a step change in the current drawn from the REFBUFOUT pins. This sudden change in load triggers a transient settling response in the reference buffer. For a fixed input voltage, any transient settling error at the end of the conversion cycle results in a change in output codes over the subsequent conversions, as shown in Figure 33. The internal reference buffer of the ADS89xxB, when used with the recommended values of $C_{REFBUF}$ and $R_{ESR}$, keeps the transient settling error at the end of each conversion cycle within 0.5-LSB. Therefore, the device supports burst-mode of operation with every conversion result being as per the datasheet specifications.

Copyright © 2016–2017, Texas Instruments Incorporated

## Feature Description (continued)

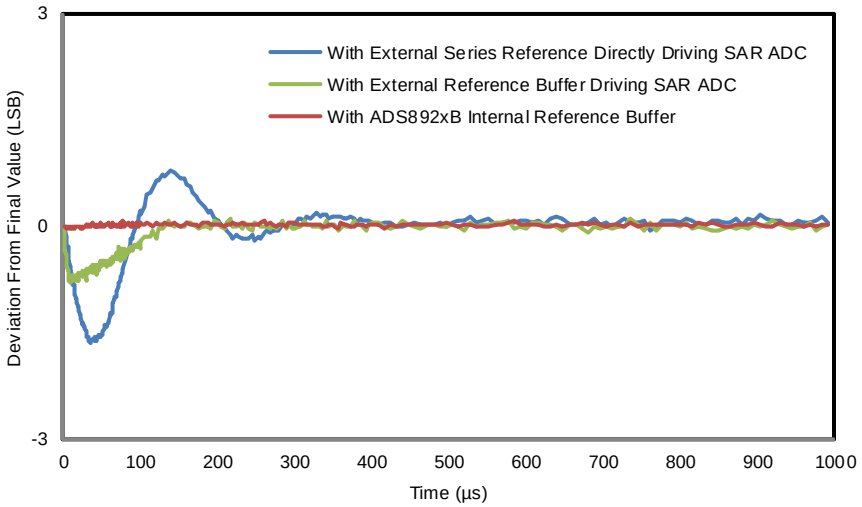



**Figure 33. ADC Output Codes in Burst-Mode Operation With Various ADC Reference Buffers**

Figure 34 shows the block diagram of the internal reference buffer.

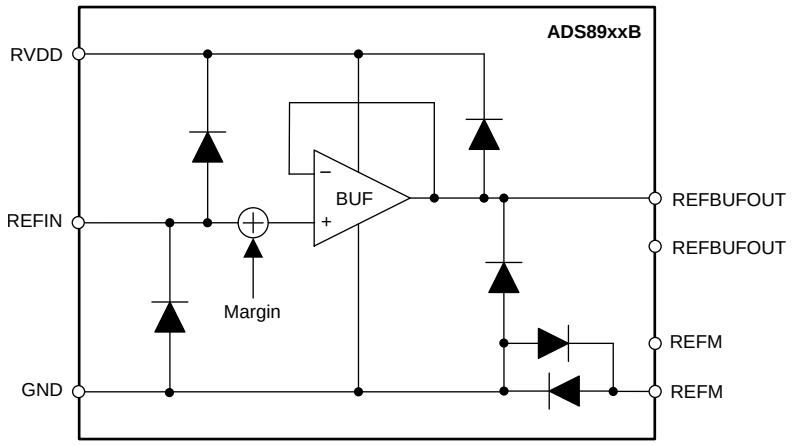



**Figure 34. Internal Reference Buffer Block Diagram**

The input range for the device is set by the external voltage applied at the REFIN pin ($V_{REF}$). The REFIN pin has electrostatic discharge (ESD) protection diodes to the RVDD and GND pins. For minimum input offset error (see $E_{(IO)}$ specified in the *Electrical Characteristics*), set the REF_SEL[2:0] bits to the value closest to $V_{REF}$ (see the OFST_CAL register).

The internal reference buffer has a typical gain of 1 V/V with minimal offset error (see $V_{(RO)}$ specified in the *Electrical Characteristics*), and the output of the buffer is available between the REFBUFOUT pins and the REFM pins. Set the REF_OFST[4:0] bits to add or subtract an intentional offset voltage (see the REF_MRG register).

Figure 35 shows the external connections required for the internal reference buffer.


Copyright © 2016–2017, Texas Instruments Incorporated

## Feature Description (continued)

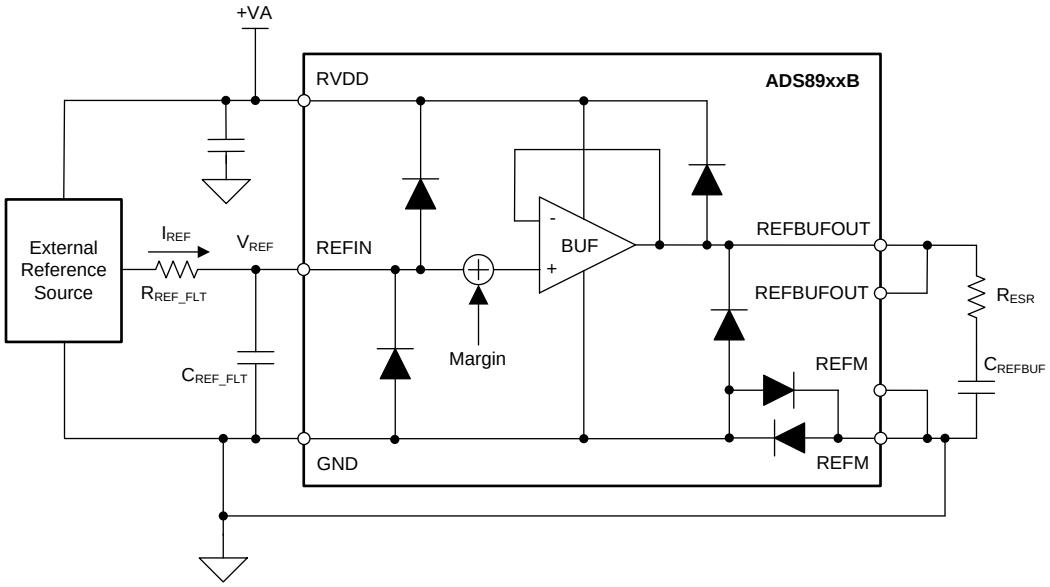



**Figure 35. External Connections for the Internal Reference Buffer**

Select $R_{REF_FLT}$ and $C_{REF_FLT}$ to limit the broadband noise contribution from the external reference source. The device takes very little current, $I_{REF}$, from the REFIN pin (typically, 0.1 µA). However, this current flows through $R_{REF_FLT}$ and may result in additional gain error.

Short the two REFBUFOUT pins externally. Short the two REFM pins to GND externally. As shown in Figure 35, place a combination of $R_{ESR}$ and $C_{REFBUF}$ (see the *Electrical Characteristics*) between the REFBUFOUT pins and the REFM pins as close to the device as possible. See the *Layout* section for layout recommendations.

### 7.3.3 Converter Module

As shown in Figure 36, the converter module samples the analog input signal (provided between the AINP and AINM pins), compares this signal with the reference voltage (between the pair of REFBUFOUT and REFM pins), and generates an equivalent digital output code.

The converter module receives $\overline{RST}$ and CONVST inputs from the interface module, and outputs the ADCST signal and the conversion result back to the interface module.

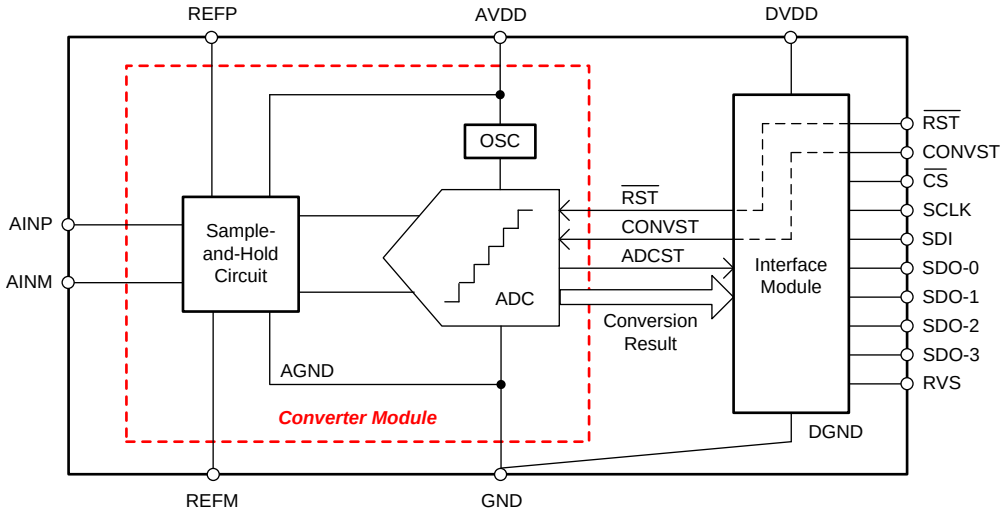



**Figure 36. Converter Module**

Copyright © 2016–2017, Texas Instruments Incorporated

## Feature Description (continued)

### 7.3.3.1 Sample-and-Hold Circuit

These devices support unipolar, fully differential, analog input signals. Figure 37 shows a small-signal equivalent circuit of the sample-and-hold circuit. Each sampling switch is represented by a resistance ($R_{S1}$ and $R_{S2}$, typically 50 Ω) in series with an ideal switch ($SW_1$ and $SW_2$). The sampling capacitors, $C_{S1}$ and $C_{S2}$, are typically 60 pF.

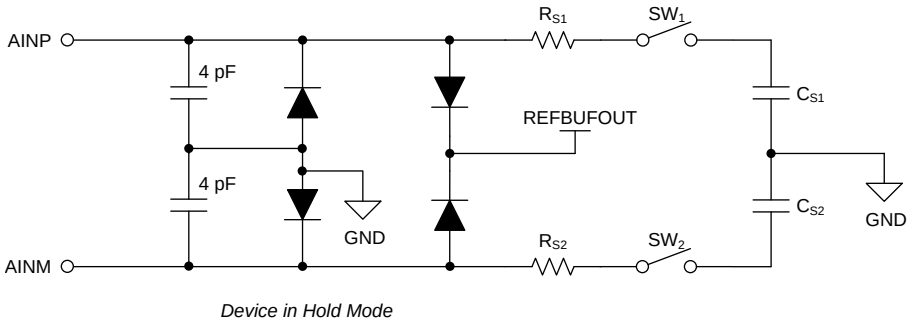



**Figure 37. Input Sampling Stage Equivalent Circuit**

During the acquisition process (ACQ state), both positive and negative inputs are individually sampled on $C_{S1}$ and $C_{S2}$, respectively. During the conversion process (CNV state), the device converts for the voltage difference between the two sampled values: $V_{AINP} - V_{AINM}$.

Each analog input pin has electrostatic discharge (ESD) protection diodes to REFBUFOUT and GND. Keep the analog inputs within the specified range to avoid turning the diodes on.

Equation 1 and Equation 2 show the full-scale input range (FSR) and common-mode voltage ($V_{CM}$), respectively, supported at the analog inputs for any external reference voltage provided on the REFIN pin ($V_{REF}$).

$$FSR = \pm V_{REF} \quad (1)$$

$$V_{CM} = \left(\frac{V_{REF}}{2}\right) \pm 0.1\ V \quad (2)$$


Copyright © 2016–2017, Texas Instruments Incorporated

## Feature Description (continued)

### 7.3.3.2 Internal Oscillator

The device family features an internal oscillator (OSC) that provides the conversion clock; see Figure 36. The conversion duration is bound by the minimum and maximum value of $t_{conv}$, as specified in the *Switching Characteristics* table.

The interface module uses this internal clock (OSC), an external clock (provided by the host controller on the SCLK pin), or a combination of both the internal and external clocks, to execute the data transfer operations between the device and host controller; see the *Interface Module* section for more details.

### 7.3.3.3 ADC Transfer Function

The device family supports unipolar, fully differential analog inputs. The device output is in two's compliment format. Figure 38 and Table 1 show the ideal transfer characteristics for the device.

The least significant bit (LSB) for the ADC is given by Equation 3:

$$1\ \text{LSB} = \frac{\text{FSR}}{2^{16}} = 2 \times \frac{V_{REF}}{2^{16}} \tag{3}$$

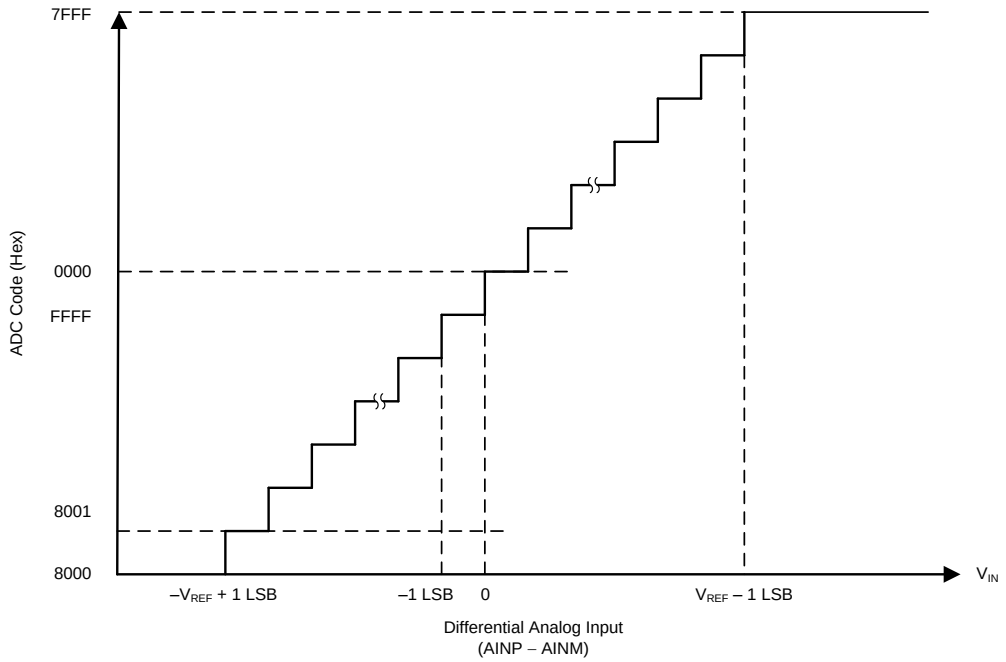



**Figure 38. Differential Transfer Characteristics**

**Table 1. Transfer Characteristics**

| DIFFERENTIAL ANALOG INPUT VOLTAGE (AINP – AINM) | OUTPUT CODE (HEX) |
|---|---|
| < $-V_{REF}$ | 8000 |
| $-V_{REF}$ + 1 LSB | 8001 |
| –1 LSB | FFFF |
| 0 | 0000 |
| 1 LSB | 0001 |
| > $V_{REF}$ – 1 LSB | 7FFF |

Copyright © 2016–2017, Texas Instruments Incorporated

### 7.3.4 Interface Module

The interface module facilitates the communication and data transfer between the device and the host controller. As shown in Figure 39, the module consists of shift registers (both input and output), configuration registers, and a protocol unit.

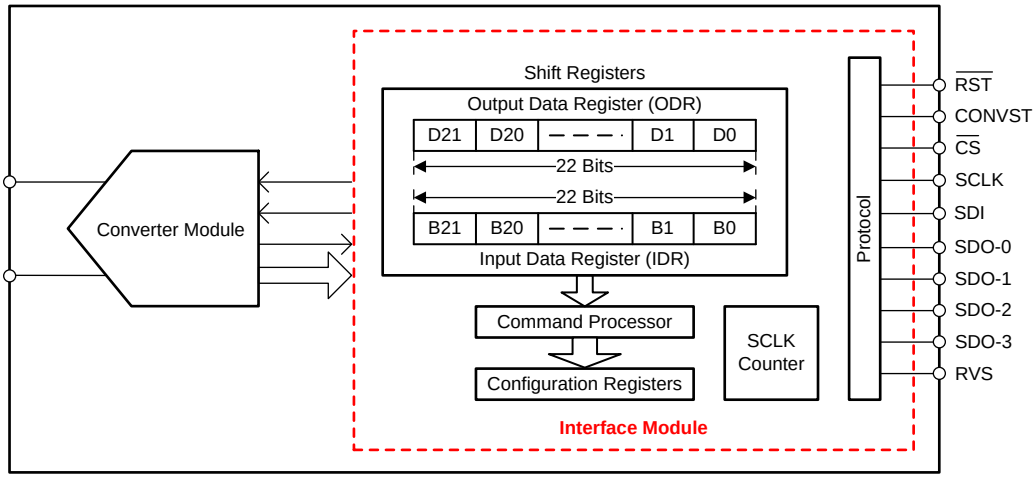



**Figure 39. Interface Module**

The *Pin Configuration and Functions* section provides descriptions of the interface pins. The *Data Transfer Frame* section details the functions of shift registers, the SCLK counter, and the command processor. The *Data Transfer Protocols* section details supported protocols. The *Register Maps* section explains the configuration registers and bit settings.


Copyright © 2016–2017, Texas Instruments Incorporated

## 7.4 Device Functional Modes

As shown in Figure 40, this device family supports three functional states: RST, ACQ, and CNV. The device state is determined by the status of the CONVST and $\overline{\text{RST}}$ control signals provided by the host controller.

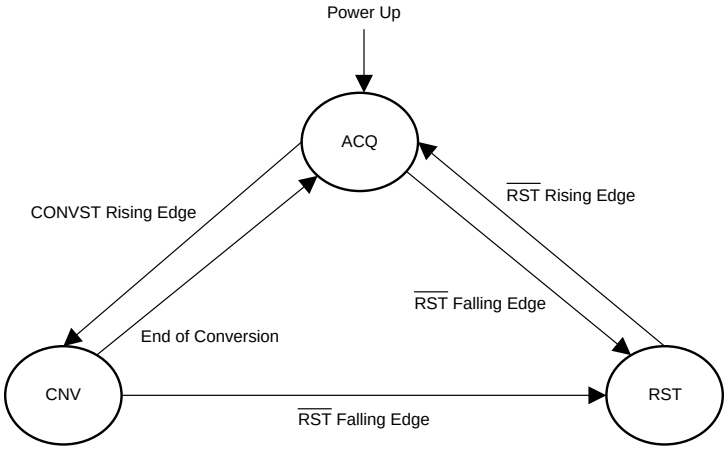



**Figure 40. Device Functional States**

### 7.4.1 RST State

The $\overline{\text{RST}}$ pin is an asynchronous digital input for the device. To enter RST state, the host controller pulls the $\overline{\text{RST}}$ pin low and keeps it low for the $t_{wl_RST}$ duration (as specified in the *Timing Requirements* table).

In RST state, all configuration registers (see the *Register Maps* section) are reset to their default values, the RVS pin remains low, and the SDO-x pins are Hi-Z.

To exit RST state, the host controller pulls the $\overline{\text{RST}}$ pin high, with CONVST and SCLK held low and $\overline{\text{CS}}$ held high, as shown in Figure 41. After a delay of $t_{d_rst}$, the device enters ACQ state and the RVS pin goes high.

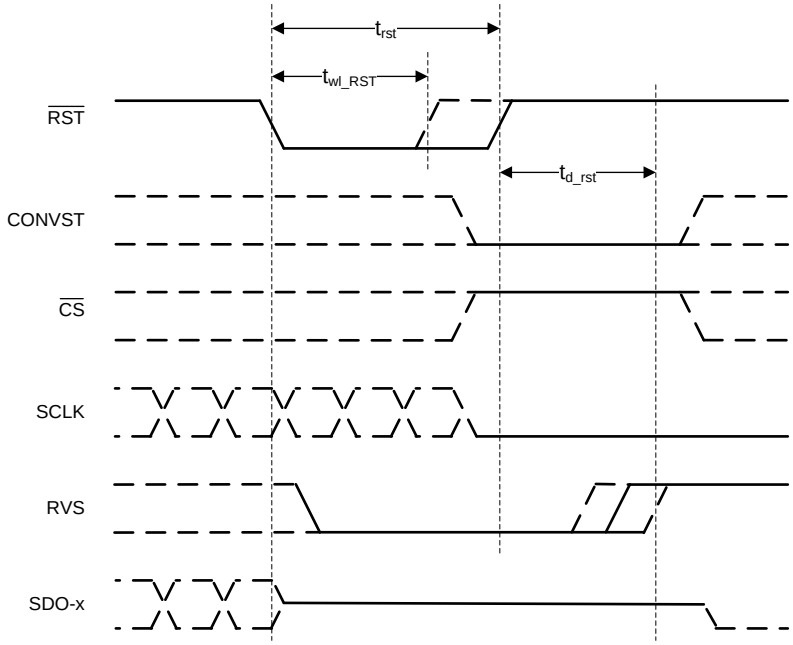



**Figure 41. Asynchronous Reset**

To operate the device in either ACQ or CNV state, $\overline{\text{RST}}$ must be held high. With $\overline{\text{RST}}$ held high, transitions on the CONVST pin determine the functional state of the device.

Copyright © 2016–2017, Texas Instruments Incorporated

## Device Functional Modes (continued)

Figure 42 shows a typical conversion process. The internal ADCST signal goes low during conversion and goes high at the end of conversion. With $\overline{CS}$ held high, RVS reflects the status of ADCST.

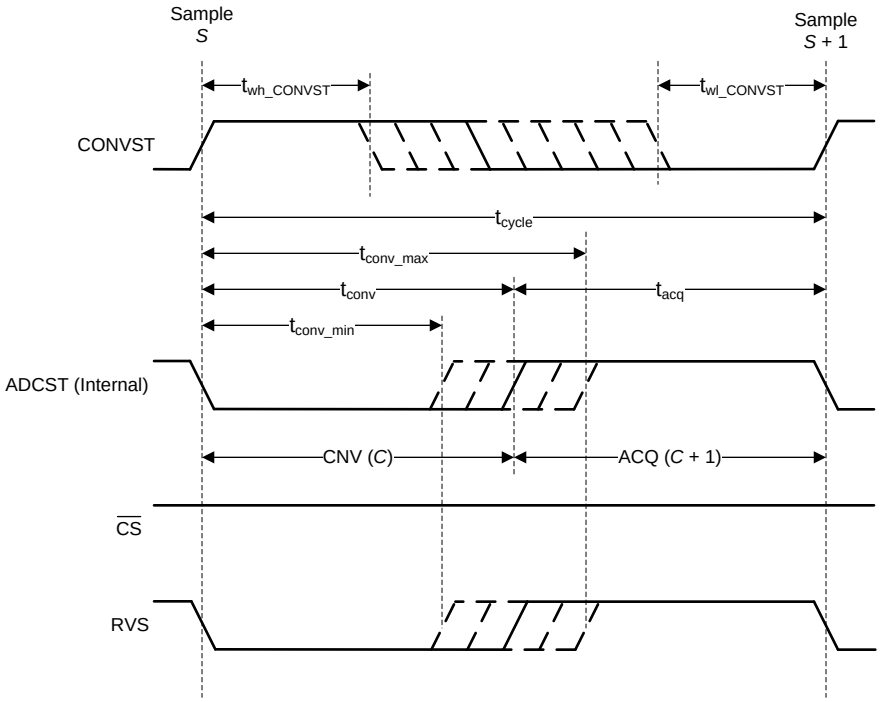



**Figure 42. Typical Conversion Process**

### 7.4.2 ACQ State

In ACQ state, the device acquires the analog input signal. The device enters ACQ state at power-up, when coming out of power down (See the PD Control section), after any asynchronous reset, and at the end of every conversion.

An $\overline{RST}$ falling edge takes the device from ACQ state to RST state. A CONVST rising edge takes the device from ACQ state to CNV state.

### 7.4.3 CNV State

The device moves from ACQ state to CNV state on a rising edge of the CONVST pin. The conversion process uses an internal clock. The device ignores any further transitions on the CONVST signal until the ongoing conversion is complete (that is, during the time interval of $t_{conv}$).

At the end of conversion, the device enters ACQ state. The cycle time for the device is given by Equation 4:

$$t_{cycle\text{-}min} = t_{conv} + t_{acq\text{-}min} \quad (4)$$

**NOTE**

The conversion time, $t_{conv}$, varies within the specified limits of $t_{conv_min}$ and $t_{conv_max}$ (as specified in the *Switching Characteristics* table). After initiating a conversion, the host controller must monitor for a low-to-high transition on the RVS pin or wait for the $t_{conv_max}$ duration to elapse before initiating a new operation (data transfer or conversion). If RVS is not monitored, substitute $t_{conv}$ in Equation 4 with $t_{conv_max}$.


Copyright © 2016–2017, Texas Instruments Incorporated

## 7.5 Programming

This device family features nine configuration registers (as described in the *Register Maps* section). To access the internal configuration registers, these devices support the commands listed in Table 2.

**Table 2. Supported Commands**

| B[21:17] | B[16:8] | B[7:0] | COMMAND ACRONYM | COMMAND DESCRIPTION |
|---|---|---|---|---|
| 00000 | 000000000 | 00000000 | NOP | No operation |
| 10000 | <9-bit address> | <8-bit unmasked bits> | CLR_BITS | Clear <8-bit unmasked bits> from <9-bit address> |
| 10001 | <9-bit address> | 00000000 | RD_REG | Read contents from the <9-bit address> |
| 10010 | <9-bit address> | <8-bit data> | WR_REG | Write <8-bit data> to the <9-bit address> |
| 10011 | <9-bit address> | <8-bit unmasked bits> | SET_BITS | Set <8-bit unmasked bits> from <9-bit address> |
| 11111 | 111111111 | 11111111 | NOP | No operation |
| Remaining combinations | xxxxxxxxx | xxxxxxxx | Reserved | These commands are reserved and treated by the device as no operation |

These devices support two types of data transfer operations: *data write* (the host controller configures the device), and *data read* (the host controller reads data from the device).

Any data write to the device is always synchronous to the external clock provided on the SCLK pin. The WR_REG command writes the 8-bit data into the 9-bit address specified in the command string. The CLR_BITS command clears the specified bits (identified by 1) at the 9-bit address (without affecting the other bits), and the SET_BITS command sets the specified bits (identified by 1) at the 9-bit address (without affecting the other bits).

The data read from the device can be synchronized to the same external clock or to an internal clock of the device by programming the configuration registers (see the *Data Transfer Protocols* section for details).

### 7.5.1 Output Data Word

In any data transfer frame, the contents of an internal, 22-bit, output data word are shifted out on the SDO pins. The D[21:6] bits of the 22-bit output data word for any frame *F* + 1, are determined by:

- Value of the DATA_VAL bit applicable to frame *F* + 1 (see the DATA_CNTL register)
- The command issued in frame *F*

If a valid RD_REG command is executed in frame *F*, then the D[21:14] bits in frame *F* + 1 reflect the contents of the selected register, and the D[13:0] bits are zeros.

If the DATA_VAL bit for frame *F* + 1 is set to 1, then the D[21:6] bits in frame *F* + 1 are replaced by the DATA_PATN[15:0] bits.

For all other combinations, the D[21:6] bits for frame *F* + 1 are the latest conversion result.

Figure 43 shows the output data word. Figure 44 shows further details of the parity computation unit illustrated in Figure 43.

Copyright © 2016–2017, Texas Instruments Incorporated

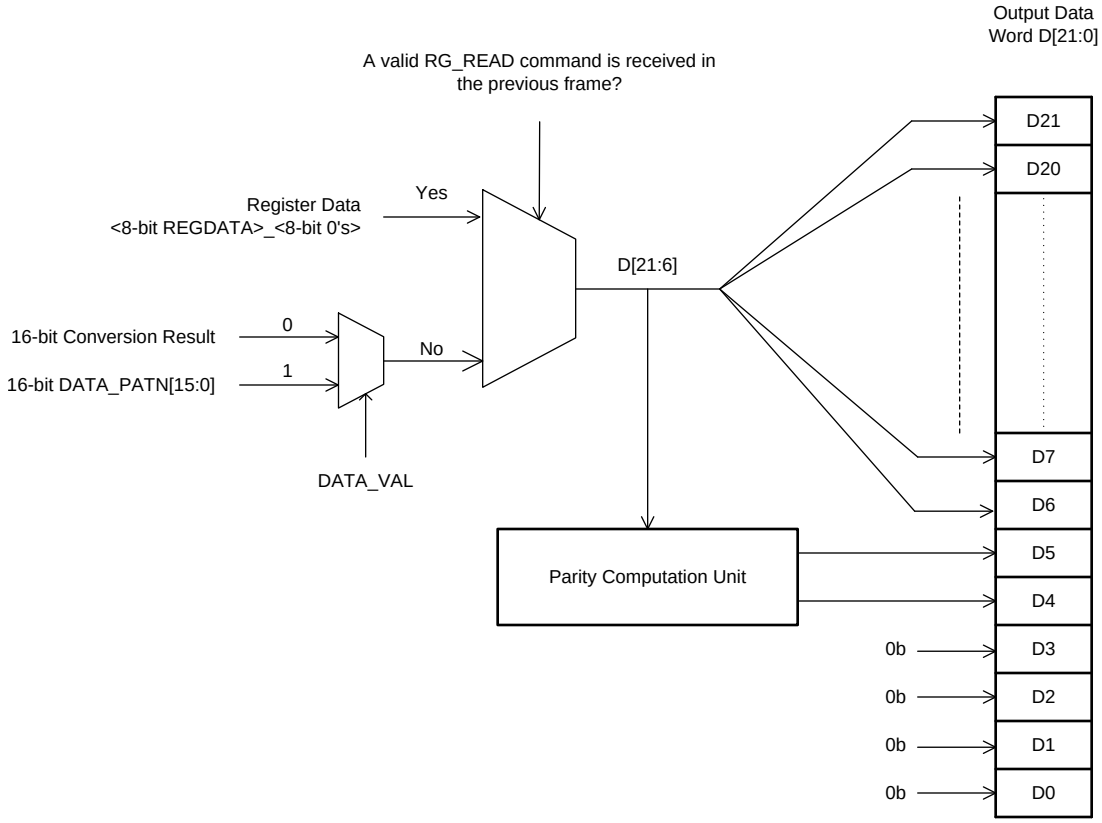



**Figure 43. Output Data Word (D[21:0])**


Copyright © 2016–2017, Texas Instruments Incorporated

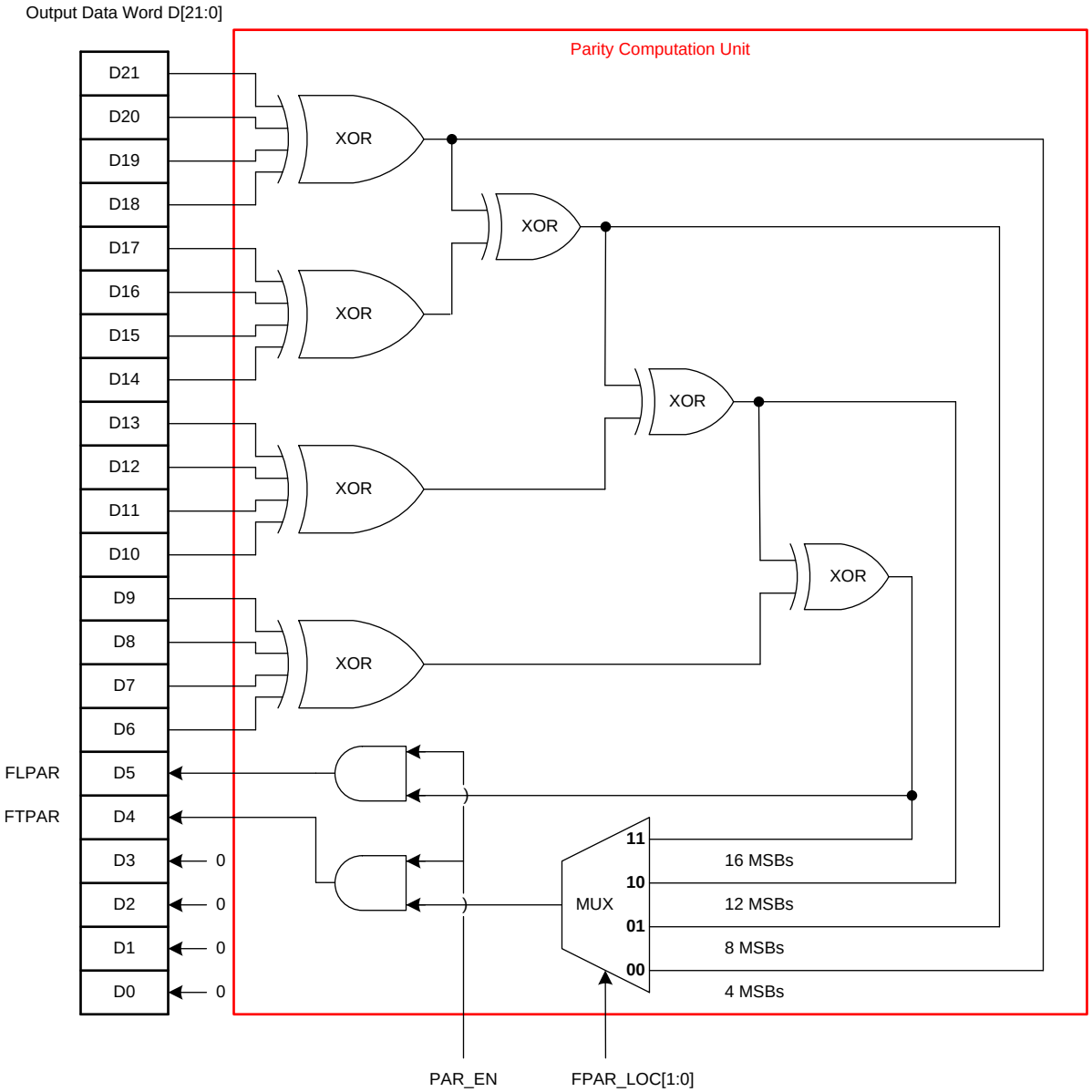



**Figure 44. Parity Bits Computation**

With the PAR_EN bit set to 0, the D[5] and D[4] bits of the output data word are set to 0 (default configuration).

When the PAR_EN bit is set to 1, the device calculates the parity bits (FLPAR and FTPAR) and appends them as bits D[5] and D[4].

- FLPAR is the even parity calculated on bits D[21:6].
- FTPAR is the even parity calculated on the bits defined by FPAR_LOC[1:0].

See the DATA_CNTL register for more details on the FPAR_LOC[1:0] bit settings. Bits D[3:0] are set to 0000b.

Copyright © 2016–2017, Texas Instruments Incorporated

### 7.5.2 Data Transfer Frame

A data transfer frame between the device and the host controller is bounded between a $\overline{CS}$ falling edge and the subsequent $\overline{CS}$ rising edge. The host controller can initiate a data transfer frame (as shown in Figure 45) at any time irrespective of the status of the CONVST signal; however, the data read during such a data transfer frame is a function of relative timing between the CONVST and $\overline{CS}$ signals.

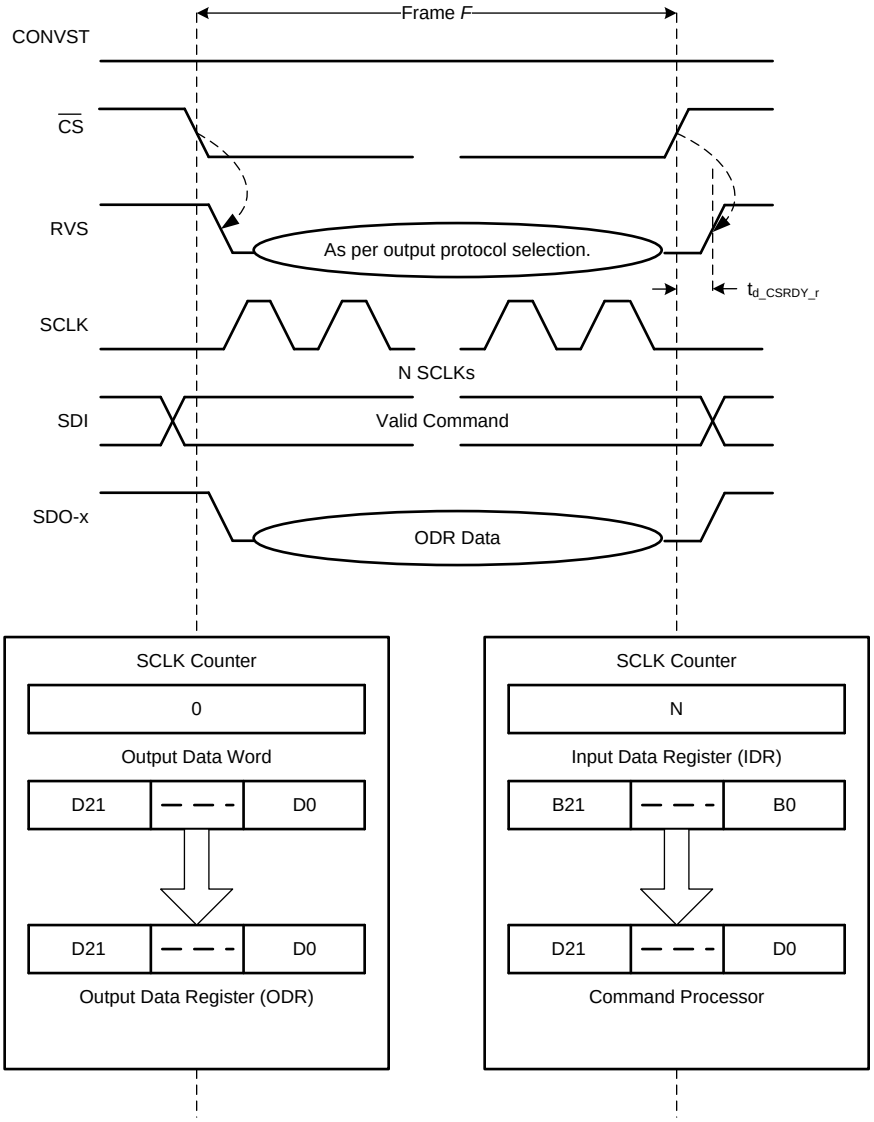



**Figure 45. Data Transfer Frame**

For this discussion, assume that the CONVST signal remains low.

A typical data transfer frame *F* follows this order:

1. The host controller pulls $\overline{CS}$ low to initiate a data transfer frame. On the $\overline{CS}$ falling edge:
   - RVS goes low, indicating the beginning of the data transfer frame.
   - The SCLK counter is reset to 0.
   - The device takes control of the data bus. As shown in Figure 45, the 22-bit contents of the output data word (see Figure 43) are loaded in to the 22-bit output data register (ODR; see Figure 39).
   - The 22-bit input data register (IDR; see Figure 39) is reset to 000000h, corresponding to a NOP command.


Copyright © 2016–2017, Texas Instruments Incorporated

2. During the frame, the host controller provides clocks on the SCLK pin. Inside the device:
   - For each SCLK capture edge, the SCLK counter is incremented and the data bit received on the SDI pin is shifted in to the IDR.
   - For each launch edge of the output clock (SCLK in this case), ODR data are shifted out on the selected SDO-x pins.
   - The status of the RVS pin depends on the output protocol selection (see the *Protocols for Reading From the Device* section).
3. The host controller pulls $\overline{CS}$ high to end the data transfer frame. On the $\overline{CS}$ rising edge:
   - The SDO-x pins go to Hi-Z.
   - RVS goes high (after a delay of $t_{d_CSRDY_r}$).
   - As illustrated in Figure 45, the 22-bit contents of the IDR are transferred to the command processor (see Figure 39) for decoding and further action.

After pulling $\overline{CS}$ high, the host controller monitors for a low-to-high transition on the RVS pin, or waits for the $t_{d_CSRDY_r}$ time (see the *Switching Characteristics* table) to elapse before initiating a new operation (data transfer or conversion). The delay, $t_{d_CSRDY_r}$, for any data transfer frame *F* varies based on the data transfer operation executed in frame *F*.

At the end of data transfer frame *F*:

- If the SCLK counter is < 22, then the IDR captured less than 22 bits from the SDI. In this case, the device treats frame *F* as a *short command frame*. At the end of a short command frame, the IDR is not updated and the device treats the frame as a no operation (NOP) command.
- If the SCLK counter = 22, then the IDR captured exactly 22 bits from SDI. In this case, the device treats the frame *F* as a *optimal command frame*. At the end of an optimal command frame, the command processor decodes the 22-bit contents of the IDR as a valid command word.
- If the SCLK counter > 22, then the IDR captured more than 22 bits from the SDI; however, only the *last 22 bits* are retained. In this case, the device treats frame F as a *long command frame*. At the end of a long command frame, the command processor treats the 22-bit contents of the IDR as a valid command word. There is no restriction on the maximum number of clocks that can be provided within any data transfer frame *F*. However, as explained above, make sure that the last 22 bits shifted into the device before the $\overline{CS}$ rising edge constitute the desired command.

In a short command frame, the write operation to the device is invalidated; however, the output data bits transferred during the short command frame are still valid output data. Therefore, the host controller can use such shorter data transfer frames to read only the required number of MSB bits from the 22-bit output data word. As shown in Figure 43, an *optimal read frame* for the ADS892xB devices must read only the 16 MSB bits of the output data word. The length of an optimal read frame depends on the output protocol selection; see the *Protocols for Reading From the Device* section for more details.

**NOTE**

The previous example shows data-read and data-write operations synchronous to the external clock provided on the SCLK pin.

However, the device also supports data read operation synchronous to the internal clock; see the *Protocols for Reading From the Device* section for more details. In this case, while the ODR contents are shifted on the SDO (or SDOs) on the launch edge of the internal clock, the device continues to capture the SDI data into the IDR (and increment the SCLK counter) on SCLK capture edges.

Copyright © 2016–2017, Texas Instruments Incorporated

### 7.5.3 Interleaving Conversion Cycles and Data Transfer Frames

The host controller operates the device at the desired throughput by interleaving the conversion cycles and the data transfer frames.

The cycle time of the device, $t_{cycle}$, is the time difference between two consecutive CONVST rising edges provided by the host controller. The response time of the device, $t_{resp}$, is the time difference between the host controller initiating conversion *C*, and the host controller receiving the complete result for conversion *C*.

Figure 46 shows three conversion cycles: *C*, *C* + 1, and *C* + 2. Conversion *C* is initiated by a CONVST rising edge at time t = 0, and the conversion result becomes available for data transfer at $t_{conv}$. However, this result is loaded into the ODR only on the subsequent $\overline{CS}$ falling edge. This $\overline{CS}$ falling edge must be provided before the completion of conversion *C* + 1 (that is, before $t_{cycle} + t_{conv}$).

To achieve the rated performance specifications, the host controller must make sure that no digital signals toggle during the quiet acquisition time ($t_{qt_acq}$) and quiet aperture time ($t_{d_cnvcap}$). Any noise during $t_{d_cnvcap}$ may negatively affect the result of the ongoing conversion, whereas any noise during $t_{qt_acq}$ may negatively affect the result of the subsequent conversion.

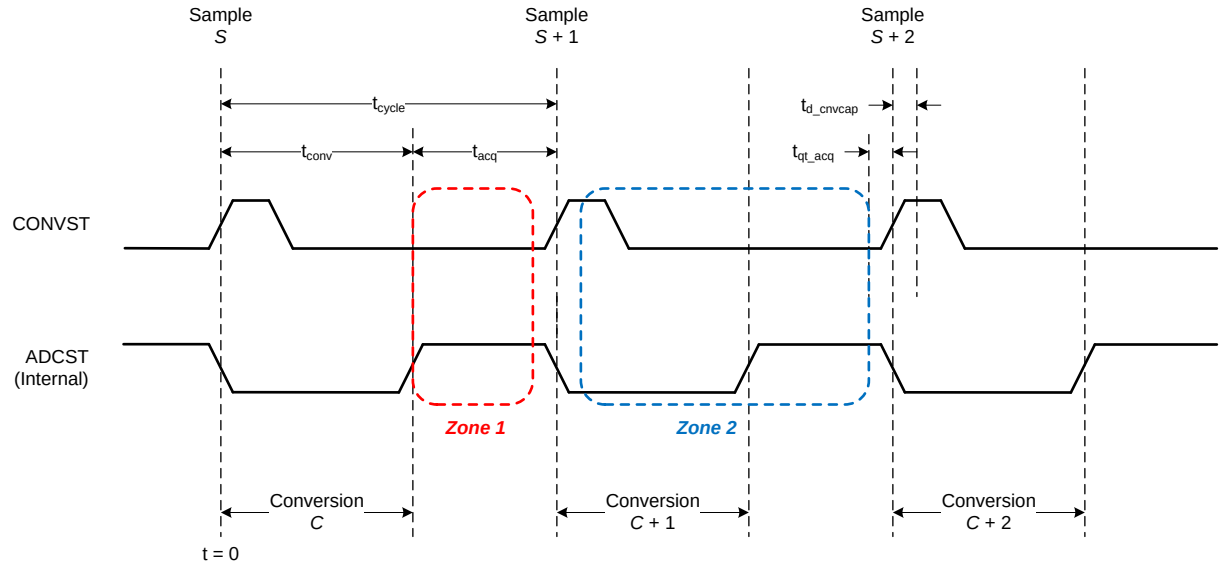



**Figure 46. Data Transfer Zones**

This architecture allows for two distinct time zones (zone 1 and zone 2) to transfer data for each conversion. Zone 1 and zone 2 for conversion *C* are defined in Table 3.

**Table 3. Data Transfer Zones Timing**

| ZONE | STARTING TIME | ENDING TIME |
|---|---|---|
| Zone 1 for conversion *C* | $t_{conv}$ | $t_{cycle} - t_{qt_acq}$ |
| Zone 2 for conversion *C* | $t_{cycle} + t_{d_cnvcap}$ | $t_{cycle} + t_{cycle} - t_{qt_acq}$ |

The response time includes the conversion time and the data transfer time, and thus is a function of the selected data transfer zone.


Copyright © 2016–2017, Texas Instruments Incorporated

Figure 47 and Figure 48 illustrate interleaving of three conversion cycles (*C*, *C* + 1, and *C* + 2) with three data transfer frames (*F*, *F* + 1, and *F* + 2) in zone 1 and in zone 2, respectively.

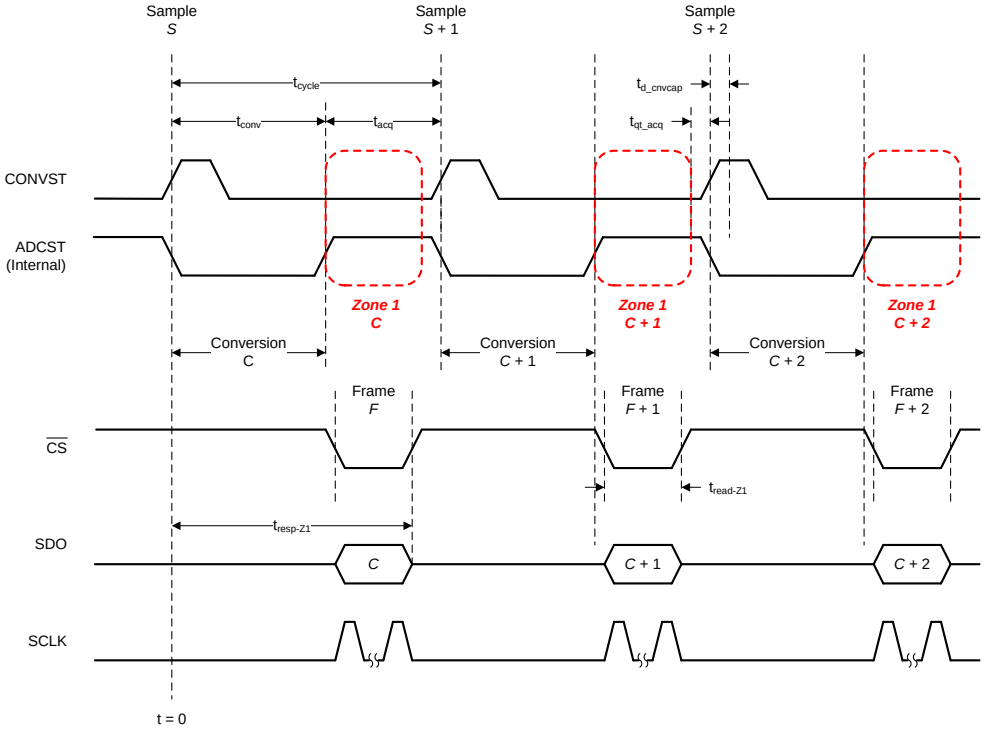



**Figure 47. Zone 1 Data Transfer**

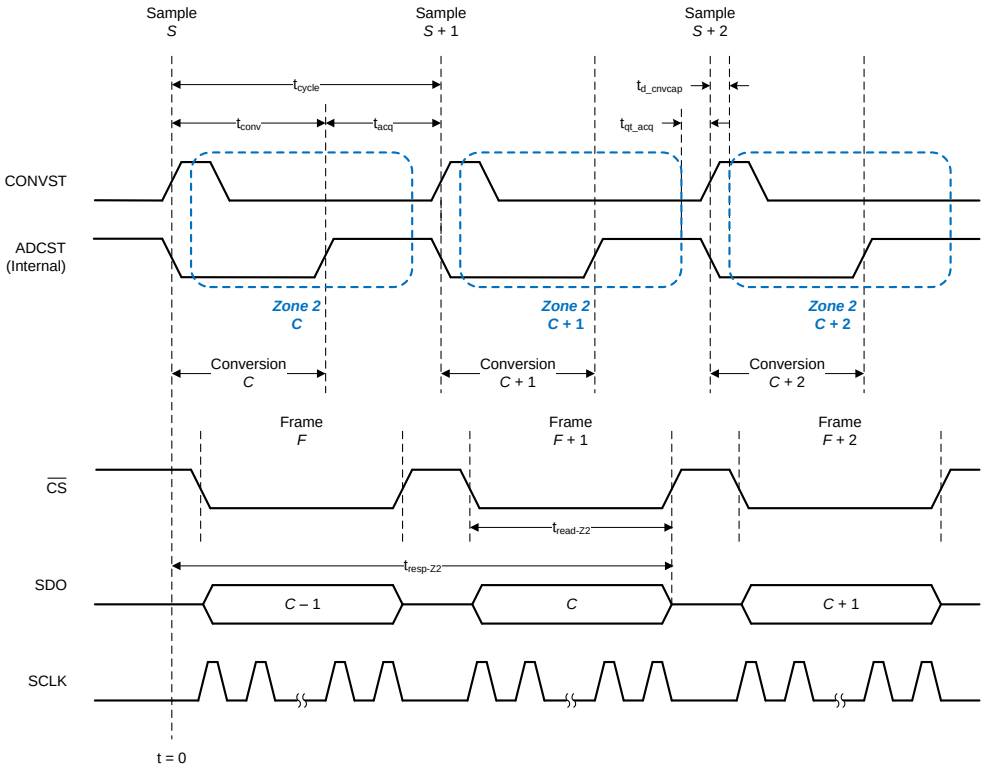



**Figure 48. Zone 2 Data Transfer**

Copyright © 2016–2017, Texas Instruments Incorporated

To achieve cycle time $t_{cycle}$, the read time in zone 1 is given by Equation 5:

$$t_{read\text{-}Z1} \leq t_{cycle} - t_{conv} - t_{qt_acq} \quad (5)$$

For an optimal data transfer frame, Equation 5 results in an SCLK frequency given by Equation 6:

$$f_{SCLK} \geq \frac{16}{t_{read\text{-}Z1}} \quad (6)$$

Then, the zone 1 data transfer achieves a response time defined by Equation 7:

$$t_{resp\text{-}Z1\text{-}min} = t_{conv} + t_{read\text{-}Z1} \quad (7)$$

At lower SCLK speeds, $t_{read\text{-}Z1}$ increases, resulting in slower response times and higher cycle times.

To achieve the same cycle time, $t_{cycle}$, the read time in zone 2 is given by Equation 8:

$$t_{read\text{-}Z2} \leq t_{cycle} - t_{d_cnvcap} - t_{qt_acq} \quad (8)$$

For an optimal data transfer frame, Equation 8 results in an SCLK frequency given by Equation 9:

$$f_{SCLK} \geq \frac{16}{t_{read_Z2}} \quad (9)$$

Then, the zone 2 data transfer achieves a response time defined by Equation 10:

$$t_{resp\text{-}Z2\text{-}min} = t_{cycle} + t_{d_cnvcap} + t_{read\text{-}Z2} \quad (10)$$

Any increase in $t_{read\text{-}Z2}$ increases response time and may increase cycle time.

For a given cycle time, the zone 1 data transfer clearly achieves faster response time, but also requires a higher SCLK speed (as evident from Equation 5, Equation 6, and Equation 7); whereas, the zone 2 data transfer clearly requires a lower SCLK speed but has a slower response time (as evident from Equation 8, Equation 9, and Equation 10).

**NOTE**

A data transfer frame can begin in zone 1, and then extend into zone 2; however, the host controller must make sure that no digital transitions occur during the $t_{qt_acq}$ and $t_{d_cnvcap}$ time intervals.

**NOTE**

For data transfer operations in zone 2 using the ADC-Clock-Master protocol (SDO_MODE[1:0] = 11b), the device supports only the external-clock-echo option (SSYNC_CLK_SEL[1:0] = 00b); see Table 9.

### 7.5.4 Data Transfer Protocols

This device family features a multiSPI digital interface that allows the host controller to operate at slower SCLK speeds and still achieve the required throughput and response time. The multiSPI digital interface module offers three options to reduce the SCLK speed required for data transfer:

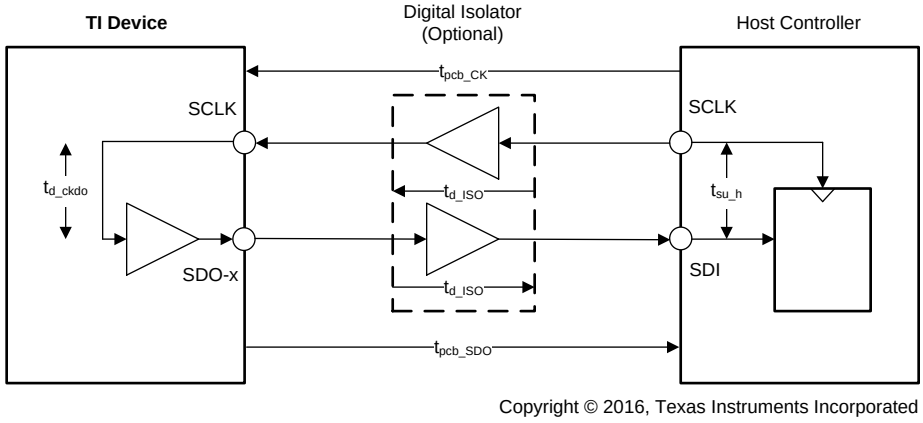
- Increase the width of the output data bus.
- Enable double data rate (DDR) transfer.
- Extended data transfer window, as shown in Figure 48.

These three options can be combined to achieve further reduction in SCLK speed.


Copyright © 2016–2017, Texas Instruments Incorporated

There are various factors that limit the maximum SCLK frequency in a system.

Figure 49 shows the delays in the communication channel between the host controller and the device in a typical serial communication.




Copyright © 2016, Texas Instruments Incorporated

**Figure 49. Delays in Serial Communication**

For example, if $t_{pcb_CK}$ and $t_{pcb_SDO}$ are the delays introduced by the printed circuit board (PCB) traces for the serial clock and SDO signals, $t_{d_CKDO}$ is the clock-to-data delay of the device, $t_{d_ISO}$ is the propagation delay introduced by the digital isolator, and $t_{su_h}$ is the setup time specification of the host controller, then the total delay in the path is given by Equation 11:

$$t_{d_total_serial} = t_{pcb_CK} + t_{d_iso} + t_{d_ckdo} + t_{d_iso} + t_{pcb_SDO} + t_{su_h} \quad (11)$$

In a standard SPI protocol, the host controller and the device launch and capture data bits on alternate SCLK edges. Therefore, the $t_{d_total_serial}$ delay must be kept to less than half of the SCLK duration. Equation 12 shows the fastest clock allowed by the SPI protocol:

$$f_{clk\text{-}SPI} \leq \frac{1}{2 \times t_{d_total\text{-}serial}} \quad (12)$$

Larger values of the $t_{d_total_serial}$ delay restricts the maximum SCLK speed for the SPI protocol, resulting in higher read and response times, and can possibly limit the throughput.

Figure 50 shows a delay ($t_{d_delcap}$) introduced in the capture path (inside the host controller).

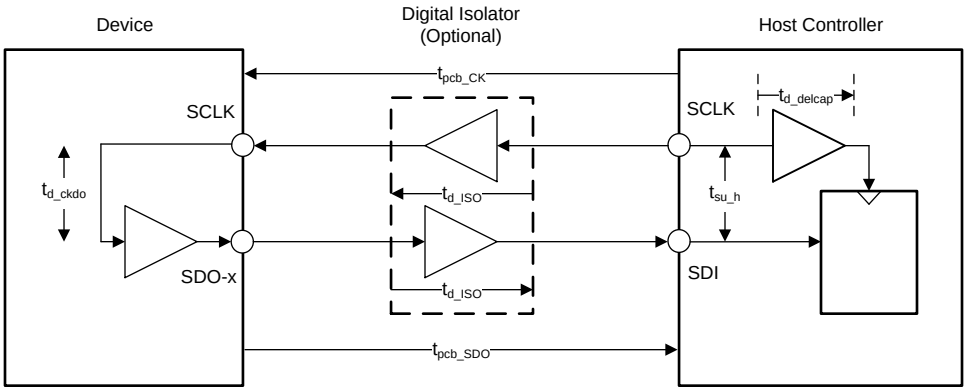



**Figure 50. Delayed Capture**

The total delay in the path modifies to Equation 13:

$$t_{d_total_serial} = t_{pcb_CK} + t_{d_iso} + t_{d_ckdo} + t_{d_iso} + t_{pcb_SDO} + t_{su_h} - t_{d_delcap} \quad (13)$$

This reduction in total delay allows the SPI protocol to operate at higher clock speeds.

The multiSPI digital interface module offers two additional options to remove the restriction on the SCLK speed:

- Early data launch (EDL) mode of operation

  In EDL mode, the device launches the output data on SDO-x pin (or pins) half a clock earlier compared to the standard SPI protocol. Therefore, Equation 12 modifies to Equation 14:

$$f_{clk\text{-}SPI} \leq \frac{1}{t_{d_total\text{-}serial}} \quad (14)$$

  The reduction in total delay allows the serial interface to operate at higher clock speeds.

- ADC-Clock-Master (*source-synchronous*) mode of operation

  As illustrated in Figure 51, in ADC-Clock-Master mode, the device provides a synchronous output clock (on the RVS pin) along with the output data (on the SDO-x pins).

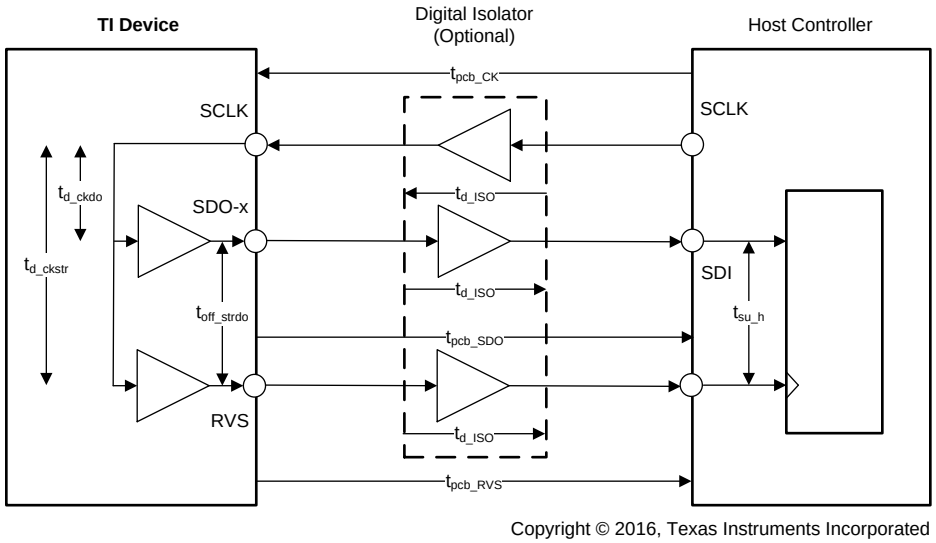



**Figure 51. Delays in ADC-Clock-Master (Source-Synchronous) Mode**

For negligible values of $t_{off_STRDO}$, the total delay in the path for a source-synchronous data transfer, is given by Equation 15:

$$t_{d_total_srcsync} = t_{pcb_RVS} - t_{pcb_SDO} + t_{su_h} \quad (15)$$

As shown by the difference between Equation 11 and Equation 15, using ADC-Clock-Master mode completely eliminates the effect of isolator delays ($t_{d_ISO}$) and clock-to-data delays ($t_{d_CKDO}$); typically, the largest contributors in the overall delay computation.

Furthermore, the actual values of $t_{pcb_RVS}$ and $t_{pcb_SDO}$ do not matter. In most cases, the $t_{d_total_srcsync}$ delay can be kept at a minimum by routing the RVS and SDO lines together on the PCB. Therefore, the ADC-Clock-Master mode allows the data transfer between the host controller and the device to operate at much higher SCLK speeds.


Copyright © 2016–2017, Texas Instruments Incorporated

#### 7.5.4.1 Protocols for Configuring the Device

As shown in Table 4, the host controller can use any of the four legacy, SPI-compatible protocols (SPI-00-S, SPI-01-S, SPI-10-S, or SPI-11-S) to write data to the device.

**Table 4. SPI Protocols for Configuring the Device**

| PROTOCOL | SCLK POLARITY (At $\overline{CS}$ Falling Edge) | SCLK PHASE (Capture Edge) | SDI_CNTL | SDO_CNTL | NO. OF SCLK (Optimal Command Frame) | TIMING DIAGRAM |
|---|---|---|---|---|---|---|
| SPI-00-S | Low | Rising | 00h | 00h | 22 | Figure 52 |
| SPI-01-S | Low | Falling | 01h | 00h | 22 | Figure 53 |
| SPI-10-S | High | Falling | 02h | 00h | 22 | Figure 54 |
| SPI-11-S | High | Rising | 03h | 00h | 22 | Figure 55 |

At power-up or after coming out of any asynchronous reset, the device supports the SPI-00-S protocol for data-read and data-write operations.

To select a different SPI-compatible protocol, program the SDI_MODE[1:0] bits in the SDI_CNTL register. This first write operation must adhere to the SPI-00-S protocol. Any subsequent data transfer frames must adhere to the newly selected protocol.

Figure 52 to Figure 55 detail the four protocols using an optimal command frame; see the *Timing Requirements* and Switching Characteristics tables for associated timing parameters.

**NOTE**

As explained in the *Data Transfer Frame* section, a valid write operation to the device requires a minimum of 22 SCLKs to be provided within a data transfer frame.

Any data write operation to the device must continue to follow the SPI-compatible protocol selected in the SDI_CNTL register, irrespective of the protocol selected for the data-read operation.

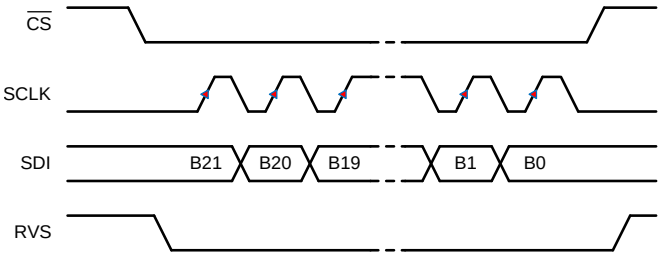



**Figure 52. SPI-00-S Protocol, Optimal Command Frame**

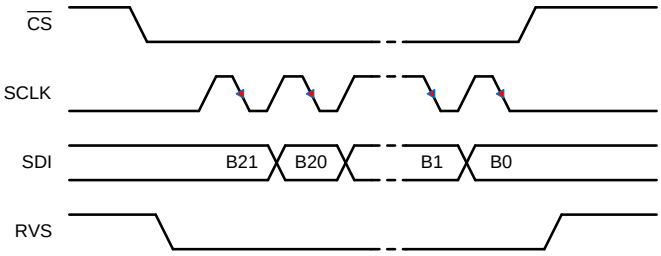



**Figure 53. SPI-01-S Protocol, Optimal Command Frame**

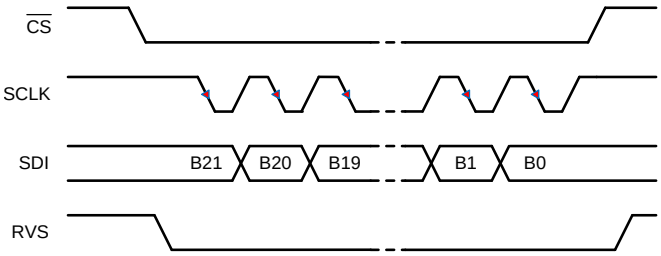



**Figure 54. SPI-10-S Protocol, Optimal Command Frame**

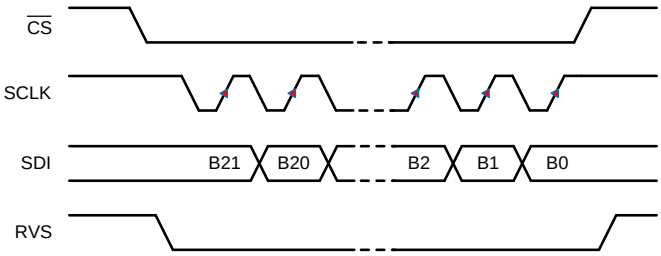



**Figure 55. SPI-11-S Protocol, Optimal Command Frame**

### 7.5.4.2 Protocols for Reading From the Device

The protocols for the data-read operation can be broadly classified into three categories:

1. Legacy, SPI-compatible (SPI-xy-S) protocol
2. SPI-compatible protocols with bus width options (SPI-xy-D and SPI-xy-Q)
3. Source-synchronous (SRC) protocols

#### 7.5.4.2.1 Legacy, SPI-Compatible (SYS-xy-S) Protocols

As shown in Table 5, the host controller can use any of the four legacy, SPI-compatible protocols (SPI-00-S, SPI-01-S, SPI-10-S, or SPI-11-S) to read data from the device.

**Table 5. SPI Protocols for Reading From the Device**

| PROTOCOL | SCLK POLARITY (At $\overline{CS}$ Falling Edge) | SCLK PHASE (Capture Edge) | MSB BIT LAUNCH EDGE | SDI_CNTL | SDO_CNTL | NO. OF SCLK (Optimal Read Frame) | TIMING DIAGRAM |
|---|---|---|---|---|---|---|---|
| SPI-00-S | Low | Rising | $\overline{CS}$ falling | 00h | 00h | 16 | Figure 56 |
| SPI-01-S | Low | Falling | 1st SCLK rising | 01h | 00h | 16 | Figure 57 |
| SPI-10-S | High | Falling | $\overline{CS}$ falling | 02h | 00h | 16 | Figure 58 |
| SPI-11-S | High | Rising | 1st SCLK falling | 03h | 00h | 16 | Figure 59 |

At power-up or after coming out of any asynchronous reset, the device supports the SPI-00-S protocol for data-read and data-write operations. To select a different SPI-compatible protocol for both the data transfer operations:

1. Program the SDI_MODE[1:0] bits in the SDI_CNTL register. This first write operation must adhere to the SPI-00-S protocol. Any subsequent data transfer frames must adhere to the newly selected protocol.
2. Set the SDO_MODE[1:0] bits = 00b in the SDO_CNTL register.

Figure 56 to Figure 59 explain the details of the four protocols using an optimal command frame to read all 22 bits of the output data word. Table 5 shows the number of SCLK required in an optimal read frame for the different output protocol selections.

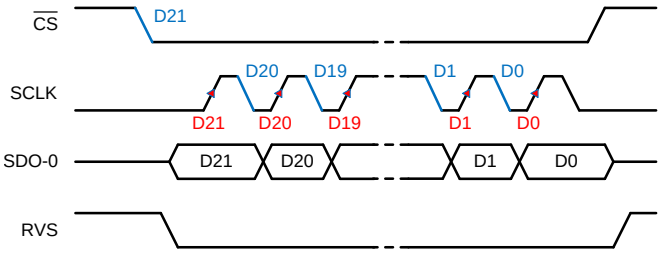



**Figure 56. SPI-00-S Protocol, 22 SCLKs**

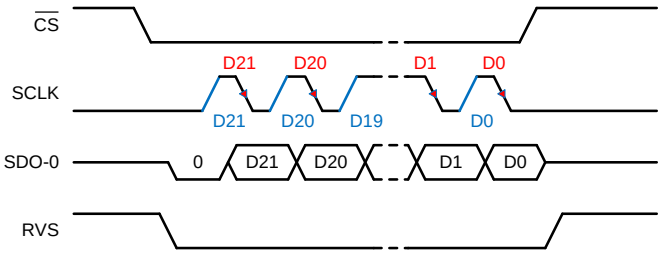



**Figure 57. SPI-01-S Protocol, 22 SCLKs**

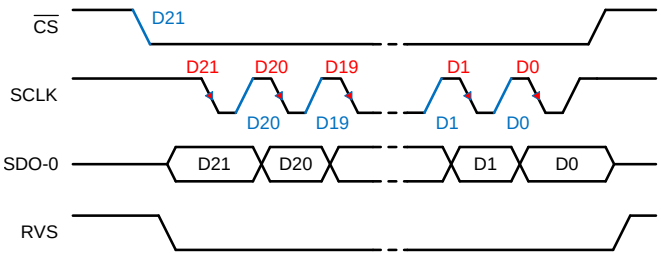



**Figure 58. SPI-10-S Protocol, 22 SCLKs**

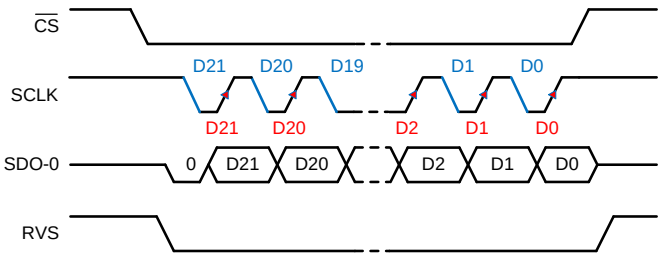



**Figure 59. SPI-11-S Protocol, 22 SCLKs**


Copyright © 2016–2017, Texas Instruments Incorporated

For SDI_MODE[1:0] = 00b or 10b, the device supports an *Early Data Launch* (EDL) option. Set SDO_MODE[1:0] = 01b in the SDO_CNTL register to enable the feature (see Table 6). Setting SDO_MODE[1:0] = 01b has no effect if SDI_MODE[1:0] = 01b or 11b.

**Table 6. SPI Protocols with Early Data Launch**

| PROTOCOL | SCLK POLARITY (At $\overline{CS}$ Falling Edge) | SCLK PHASE (Capture Edge) | MSB BIT LAUNCH EDGE | SDI_CNTL | SDO_CNTL | NO. OF SCLK (Optimal Read Frame) | TIMING DIAGRAM |
|---|---|---|---|---|---|---|---|
| SPI-00-S-EDL | Low | Rising | $\overline{CS}$ falling | 00h | 01h | 16 | Figure 56 |
| SPI-10-S-EDL | High | Falling | $\overline{CS}$ falling | 02h | 01h | 16 | Figure 58 |

As shown in Figure 60, and Figure 61, the device launches the output data bit on the SDO-0 pin half clock earlier compared to the standard SPI protocol.

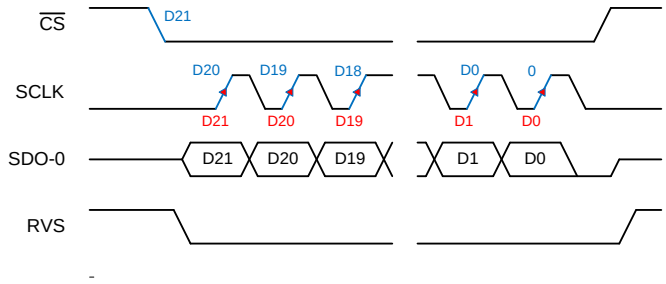



**Figure 60. SPI-00-S-EDL Protocol, 22 SCLKs**

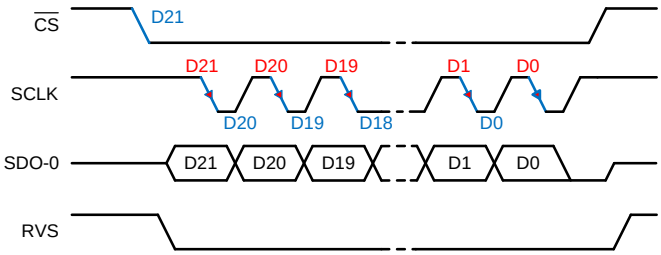



**Figure 61. SPI-10-S-EDL Protocol, 22 SCLKs**

When using these SPI-compatible protocols, the RVS output remains low throughout the data transfer frame; see the *Timing Requirements* and Switching Characteristics tables for associated timing parameters.

With SDO_CNTL[7:0] = 00h or 01h, if the host controller uses a long data transfer frame, the device exhibits daisy-chain operation (see the *Multiple Devices: Daisy-Chain Topology* section).

**NOTE**

Use SPI-compatible protocols to execute the RD_REG, WR_REG, CLR_BITS, and SET_BITS commands specified in Table 2.

Copyright © 2016–2017, Texas Instruments Incorporated

#### 7.5.4.2.2 SPI-Compatible Protocols with Bus Width Options

The device provides an option to increase the SDO bus width from one bit (default, single SDO) to two bits (dual SDO) or four bits (quad SDO) when operating with any of the four legacy, SPI-compatible protocols.

Set the SDO_WIDTH[1:0] bits in the SDO_CNTL register to select the SDO bus width. The SCLK launch edge depends on the SPI protocol selection (as shown in Table 7).

**Table 7. SPI-Compatible Protocols with Bus Width Options**

| PROTOCOL | SCLK POLARITY (At $\overline{CS}$ Falling Edge) | SCLK PHASE (Capture Edge) | MSB BIT LAUNCH EDGE | SDI_CNTL | SDO_CNTL | #SCLK (Optimal Read Frame) | TIMING DIAGRAM |
|---|---|---|---|---|---|---|---|
| SPI-00-D | Low | Rising | $\overline{CS}$ falling | 00h | 08h | 8 | Figure 62 |
| SPI-01-D | Low | Falling | First SCLK rising | 01h | 08h | 8 | Figure 63 |
| SPI-10-D | High | Falling | $\overline{CS}$ falling | 02h | 08h | 8 | Figure 64 |
| SPI-11-D | High | Rising | First SCLK falling | 03h | 08h | 8 | Figure 65 |
| SPI-00-Q | Low | Rising | $\overline{CS}$ falling | 00h | 0Ch | 4 | Figure 66 |
| SPI-01-Q | Low | Falling | First SCLK rising | 01h | 0Ch | 4 | Figure 67 |
| SPI-10-Q | High | Falling | $\overline{CS}$ falling | 02h | 0Ch | 4 | Figure 68 |
| SPI-11-Q | High | Rising | First SCLK falling | 03h | 0Ch | 4 | Figure 69 |

In dual-SDO mode (SDO_WIDTH[1:0] = 10b), two bits of data are launched on the two SDO pins (SDO-0 and SDO-1) on every SCLK launch edge.

In quad-SDO mode (SDO_WIDTH[1:0] = 11b), four bits of data are launched on the four SDO pins (SDO-0, SDO-1, SDO-2, and SDO-3) on every SCLK launch edge.

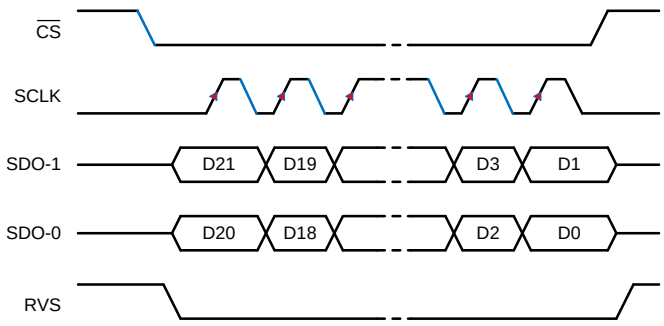



**Figure 62. SPI-00-D Protocol**

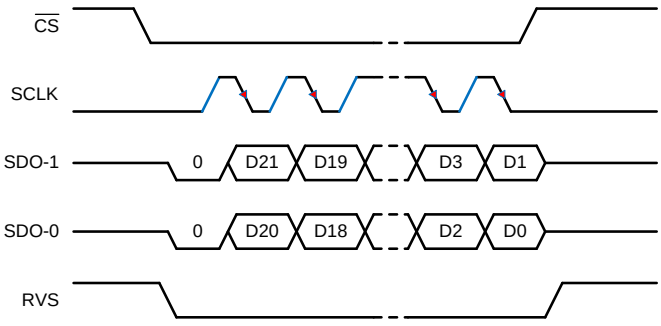



**Figure 63. SPI-01-D Protocol**

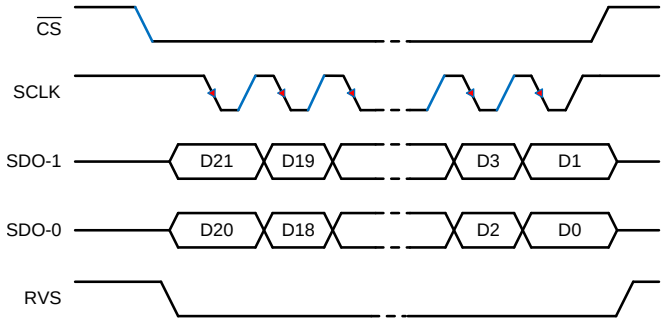



**Figure 64. SPI-10-D Protocol**

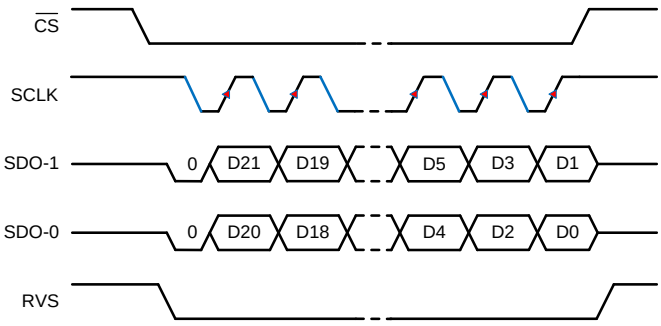



**Figure 65. SPI-11-D Protocol**


Copyright © 2016–2017, Texas Instruments Incorporated

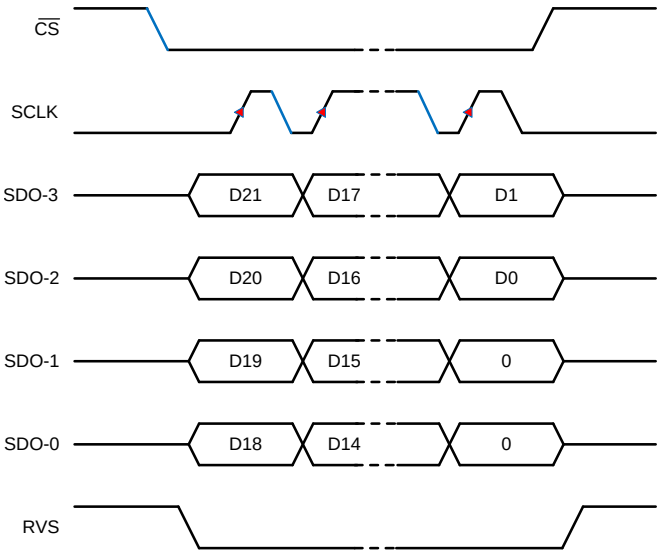



**Figure 66. SPI-00-Q Protocol**

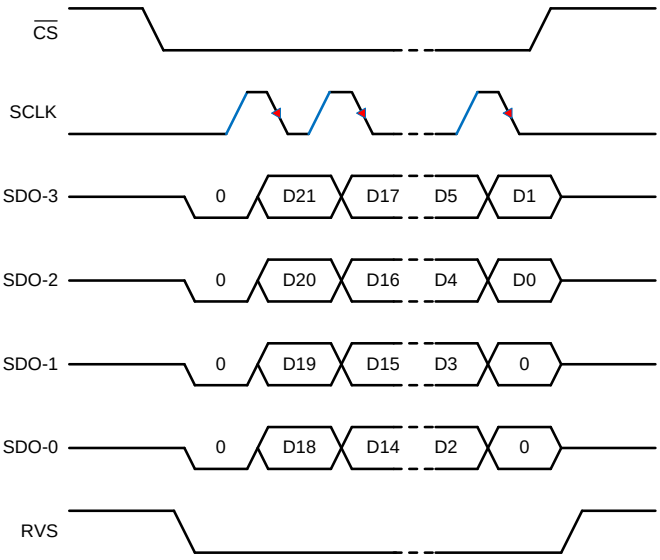



**Figure 67. SPI-01-Q Protocol**

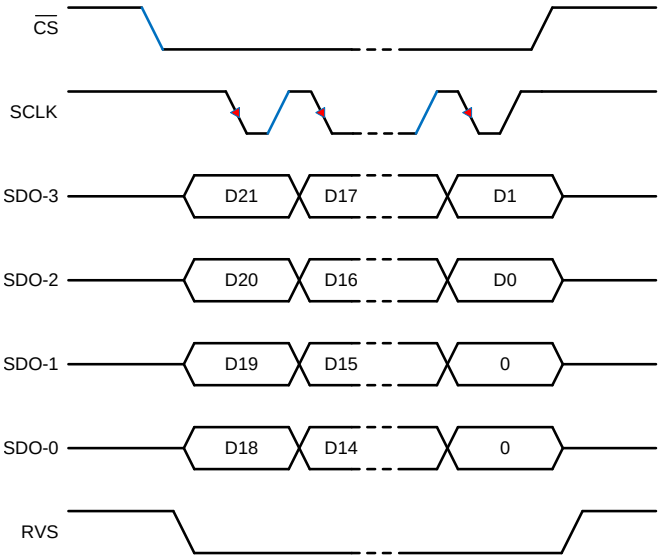



**Figure 68. SPI-10-Q Protocol**

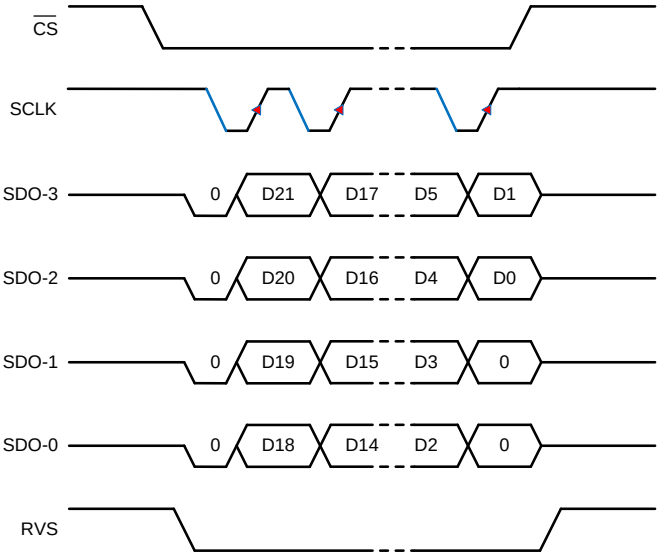



**Figure 69. SPI-11-Q Protocol**

For SDI_MODE[1:0] = 00b or 10b, the device supports an early data launch (EDL) option. Set SDO_MODE[1:0] = 01b in the SDO_CNTL register to enable the feature (see Table 8). Setting SDO_MODE[1:0] = 01b has no effect if SDI_MODE[1:0] = 01b or 11b.

**Table 8. SPI Protocols with Early Data Launch**

| PROTOCOL | SCLK POLARITY (At $\overline{CS}$ Falling Edge) | SCLK PHASE (Capture Edge) | MSB BIT LAUNCH EDGE | SDI_CNTL | SDO_CNTL | NO. OF SCLK (Optimal Read Frame) | TIMING DIAGRAM |
|---|---|---|---|---|---|---|---|
| SPI-00-D-EDL | Low | Rising | $\overline{CS}$ falling | 00h | 09h | 8 | Figure 62 |
| SPI-10-D-EDL | High | Falling | $\overline{CS}$ falling | 02h | 09h | 8 | Figure 64 |
| SPI-00-Q-EDL | Low | Rising | $\overline{CS}$ falling | 00h | 0Dh | 4 | Figure 66 |
| SPI-10-Q-EDL | High | Falling | $\overline{CS}$ falling | 02h | 0Dh | 4 | Figure 68 |

Copyright © 2016–2017, Texas Instruments Incorporated

As shown in Figure 60, and Figure 61, the device launches the output data bits on the SDO-x pins half clock earlier compared to the standard SPI protocol.

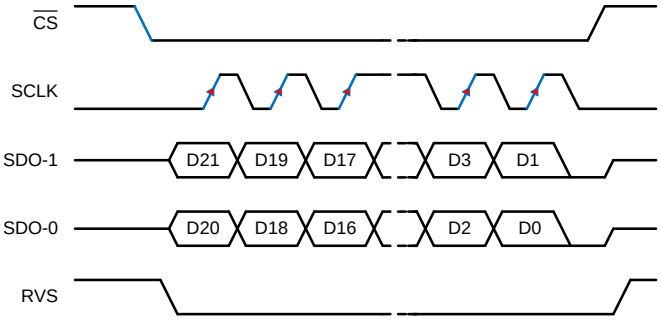



**Figure 70. SPI-00-D-EDL Protocol**

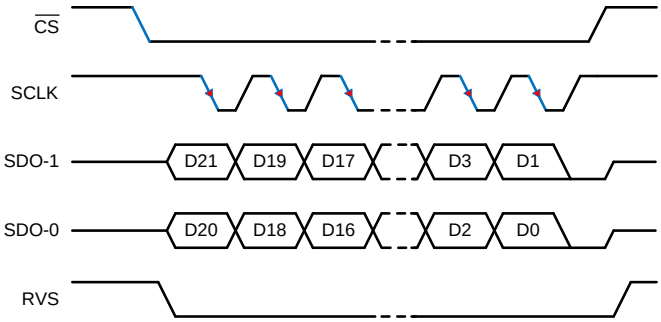



**Figure 71. SPI-10-D-EDL Protocol**

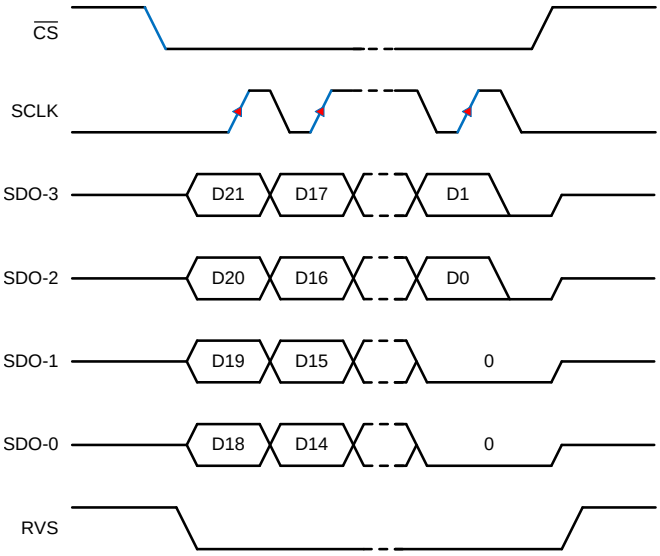



**Figure 72. SPI-00-Q-EDL Protocol**

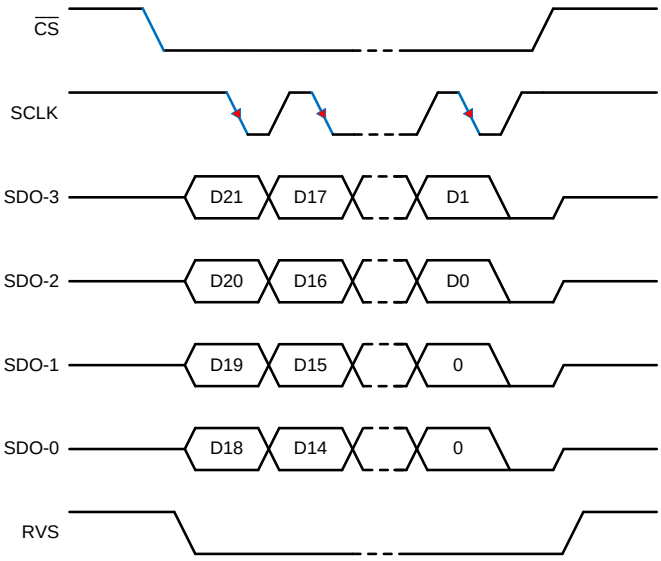



**Figure 73. SPI-10-Q-EDL Protocol**

When using any of the SPI-compatible protocols, the RVS output remains low throughout the data transfer frame; see the *Timing Requirements* and Switching Characteristics tables for associated timing parameters.

Figure 62 to Figure 73 illustrate how the wider data bus allows the host controller to read all 22 bits of the output data word using shorter data transfer frames. Table 7 and Table 8 show the number of SCLK required in an optimal read frame for the different output protocol selections.

**NOTE**

With SDO_CNTL[7:0] ≠ 00h or 01h, a long data transfer frame does not result in daisy-chain operation. On SDO pin (or pins), the 22 bits of output data word are followed by zeros.


Copyright © 2016–2017, Texas Instruments Incorporated

#### 7.5.4.2.3 Source-Synchronous (SRC) Protocols

As described in the *Data Transfer Protocols* section, the multiSPI digital interface supports an ADC-Clock-Master or a *source-synchronous* mode of data transfer between the device and host controller. In this mode, the device provides an output clock that is synchronous with the output data. Furthermore, the host controller can also select the output clock source, data bus width, and data transfer rate.

##### *7.5.4.2.3.1 Output Clock Source Options with SRC Protocols*

In all SRC protocols, the RVS pin provides the output clock. The device allows this output clock to be synchronous to either the external clock provided on the SCLK pin or to the internal clock of the device. Furthermore, this internal clock can be divided by a factor of two or four to lower the data rates.

As shown in Figure 74, set the SSYNC_CLK_SEL[1:0] bits in the SDO_CNTL register to select the output clock source.

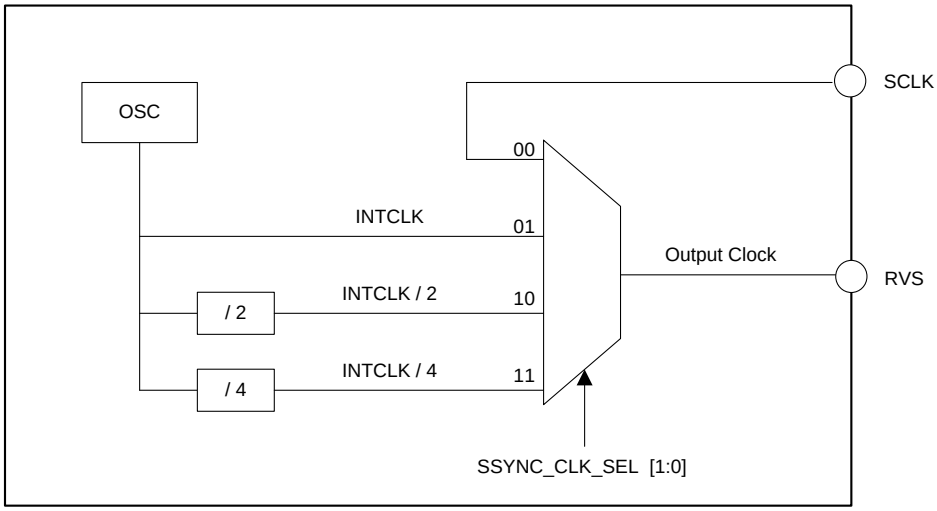



**Figure 74. Output Clock Source Options With SRC Protocols**

#### 7.5.4.2.3.2 Bus Width Options With SRC Protocols

The device provides an option to increase the SDO bus width from one bit (default, single SDO) to two bits (dual SDO) or to four bits (quad SDO) when operating with any of the SRC protocols. Set the SDO_WIDTH[1:0] bits in the SDO_CNTL register to select the SDO bus width.

In dual-SDO mode (SDO_WIDTH[1:0] = 10b), two bits of data are launched on the two SDO pins (SDO-0 and SDO-1) on every SCLK rising edge.

In quad-SDO mode (SDO_WIDTH[1:0] = 11b), four bits of data are launched on the four SDO pins (SDO-0, SDO-1, SDO-2, and SDO-3) on every SCLK rising edge.

#### 7.5.4.2.3.3 Output Data Rate Options With SRC Protocols

The device provides an option to transfer the data to the host controller at a single data rate (default, SDR) or at a double data rate (DDR). Set the DATA_RATE bit in the SDO_CNTL register to select the data transfer rate.

In SDR mode (DATA_RATE = 0b), the RVS pin toggles from low to high, and the output data bits are launched on the SDO pins on the output clock rising edge.

In DDR mode (DTA_RATE = 1b), the RVS pin toggles (from low-to-high or high-to-low), and the output data bits are launched on the SDO pins on every output clock edge, starting with the first rising edge.

The device supports all 24 combinations of output clock source, bus width, and output data rate, as shown in Table 9.

**Table 9. SRC Protocol Combinations**

| PROTOCOL | OUTPUT CLOCK SOURCE | BUS WIDTH | OUTPUT DATA RATE | SDI_CNTL | SDO_CNTL | #OUTPUT CLOCK (Optimal Read Frame) | TIMING DIAGRAM |
|---|---|---|---|---|---|---|---|
| SRC-EXT-SS | SCLK(1) | Single | SDR | 00h, 01h, 02h, or 03h(2) | 03h | 8 | Figure 75 |
| SRC-INT-SS | INTCLK(3) | Single | SDR | | 43h | 8 | Figure 76 |
| SRC-IB2-SS | INTCLK / 2(3) | Single | SDR | | 83h | 8 | |
| SRC-IB4-SS | INTCLK / 4(3) | Single | SDR | | C3h | 8 | |
| SRC-EXT-DS | SCLK(1) | Dual | SDR | | 0Bh | 8 | Figure 79 |
| SRC-INT-DS | INTCLK(3) | Dual | SDR | | 4Bh | 8 | Figure 80 |
| SRC-IB2-DS | INTCLK / 2(3) | Dual | SDR | | 8Bh | 8 | |
| SRC-IB4-DS | INTCLK / 4(3) | Dual | SDR | | CBh | 8 | |
| SRC-EXT-QS | SCLK(1) | Quad | SDR | | 0Fh | 4 | Figure 83 |
| SRC-INT-QS | INTCLK(3) | Quad | SDR | | 4Fh | 4 | Figure 84 |
| SRC-IB2-QS | INTCLK / 2(3) | Quad | SDR | | 8Fh | 4 | |
| SRC-IB4-QS | INTCLK / 4(3) | Quad | SDR | | CFh | 4 | |
| SRC-EXT-SD | SCLK(1) | Single | DDR | | 13h | 8 | Figure 77 |
| SRC-INT-SD | INTCLK(3) | Single | DDR | | 53h | 8 | Figure 78 |
| SRC-IB2-SD | INTCLK / 2(3) | Single | DDR | | 93h | 8 | |
| SRC-IB4-SD | INTCLK / 4(3) | Single | DDR | | D3h | 8 | |
| SRC-EXT-DD | SCLK(1) | Dual | DDR | | 1Bh | 4 | Figure 81 |
| SRC-INT-DD | INTCLK(3) | Dual | DDR | | 5Bh | 4 | Figure 82 |
| SRC-IB2-DD | INTCLK / 2(3) | Dual | DDR | | 9Bh | 4 | |
| SRC-IB4-DD | INTCLK / 4(3) | Dual | DDR | | DBh | 4 | |
| SRC-EXT-QD | SCLK(1) | Quad | DDR | | 1Fh | 2 | Figure 85 |
| SRC-INT-QD | INTCLK(3) | Quad | DDR | | 5Fh | 2 | Figure 86 |
| SRC-IB2-QD | INTCLK / 2(3) | Quad | DDR | | 9Fh | 2 | |
| SRC-IB4-QD | INTCLK / 4(3) | Quad | DDR | | DFh | 2 | |

(1) The EXTCLK option is not recommended when operating with $DV_{DD}$ < 2.35 V.
(2) Any of the four values can be used; see the *Protocols for Configuring the Device* section for more information.
(3) The device supports INTCLK, INTCLK / 2, and INTCLK / 4 options only for data transfer operations in zone 1. The EXTCLK option is supported in zone 1 and zone 2; see Figure 46.


Copyright © 2016–2017, Texas Instruments Incorporated

Figure 75 to Figure 86 show the details of various source synchronous protocols. Table 9 shows the number of output clocks required in an optimal read frame for the different output protocol selections.

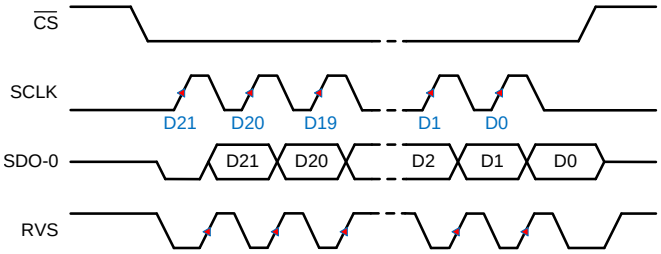



**Figure 75. SRC-EXT-SS: SRC, SCLK, Single SDO, SDR**

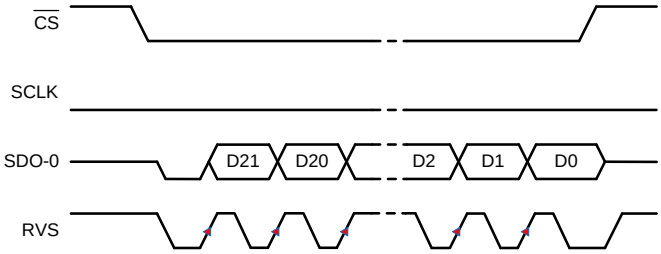



**Figure 76. SRC-INT-SS: SRC, INTCLK, Single SDO, SDR**

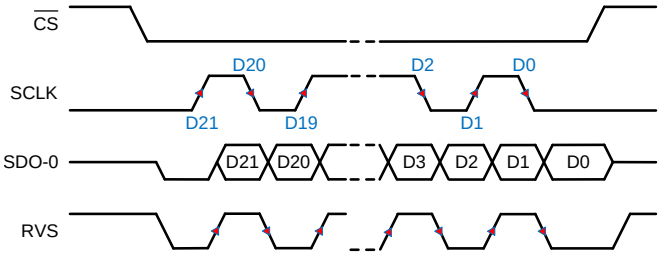



**Figure 77. SRC-EXT-SD: SRC, SCLK, Single SDO, DDR**

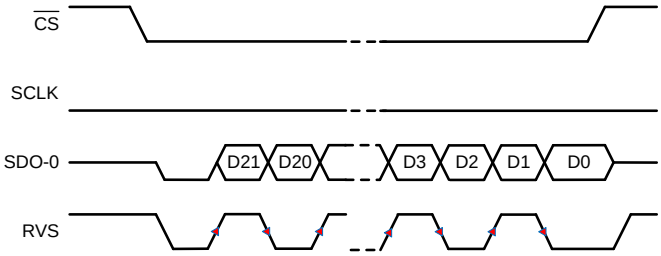



**Figure 78. SRC-INT-SD: SRC, INTCLK, Single SDO, DDR**

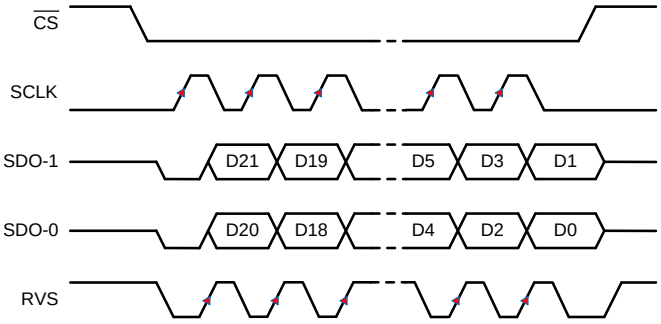



**Figure 79. SRC-EXT-DS: SRC, SCLK, Dual SDO, SDR**

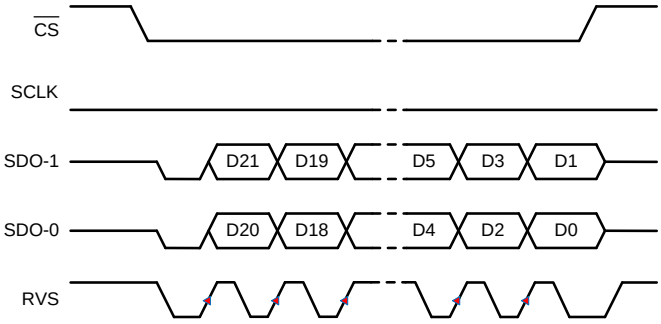



**Figure 80. SRC-INT-DS: SRC, INTCLK, Dual SDO, SDR**

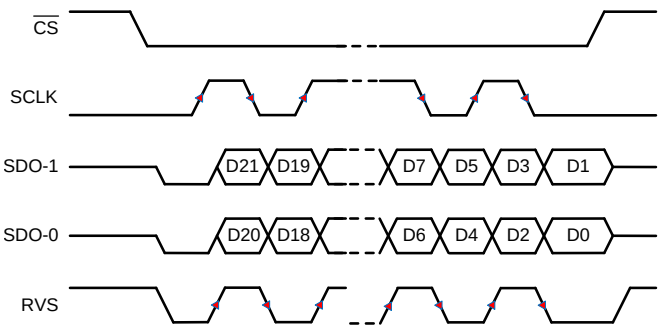



**Figure 81. SRC-EXT-DD: SRC, SCLK, Dual SDO, DDR**

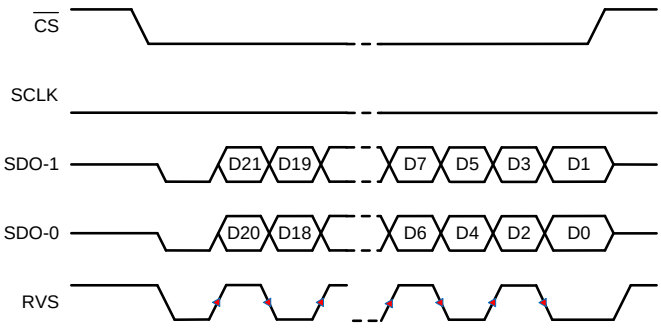



**Figure 82. SRC-INT-DD: SRC, INTCLK, Dual SDO, DDR**

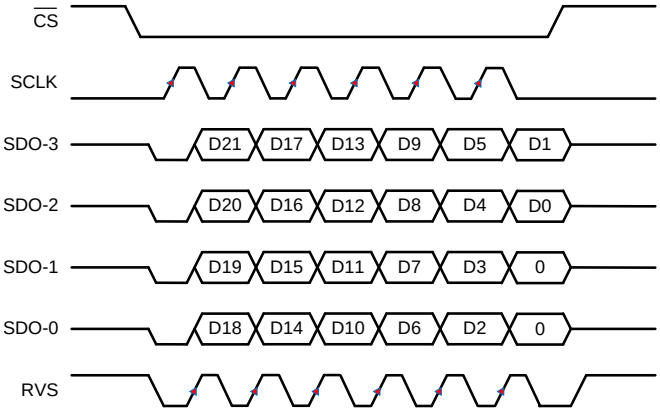



**Figure 83. SRC-EXT-QS: SRC, SCLK, Quad SDO, SDR**

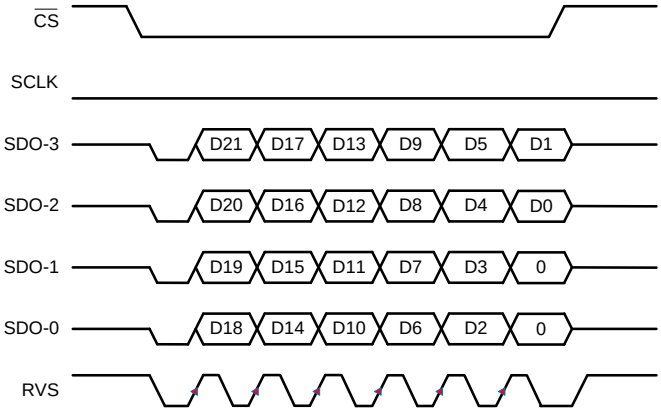



**Figure 84. SRC-INT-QS: SRC, INTCLK, Quad SDO, SDR**

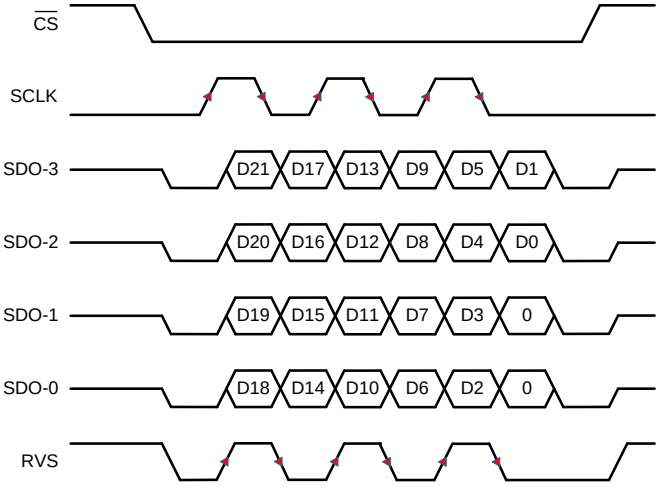



**Figure 85. SRC-EXT-QD: SRC, SCLK, Quad SDO, DDR**

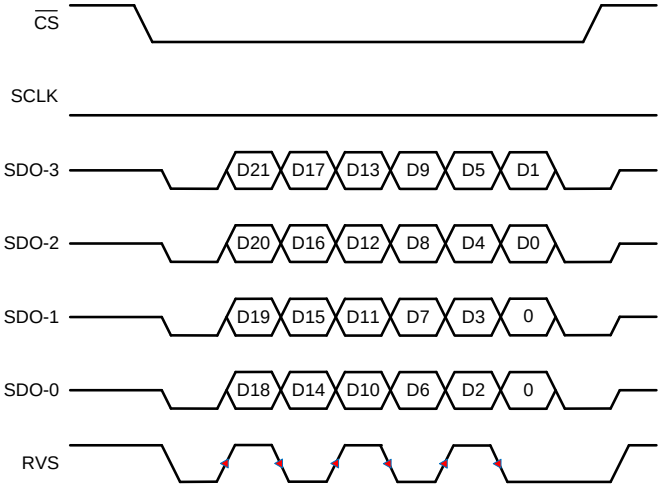



**Figure 86. SRC-INT-QD: SRC, INTCLK, Quad SDO, DDR**

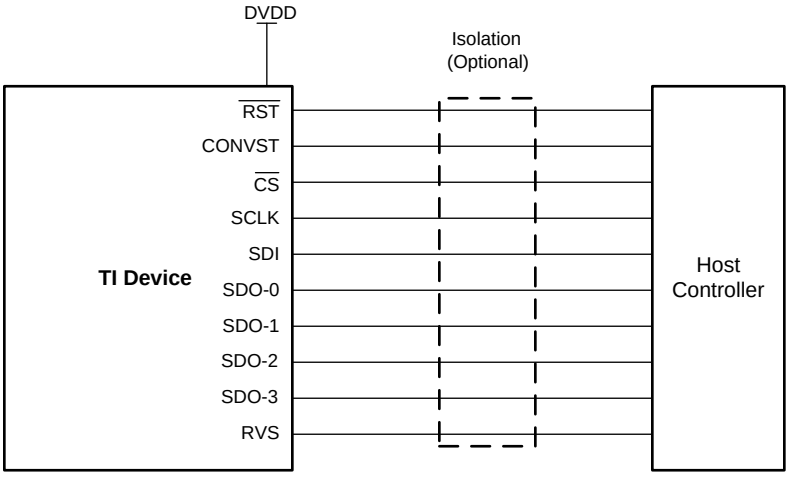

Copyright © 2016–2017, Texas Instruments Incorporated

### 7.5.5 Device Setup

The multiSPI digital interface and the device configuration registers offer multiple operation modes. This section describes how to select the hardware connection topology to meet different system requirements.

#### *7.5.5.1 Single Device: All multiSPI Options*

Figure 87 shows the connections between a host controller and a single device in order to exercise all options provided by the multiSPI digital interface.

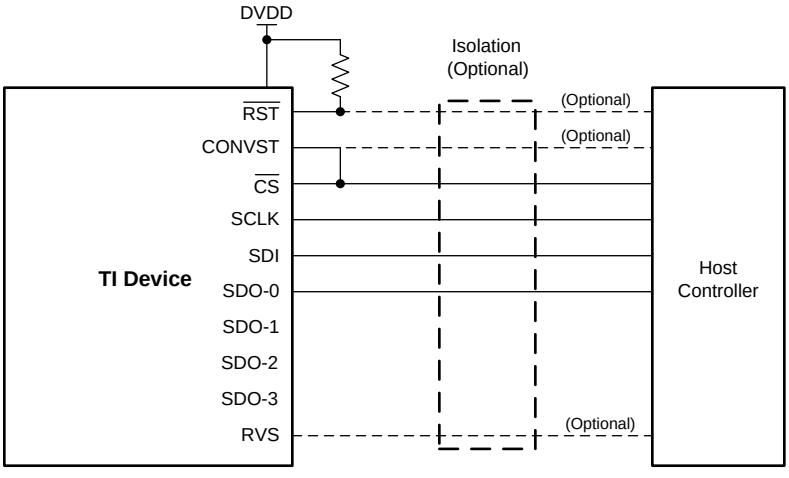



Copyright © 2016, Texas Instruments Incorporated

**Figure 87. MultiSPI Digital Interface, All Pins**

#### *7.5.5.2 Single Device: Minimum Pins for a Standard SPI Interface*

Figure 88 shows the minimum-pin interface for applications using a standard SPI protocol.




Copyright © 2016, Texas Instruments Incorporated

**Figure 88. SPI Interface, Minimum Pins**

The $\overline{CS}$, SCLK, SDI, and SDO-0 pins constitute a standard SPI port of the host controller. The CONVST pin is tied to $\overline{CS}$, and the $\overline{RST}$ pin is tied to DVDD. The SDO-1, SDO-2, and SDO-3 pins have no external connections. The following features are also available:

- Control the CONVST pin independently to get additional timing flexibility.
- Control $\overline{RST}$ pin independently to add asynchronous reset functionality.
- Monitor the RVS pin for additional timing benefits.

### 7.5.5.3 Multiple Devices: Daisy-Chain Topology

A typical connection diagram showing multiple devices in a daisy-chain topology is shown in Figure 89.

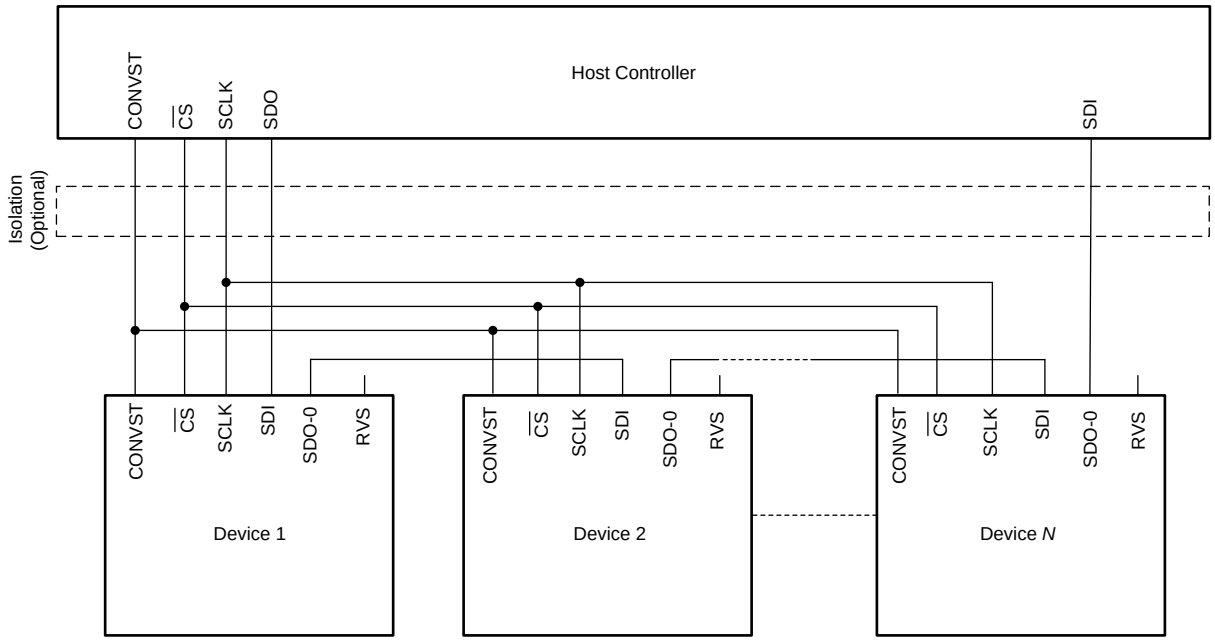



**Figure 89. Daisy-Chain Connections**

The CONVST, $\overline{CS}$, and SCLK inputs of all devices are connected together and controlled by a single CONVST, $\overline{CS}$, and SCLK pin of the host controller, respectively. The SDI input pin of the first device in the chain (Device 1) is connected to the SDO pin of the host controller, the SDO-0 output pin of Device 1 is connected to the SDI input pin of Device 2, and so on. The SDO-0 output pin of the last device in the chain (Device *N*) is connected to the SDI pin of the host controller.

To operate multiple devices in a daisy-chain topology, the host controller sets the configuration registers in each device with identical values and operates with any of the legacy, SPI-compatible protocols for data-read and data-write operations (SDO_CNT[7:0] = 00h or 01h). With these configurations settings, the 22-bit ODR and 22-bit IDR registers in each device collapse to form a single, 22-bit unified shift register (USR) per device, as shown in Figure 90.

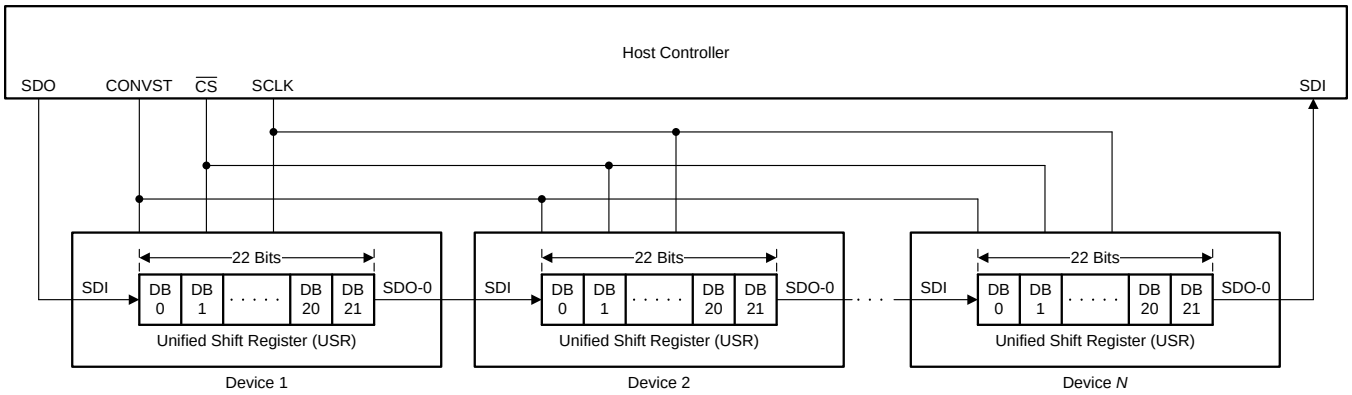



**Figure 90. Unified Shift Register**


Copyright © 2016–2017, Texas Instruments Incorporated

All devices in the daisy-chain topology sample the respective device analog input signals on the CONVST rising edge. The data transfer frame starts with a $\overline{CS}$ falling edge. On each SCLK launch edge, every device in the chain shifts out the MSB of the respective USR on to the respective SDO-0 pin. On every SCLK capture edge, each device in the chain shifts in data received on the respective SDI pin as the LSB bit of the respective USR. Therefore, in a daisy-chain configuration, the host controller receives the data of Device *N*, followed by the data of Device *N* – 1, and so on (MSB-first). On the $\overline{CS}$ rising edge, each device decodes the contents in the respective USR, and takes appropriate action.

A typical timing diagram for three devices connected in daisy-chain topology using the SPI-00-S protocol is shown in Figure 91.

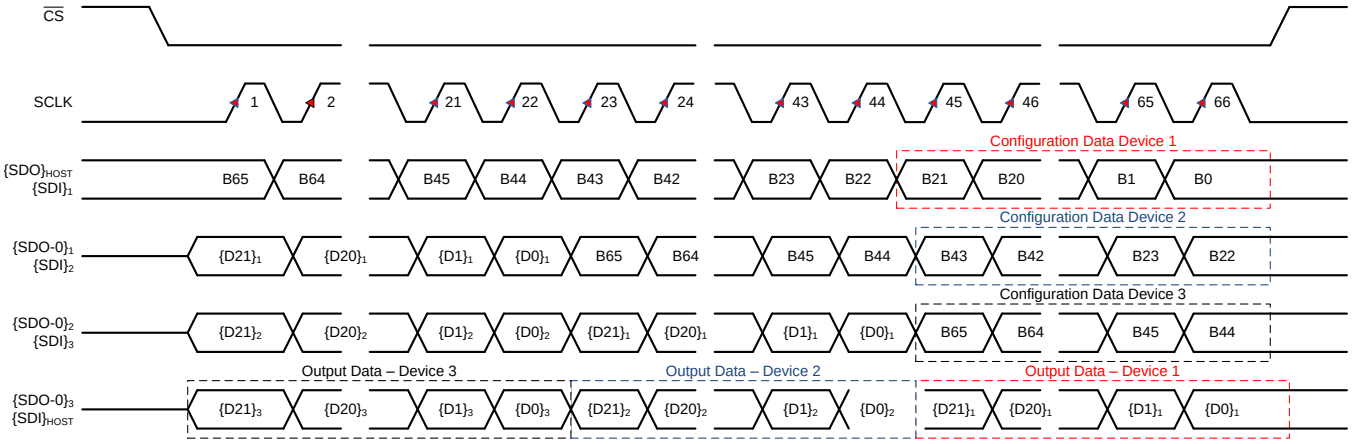



**Figure 91. Three-Device, Daisy-Chain Timing**

In daisy-chain topology, the overall throughput of the system is proportionally reduced as more devices are connected in the daisy-chain.

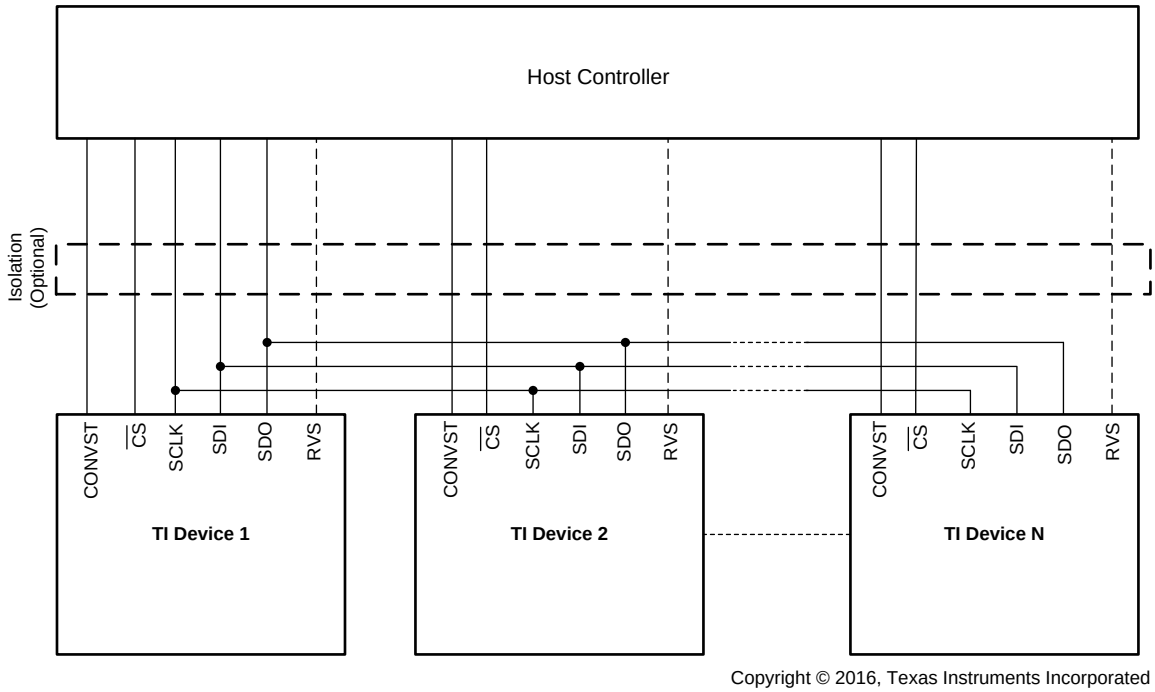
**NOTE**

For *N* devices connected in daisy-chain topology, an optimal data transfer frame must contain 22 × *N* SCLK capture edges. For a longer data transfer frame (number of SCLK in the frame > 22 × *N*), the host controller must appropriately align the configuration data for each device before bringing $\overline{CS}$ high. A shorter data transfer frame (number of SCLK in the frame < 22 × *N*) might result in an erroneous device configuration, and *must be avoided*.

Copyright © 2016–2017, Texas Instruments Incorporated

### 7.5.5.4 Multiple Devices: Star Topology

A typical connection diagram showing multiple devices in a star topology is shown in Figure 92. The CONVST, SDI, and SCLK inputs of all devices are connected together, and are controlled by a single CONVST, SDO, and SCLK pin of the host controller, respectively. Similarly, the SDO output pin of all devices are tied together and connected to the a single SDI input pin of the host controller. The $\overline{CS}$ input pin of each device is individually controlled by separate $\overline{CS}$ control lines from the host controller.




Copyright © 2016, Texas Instruments Incorporated

**Figure 92. Star-Topology Connection**

The timing diagram for three devices connected in the star topology is shown in Figure 93. In order to avoid any conflict related to multiple devices driving the SDO line at the same time, make sure that the host controller pulls down the $\overline{CS}$ signal for *only one device at any particular time*.

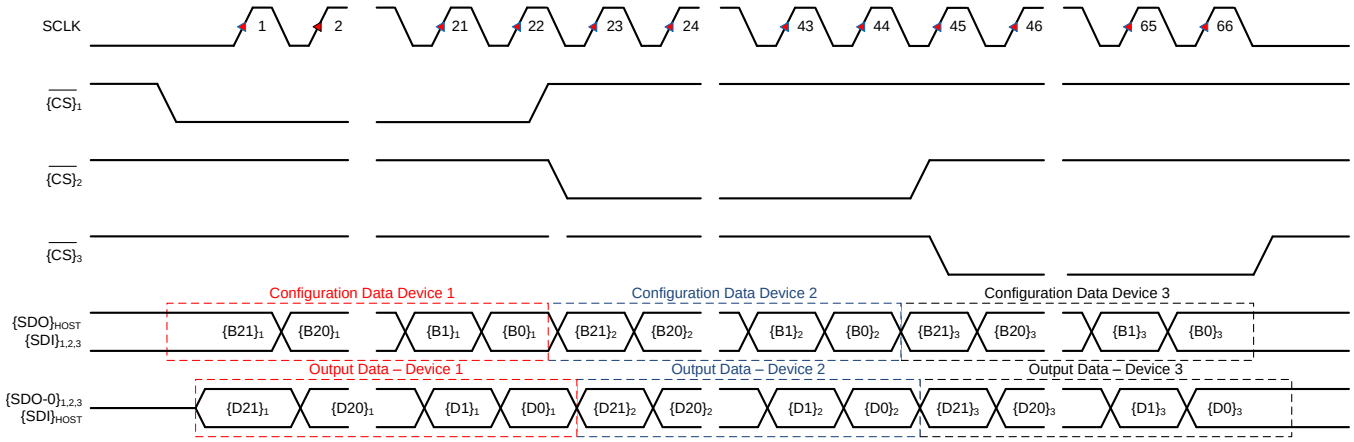



**Figure 93. Three-Device, Star Connection Timing**


Copyright © 2016–2017, Texas Instruments Incorporated

## 7.6 Register Maps

### 7.6.1 Device Configuration and Register Maps

The device features nine configuration registers, mapped as described in Table 10.

**Table 10. Configuration Registers Mapping**

| ADDRESS | REGISTER NAME | REGISTER DESCRIPTION |
|---|---|---|
| 004h | PD_CNTL | Low-power modes control |
| 008h | SDI_CNTL | SDI input protocol selection |
| 00Ch | SDO_CNTL | SDO output protocol selection |
| 010h | DATA_CNTL | Output data word configuration |
| 014h | PATN_LSB | Eight least significant bits (LSB) of the output pattern |
| 015h | PATN_MID | Eight middle bits of the output pattern |
| 016h | PATN_MSB | Four most significant bits (MSB) of the output pattern |
| 020h | OFST_CAL | Offset calibration |
| 030h | REF_MRG | Reference margin |

#### *7.6.1.1 PD_CNTL Register (address = 04h) [reset = 00h]*

This register controls the low-power modes offered by the device.

**Figure 94. PD_CNTL Register**

| 7 | 6 | 5 | 4 | 3 | 2 | 1 | 0 |
|---|---|---|---|---|---|---|---|
| 0 | 0 | 0 | 0 | 0 | PD_REFBUF | PD_ADC | 0 |
| R-0b | R-0b | R-0b | R-0b | R-0b | R/W-0b | R/W-0b | R-0b |

LEGEND: R/W = Read/Write; R = Read only; -n = value after reset

**Table 11. PD_CNTL Register Field Descriptions**

| Bit | Field | Type | Reset | Description |
|---|---|---|---|---|
| 7-3 | 0 | R | 00000b | Reserved bits. Reads return 00000b. |
| 2 | PD_REFBUF | R/W | 0b | This bit powers down the internal reference buffer.<br>0b = Internal reference buffer is powered up<br>1b = Internal reference buffer is powered down |
| 1 | PD_ADC | R/W | 0b | This bit powers down the converter module.<br>0b = converter module is powered up<br>1b = converter module is powered down |
| 0 | 0 | R | 0b | Reserved bits. Do not write. Reads return 0b. |

To power-down the converter module, set the PD_ADC bit in the PD_CNTL register. The converter module powers down on the rising edge of $\overline{CS}$. To power-up the converter module, reset the PD_ADC bit in the PD_CNTL register. The converter module starts to power-up on the rising edge of $\overline{CS}$. Wait for $t_{PU_ADC}$ before initiating any conversion or data transfer operation.

To power-down the internal reference buffer, set the PD_REFBUF bit in the PD_CNTL register. The internal reference buffer powers down on the rising edge of $\overline{CS}$. To power-up the internal reference buffer, reset the PD_REFBUF bit in the PD_CNTL register. The internal reference buffer starts to power-up on the rising edge of $\overline{CS}$. Wait for $t_{PU_REFBUF}$ before initiating any conversion.

Copyright © 2016–2017, Texas Instruments Incorporated

### 7.6.1.2 SDI_CNTL Register (address = 008h) [reset = 00h]

This register selects the SPI protocol for writing data to the device.

**Figure 95. SDI_CNTL Register**

| 7 | 6 | 5 | 4 | 3 | 2 | 1 | 0 |
|---|---|---|---|---|---|---|---|
| 0 | 0 | 0 | 0 | 0 | 0 | SDI_MODE[1:0] | |
| R-0b | R-0b | R-0b | R-0b | R-0b | R-0b | R/W-00b | |

LEGEND: R/W = Read/Write; R = Read only; -n = value after reset

**Table 12. SDI_CNTL Register Field Descriptions**

| Bit | Field | Type | Reset | Description |
|---|---|---|---|---|
| 7-2 | 0 | R | 000000b | Reserved bits. Do not write. Reads return 000000b. |
| 1-0 | SDI_MODE[1:0] | R/W | 00b | These bits select the protocol for writing data into the device.<br>00b = Standard SPI with CPOL = 0 and CPHASE = 0<br>01b = Standard SPI with CPOL = 0 and CPHASE = 1<br>10b = Standard SPI with CPOL = 1 and CPHASE = 0<br>11b = Standard SPI with CPOL = 1 and CPHASE = 1 |

### 7.6.1.3 SDO_CNTL Register (address = 0Ch) [reset = 00h]

This register configures the protocol for reading data from the device.

**Figure 96. SDO_CNTL Register**

| 7 | 6 | 5 | 4 | 3 | 2 | 1 | 0 |
|---|---|---|---|---|---|---|---|
| SSYNC_CLK_SEL[1:0] | | 0 | DATA_RATE | SDO_WIDTH[1:0] | | SDO_MODE[1:0] | |
| R/W-00b | | R-0b | R/W-0b | R/W-00b | | R/W-00b | |

LEGEND: R/W = Read/Write; R = Read only; -n = value after reset

**Table 13. SDO_CNTL Register Field Descriptions**

| Bit | Field | Type | Reset | Description |
|---|---|---|---|---|
| 7-6 | SSYNC_CLK_SEL[1:0] | R/W | 00b | These bits select the source and frequency of the clock for the ADC-Clock-Master mode, and are valid only if SDO_MODE[1:0] = 11b.<br>00b = External SCLK echo<br>01b = Internal clock (INTCLK)<br>10b = Internal clock / 2 (INTCLK / 2)<br>11b = Internal clock / 4 (INTCLK / 4) |
| 5 | 0 | R | 0b | Reserved bit. Do not write. Reads return 0b. |
| 4 | DATA_RATE | R/W | 0b | This bit is ignored if SDO_MODE[1:0] = 00b. When SDO_MODE[1:0] = 11b:<br>0b = SDOs are updated at single data rate (SDR) with respect to the output clock<br>1b = SDOs are updated at double data rate (DDR) with respect to the output clock |
| 3-2 | SDO_WIDTH[1:0] | R/W | 00b | These bits set the width of the output bus.<br>0xb = Data are output only on SDO-0<br>10b = Data are output only on SDO-0 and SDO-1<br>11b = Data are output on SDO-0, SDO-1, SDO-2, and SDO-3 |
| 1-0 | SDO_MODE[1:0] | R/W | 00b | These bits select the protocol for reading data from the device.<br>00b = SDO follows the SPI protocol selected in the SDI_CNTL register<br>01b = SDO follows the SPI protocol selected in the SDI_CNTL register but with *Early Data Launch* feature enabled. See Table 6.<br>10b = Invalid configuration, not supported by the device<br>11b = SDO follows the source-synchronous protocol |


Copyright © 2016–2017, Texas Instruments Incorporated

#### 7.6.1.4 DATA_CNTL Register (address = 010h) [reset = 00h]

This register configures the contents of the 22-bit output data word (D[21:0]).

**Figure 97. DATA_CNTL Register**

| 7 | 6 | 5 | 4 | 3 | 2 | 1 | 0 |
|---|---|---|---|---|---|---|---|
| 0 | 0 | 0 | 0 | FPAR_LOC[1:0] | | PAR_EN | DATA_VAL |
| R-0b | R-0b | R-0b | R-0b | R/W-00b | | R/W-0b | R/W-0b |

LEGEND: R/W = Read/Write; R = Read only; -n = value after reset

**Table 14. DATA_CNTL Register Field Descriptions**

| Bit | Field | Type | Reset | Description |
|---|---|---|---|---|
| 7-4 | 0 | R | 0000b | Reserved bits. Reads return 0000b. |
| 3-2 | FPAR_LOC[1:0] | R/W | 00b | These bits control the data span for calculating the FTPAR bit (bit D[4] in the output data word).<br>00b = D[4] reflects even parity calculated for 4 MSB<br>01b = D[4] reflects even parity calculated for 8 MSB<br>10b = D[4] reflects even parity calculated for 12 MSB<br>11b = D[4] reflects even parity calculated for all 16 bits (that is, the same as FLPAR) |
| 1 | PAR_EN | R/W | 0b | 0b = Output data does not contain any parity information<br>D[5] = 0<br>D[4] = 0<br>1b = Parity information is appended to the LSB of the output data<br>D[5] = Even parity calculated on bits D[21:6]<br>D[4] = Even parity computed on selected number of MSB of D[21:6] as per FPAR_LOC[1:0] setting<br>See Figure 44 for further details of parity computation. |
| 0 | DATA_VAL | R/W | 0b | These bits control bits D[21:6] of the output data word.<br>0b = 16-bit conversion output<br>1b = 16-bit contents of the fixed-pattern registers<br>See PATN CNTL for more details. |

Copyright © 2016–2017, Texas Instruments Incorporated

### 7.6.1.5 PATN_LSB Register (address = 014h) [reset = 00h]

This register controls the eight LSB of the output pattern when DATA_VAL = 1b; see Figure 101.

**Figure 98. PATN_LSB Register**

| 7 | 6 | 5 | 4 | 3 | 2 | 1 | 0 |
|---|---|---|---|---|---|---|---|
| PATN_LSB_BITS | | | | | | | |
| R/W-00000000b | | | | | | | |

LEGEND: R/W = Read/Write; R = Read only; -n = value after reset

**Table 15. PATN_LSB Register Field Descriptions**

| Bit | Field | Type | Reset | Description |
|---|---|---|---|---|
| 7-0 | PATN_LSB_BITS | R/W | 00000000b | 8 LSB of the output pattern |

### 7.6.1.6 PATN_MID Register (address = 015h) [reset = 00h]

This register controls the middle eight bits of the output pattern when DATA_VAL = 1b; see Figure 101.

**Figure 99. PATN_MID Register**

| 7 | 6 | 5 | 4 | 3 | 2 | 1 | 0 |
|---|---|---|---|---|---|---|---|
| PATN_MID_BITS | | | | | | | |
| R/W-00000000b | | | | | | | |

LEGEND: R/W = Read/Write; R = Read only; -n = value after reset

**Table 16. PATN_MID Register Field Descriptions**

| Bit | Field | Type | Reset | Description |
|---|---|---|---|---|
| 7-0 | PATN_MID_BITS | R/W | 00000000b | 8 middle bits of the output pattern |

### 7.6.1.7 PATN_MSB Register (address = 016h) [reset = 00h]

This register controls the four MSB of the output pattern when DATA_VAL = 1b; see Figure 101.

**Figure 100. PATN_MSB Register**

| 7 | 6 | 5 | 4 | 3 | 2 | 1 | 0 |
|---|---|---|---|---|---|---|---|
| 0 | 0 | 0 | 0 | PATN_MSB_BITS | | | |
| R-0b | R-0b | R-0b | R-0b | R/W-0000b | | | |

LEGEND: R/W = Read/Write; R = Read only; -n = value after reset

**Table 17. PATN_MSB Register Field Descriptions**

| Bit | Field | Type | Reset | Description |
|---|---|---|---|---|
| 7-4 | 0 | R | 0000b | Reserved bits. Reads return 0000b. |
| 3-0 | PATN_MSB_BITS | R/W | 0000b | 4 MSB of the output pattern |

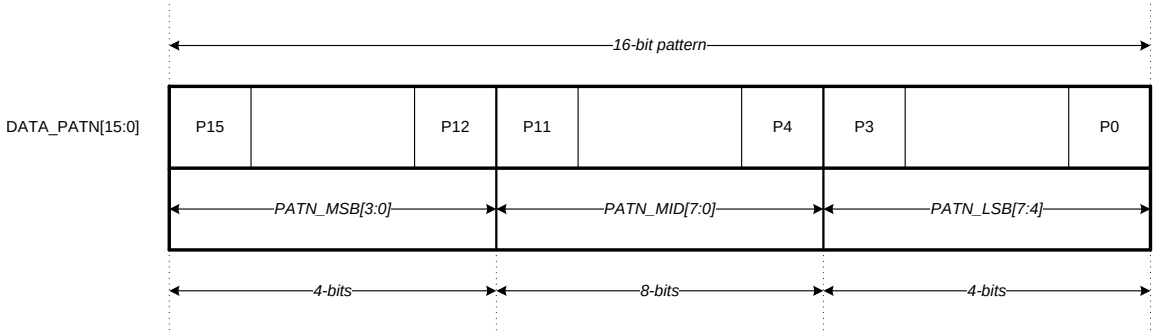



**Figure 101. DATA_PATN[15:0]**


Copyright © 2016–2017, Texas Instruments Incorporated

#### 7.6.1.8 OFST_CAL Register (address = 020h) [reset = 00h]

This register selects the external reference range for optimal offset calibration.

**Figure 102. OFST_CAL Register**

| 7 | 6 | 5 | 4 | 3 | 2 | 1 | 0 |
|---|---|---|---|---|---|---|---|
| 0 | 0 | 0 | 0 | 0 | REF_SEL[2:0] | | |
| R-0b | R-0b | R-0b | R-0b | R-0b | R/W-000b | | |

LEGEND: R/W = Read/Write; R = Read only; -n = value after reset

**Table 18. OFST_CAL Register Field Descriptions**

| Bit | Field | Type | Reset | Description |
|---|---|---|---|---|
| 7-3 | 0 | R | 00000b | Reserved bits. Reads return 00000b. |
| 2-0 | REF_SEL[2:0] | R/W | 000b | These bits select the external reference range for optimal offset.<br>000b = Optimum offset calibration for $V_{REF}$ = 5.0 V<br>001b = Optimum offset calibration for $V_{REF}$ = 4.5 V<br>010b = Optimum offset calibration for $V_{REF}$ = 4.096 V<br>011b = Optimum offset calibration for $V_{REF}$ = 3.3 V<br>100b = Optimum offset calibration for $V_{REF}$ = 3.0 V<br>101b = Optimum offset calibration for $V_{REF}$ = 2.5 V<br>110b = Optimum offset calibration for $V_{REF}$ = 5.0 V<br>111b = Optimum offset calibration for $V_{REF}$ = 5.0 V |

Copyright © 2016–2017, Texas Instruments Incorporated

### 7.6.1.9 REF_MRG Register (address = 030h) [reset = 00h]

This register selects the margining to be added to or subtracted from the reference buffer output; see the *Reference Buffer Module* section.

**Figure 103. REF_MRG Register**

| 7 | 6 | 5 | 4 | 3 | 2 | 1 | 0 |
|---|---|---|---|---|---|---|---|
| 0 | 0 | EN_MARG | REF_OFST[4:0] | | | | |
| R-0b | R-0b | R/W-0b | R/W-00000b | | | | |

LEGEND: R/W = Read/Write; R = Read only; -n = value after reset

**Table 19. REF_MRG Register Field Descriptions**

| Bit | Field | Type | Reset | Description |
|---|---|---|---|---|
| 7-6 | 0 | R | 00b | Reserved bits. Reads return 00b. |
| 5 | EN_MARG | R/W | 0b | This bit enables margining feature.<br>0b = Margining is disabled<br>1b = Margining is enabled |
| 4-0 | REF_OFST[4:0] | R/W | 00000b | These bits select the reference offset value as per Table 20. |

**Table 20. REF_OFST[4:0] settings**

| REF_OFST[4:0] | $\Delta V_{REFBUFOUT}$ (typical (1)) |
|---|---|
| 00000b | 0 mV |
| 00001b | 280 µV |
| 00010b | 580 µV |
| 00011b | 840 µV |
| 00100b | 1.12 mV |
| 00101b | 1.4 mV |
| 00110b | 1.68 mV |
| 00111b | 1.96 mV |
| 01000b | 2.24 mV |
| 01001b | 2.52 mV |
| 01010b | 2.8 mV |
| 01011b | 3.08 mV |
| 01100b | 3.36 mV |
| 01101b | 3.64 mV |
| 01110b | 3.92 mV |
| 01111b | 4.2 mV |
| 10000b | –4.5 mV |
| 10001b | –4.22 mV |
| 10010b | –3.94 mV |
| 10011b | –3.66 mV |
| 10100b | –3.38 mV |
| 10101b | –3.1 mV |
| 10110b | –2.82 mV |
| 10111b | –2.54 mV |
| 11000b | –2.26 mV |
| 11001b | –1.98 mV |
| 11010b | –1.7 mV |
| 11011b | –1.42 mV |
| 11100b | –1.14 mV |
| 11101b | –860 µV |
| 11110b | –580 µV |
| 11111b | –280 µV |

(1) The actual $V_{REFBUFOUT}$ value may vary by ±10% from Table 20


Copyright © 2016–2017, Texas Instruments Incorporated

# 8 Application and Implementation

**NOTE**

Information in the following applications sections is not part of the TI component specification, and TI does not warrant its accuracy or completeness. TI's customers are responsible for determining suitability of components for their purposes. Customers should validate and test their design implementation to confirm system functionality.

## 8.1 Application Information

The two primary circuits required to maximize the performance of a high-precision, successive approximation register (SAR), analog-to-digital converter (ADC) are the input driver and the reference driver circuits. This section presents general principles for designing these circuits, followed by an application circuit designed using the ADS892xB.

### 8.1.1 ADC Reference Driver

The external reference source must provide low-drift and very accurate voltage at the REFIN pin of the ADS892xB. The output broadband noise of most references can be in the order of a few hundred $\mu V_{RMS}$. Therefore, to prevent any degradation in the noise performance of the ADC, appropriately filter the output of the voltage reference by using a low-pass filter with a cutoff frequency of a few hundred hertz.

The internal reference buffer of the ADS892xB provides the dynamic load posed on the REFBUFOUT pin during the conversion process. Decouple the REFBUFOUT pin with the REFM pin using the recommended $C_{REFBUF}$ and $R_{ESR}$. See the Layout section for layout recommendations.

### 8.1.2 ADC Input Driver

The input driver circuit for a high-precision ADC mainly consists of two parts: a driving amplifier and a charge kickback filter. The amplifier is used for signal conditioning of the input signal and the low output impedance of the amplifier provides a buffer between the signal source and the switched capacitor inputs of the ADC. The charge kickback filter helps attenuate the sampling charge injection from the switched-capacitor input stage of the ADC, and band-limits the wideband noise contributed by the front-end circuit. Careful design of the front-end circuit is critical to meet the linearity and noise performance of the ADS892xB.

#### *8.1.2.1 Charge-Kickback Filter*

The charge-kickback filter is an RC filter at the input pins of the ADC that filters the broadband noise from the front-end drive circuitry, and attenuates the sampling charge injection from the switched-capacitor input stage of the ADC. A filter capacitor, $C_{FLT}$, is connected from each input pin of the ADC to the ground (as shown in Figure 104). This capacitor helps reduce the sampling charge injection and provides a charge bucket to quickly charge the internal sample-and-hold capacitors during the acquisition process. Generally, the value of this capacitor must be at least 20 times the specified value of the ADC sampling capacitance. For the ADS892xB, the input sampling capacitance is equal to 60 pF; therefore, for optimal performance, keep $C_{FLT}$ greater than 1.2 nF. This capacitor must be a COG- or NPO-type. The type of dielectric used in COG or NPO ceramic capacitors provides the most stable electrical properties over voltage, frequency, and temperature changes.

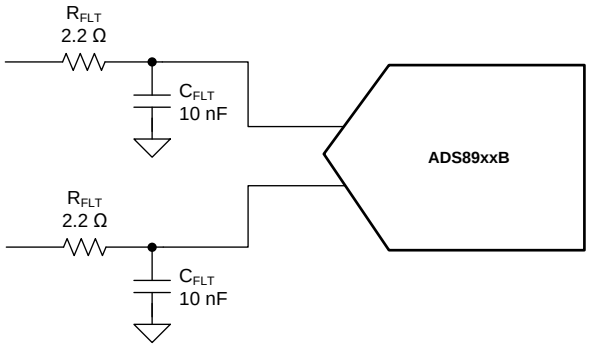



**Figure 104. Charge Kickback Filter Configuration**

## Application Information (continued)

Driving capacitive loads can degrade the phase margin of the input amplifier, thus making the amplifier marginally unstable. To avoid amplifier stability issues, series isolation resistors ($R_{FLT}$) are used at the output of the amplifiers. A higher value of $R_{FLT}$ helps with amplifier stability, but adds distortion as a result of interactions with the nonlinear input impedance of the ADC. Distortion increases with source impedance, input signal frequency, and input signal amplitude. Therefore, the selection of $R_{FLT}$ requires balancing the stability of the driver amplifier and distortion performance of the design. Always verify the stability and settling behavior of the driving amplifier and charge-kickback filter by TINA-TI™ SPICE simulation. Keep the tolerance of the selected resistors less than 1% to keep the inputs balanced.

### *8.1.2.2 Input Amplifier Selection*

Selection criteria for the input amplifiers is highly dependent on the input signal type, as well as the performance goals, of the data acquisition system. Some key amplifier specifications to consider when selecting an appropriate amplifier to drive the inputs of the ADC are:

- *Small-signal bandwidth.* Select the small-signal bandwidth of the input amplifiers to be as high as possible after meeting the power budget of the system. Higher bandwidth reduces the closed-loop output impedance of the amplifier, thus allowing the amplifier to more easily drive the ADC sample-and-hold capacitor and the RC filter (Charge-Kickback Filter) at the inputs of the ADC. Higher bandwidth amplifiers offer faster settling times while driving the capacitive load of the charge-kickback filter, thus reducing harmonic distortion at higher input frequencies. In order to maintain the overall stability of the input driver circuit, select the amplifier with a unity gain bandwidth (UGB) as described in Equation 16:

$$UGB \geq 4 \times \left( \frac{1}{2\pi \times R_{FLT} \times C_{FLT}} \right) \tag{16}$$

- *Distortion.* Both the ADC and the input driver introduce distortion in a data acquisition block. To make sure that the distortion performance of the data acquisition system is not limited by the front-end circuit, the distortion of the input driver must be at least 10 dB less than the distortion of the ADC, as shown in Equation 17.

$$THD_{AMP} \leq THD_{ADC} - 10\,(dB) \tag{17}$$

- *Noise.* Noise contribution of the front-end amplifiers must be as low as possible to prevent any degradation in SNR performance of the system. Generally, to make sure that the noise performance of the data acquisition system is not limited by the front-end circuit, the total noise contribution from the front-end circuit must be kept below 20% of the input-referred noise of the ADC. Noise from the input driver circuit is band-limited by designing a low cutoff frequency, charge-kickback filter, as explained in Equation 18.

$$N_G \times \sqrt{2} \times \sqrt{\left( \frac{V_{1/f_AMP_PP}}{6.6} \right)^2 + e_{n_RMS}^2 \times \frac{\pi}{2} \times f_{-3dB}} \leq \frac{1}{5} \times \frac{V_{REF}}{\sqrt{2}} \times 10^{-\left(\frac{SNR(dB)}{20}\right)} \tag{18}$$

where:

- $V_{1\,/\,f_AMP_PP}$ is the peak-to-peak flicker noise in µV
- $e_{n_RMS}$ is the amplifier broadband noise density in nV/√Hz
- $f_{-3dB}$ is the 3-dB bandwidth of the charge-kickback filter
- $N_G$ is the noise gain of the front-end circuit that is equal to 1 in a buffer configuration

- *Settling Time.* For dc signals with fast transients that are common in a multiplexed application, the input signal must settle within an 16-bit accuracy at the device inputs during the acquisition time window. This condition is critical to maintain the overall linearity performance of the ADC. Typically, amplifier data sheets specify the output settling performance only up to 0.1% to 0.001%, which may not be sufficient for the desired 16-bit accuracy. Therefore, always verify the settling behavior of the input driver by TINA-TI SPICE simulations before selecting the amplifier.


Copyright © 2016–2017, Texas Instruments Incorporated

## 8.2 Typical Application

### 8.2.1 Data Acquisition (DAQ) Circuit for Lowest Distortion and Noise Performance With Differential Input

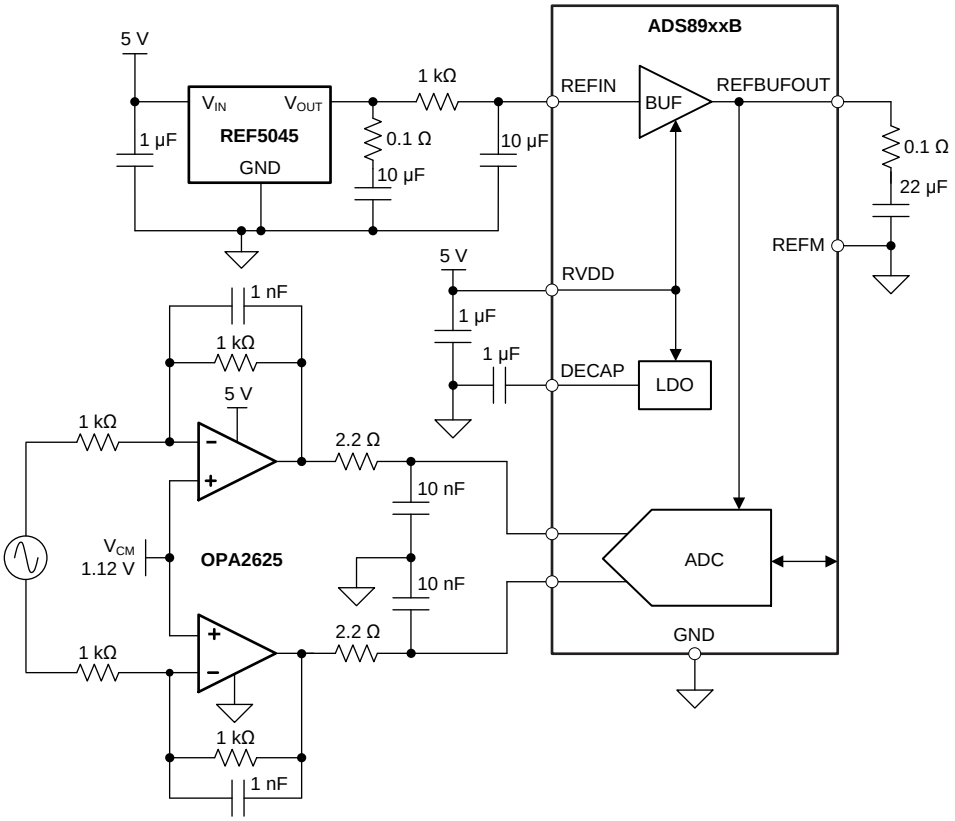



**Figure 105. Differential-Input DAQ Circuit for Lowest Distortion and Noise Using the ADS892xB**

#### 8.2.1.1 Design Requirements

For this example, the design parameters are listed in Table 21.

**Table 21. Design Parameters**

| DESIGN PARAMETER | EXAMPLE VALUE |
|---|---|
| ADC sample rate | Maximum-specified throughput |
| Input signal | 2-kHz input, 4.5-$V_{PP}$ fully differential |
| Noise performance, SNR | > 96-dB |
| Distortion, THD | < –120-dB |
| Linearity, INL | < ±0.5-LSB |
| Reference | 4.5 V |
| Power supply | < 5.5-V analog, 3.3-V I/O |

#### 8.2.1.2 Detailed Design Procedure

The application circuit is illustrated in Figure 105. For simplicity, power-supply decoupling capacitors are not shown in these circuit diagrams; see the *Power-Supply Recommendations* section for suggested guidelines.

The reference voltage of 4.5 V is generated by the high-precision, low-noise REF5045 circuit. The output broadband noise of the reference is heavily filtered by a low-pass filter with a 3-dB cutoff frequency of 16 Hz.

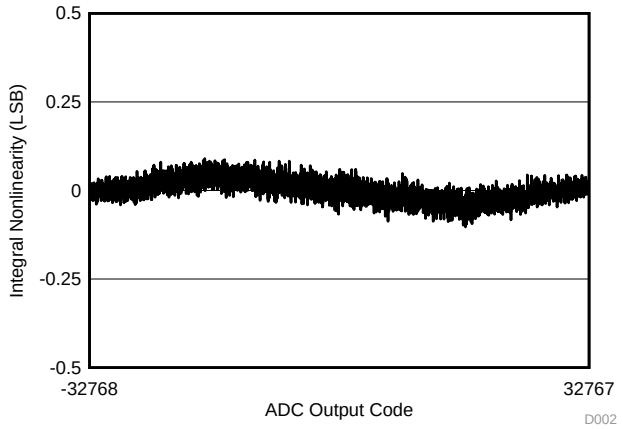
Generally, the distortion from the input driver must be at least 10 dB less than the ADC distortion. The low-power OPA2625 (a high-bandwidth, low-distortion, high-precision amplifier in an inverting gain configuration) as an input driver provides exceptional ac performance because of its extremely low-distortion and high-bandwidth specifications. The distortion resulting from variation in the common-mode signal is eliminated by using the OPA2625 in an inverting gain configuration. To exercise the complete dynamic range of the device, the common-mode voltage at the ADS892xB inputs is established at a value of 2.25 V (4.5 V / 2) by using the noninverting pins of the OPA2625 amplifiers. In addition, the components of the charge kickback filter keep the noise from the front-end circuit low without adding distortion to the input signal.

For a complete schematic, see the *ADS8920BEVM-PDK user's guide* located in the *ADS8920B SAR Analog to Digital Converter Evaluation Module* web folder at www.ti.com.

A similar circuit is used in reference design TIPD211, a step-by-step process to design a *20-Bit, 1-MSPS, 4-Ch Small Form Factor Design for Test and Measurement Applications* using four ADS8900B SAR ADCs, four OPA2625 precision amplifiers and one REF5050 precision reference.

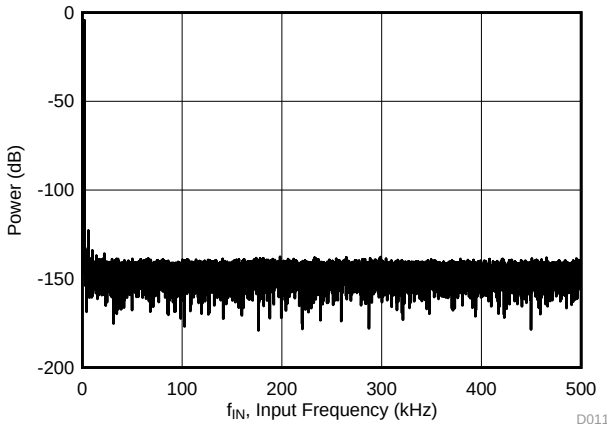
For step-by-step design procedure, circuit schematics, bill of materials, PCB files, simulation results, and test results, refer to TI Precision Design TIPD211, *18-Bit, 1-MSPS, 4-Ch Small Form Factor Design for Test and Measurement Applications* (TIDUBW7).

### 8.2.1.3 Application Curves



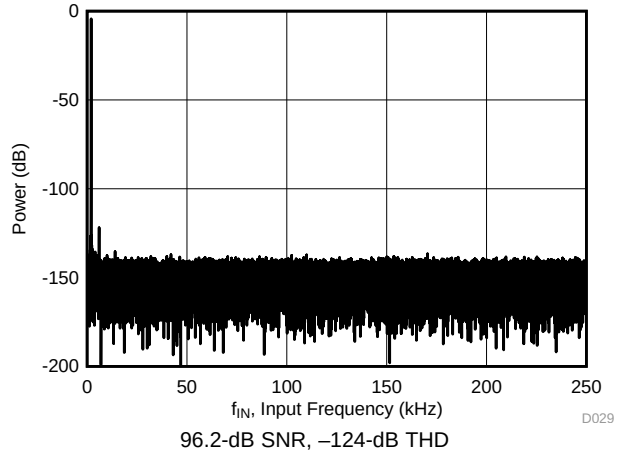

16-bit NMC DNL, ±0.2-LSB INL

**Figure 106. Typical Linearity**



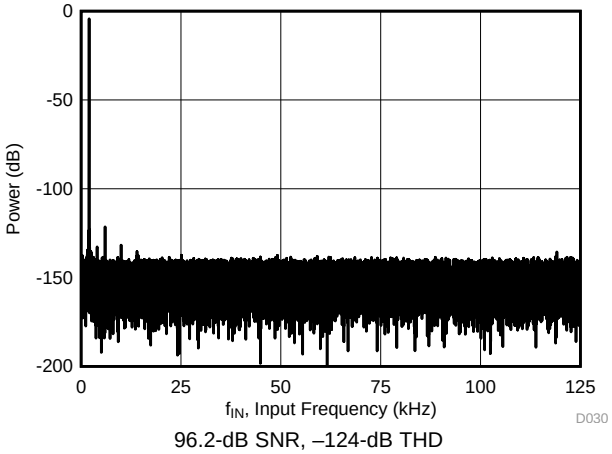

96.2-dB SNR, –124-dB THD

**Figure 107. Noise-Performance FFT Plot - ADS8920B**




96.2-dB SNR, –124-dB THD

**Figure 108. Noise-Performance FFT Plot - ADS8922B**




96.2-dB SNR, –124-dB THD

**Figure 109. Noise-Performance FFT Plot - ADS8924B**


Copyright © 2016–2017, Texas Instruments Incorporated

### 8.2.2 DAQ Circuit With FDA Input Driver and Single-Ended or Differential Input

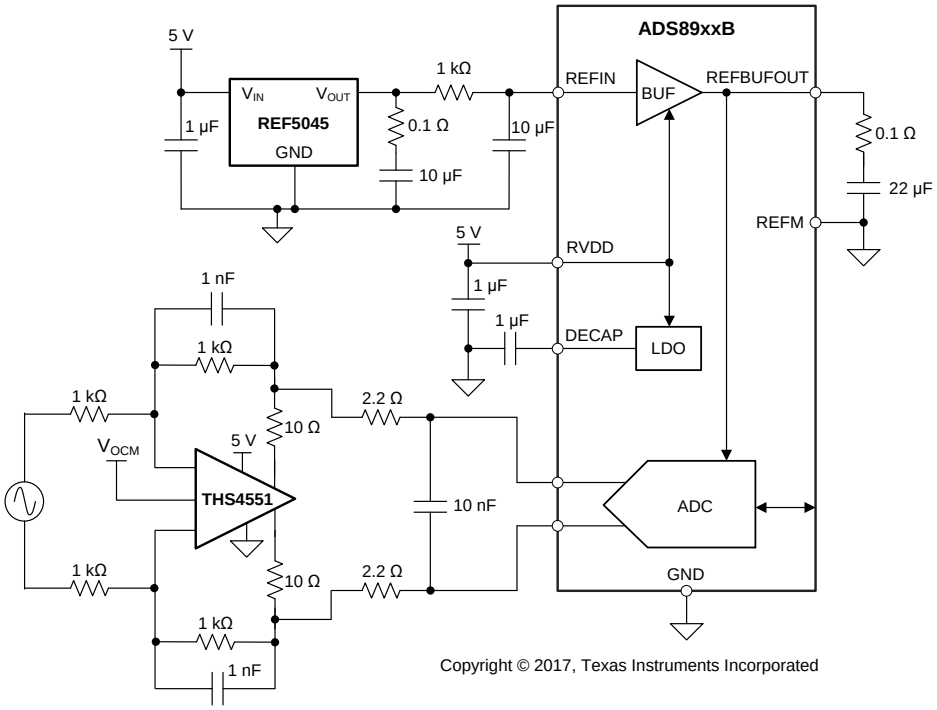



**Figure 110. DAQ Circuit With FDA Input Driver and Differential Input**

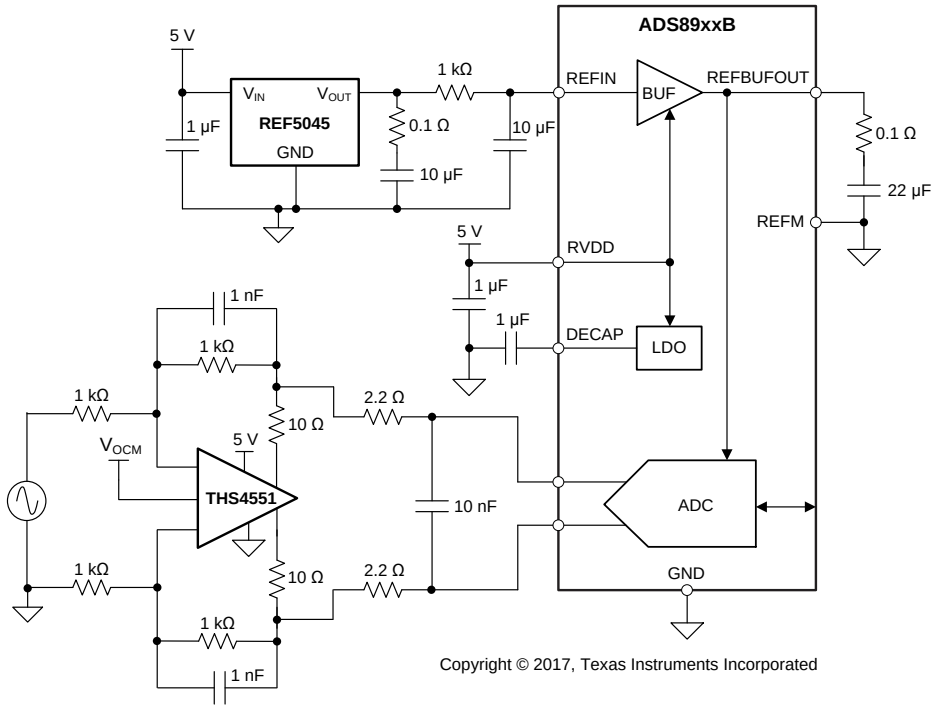



**Figure 111. DAQ Circuit With FDA Input Driver and Single-Ended Input**

### 8.2.3 Design Requirements

For this example, the design parameters are listed in Table 22.

**Table 22. Design Parameters**

| DESIGN PARAMETER | EXAMPLE VALUE |
|---|---|
| ADC sample rate | Maximum-specified throughput |
| Input signal | 2-kHz input, ±4.5-$V_{PP}$ fully differential and ±4.5-$V_{PP}$ single-ended bipolar signal |
| Noise performance, SNR | > 96-dB |
| Distortion, THD | < –120-dB |
| Linearity, INL | < ±0.5-LSB |
| Reference | 4.5 V |
| Power supply | < 5.4-V analog, 3.3-V I/O |

### 8.2.4 Detailed Design Procedure

The application circuits are shown in Figure 110 and Figure 111. In both applications, the input signal is processed through a high-bandwidth, low-distortion, fully-differential amplifier (FDA) designed in a gain of 1 V/V and a low-pass RC filter before going to the ADC.

The reference voltage of 4.5 V generated by the high-precision, low-noise REF5045 circuit. The output broadband noise of the reference is heavily filtered by a low-pass filter with a 3-dB cutoff frequency of 16 Hz.

Generally, the distortion from the input driver must be at least 10 dB less than the ADC distortion. The distortion resulting from variation in the common-mode signal is eliminated by using the FDA in an inverting gain configuration that establishes a fixed common-mode level for the circuit. This configuration also eliminates the requirement of a rail-to-rail swing at the amplifier input. Therefore, these circuits use the low-power THS4551 as an input driver that provides exceptional ac performance because of its extremely low-distortion and high bandwidth specifications. In addition, the components of the charge kickback filter keep the noise from the front-end circuit low without adding distortion to the input signal.

The circuit in Figure 110 shows a fully-differential data acquisition (DAQ) block optimized for low distortion and noise using the THS4551 and ADS892xB. This front-end circuit configuration requires a differential signal at the input of the FDA and provides a differential output to drive the ADC inputs. The common-mode voltage of the input signal provided to the ADC is set by the $V_{OCM}$ pin of the THS4551 (not shown in Figure 110). To use the complete dynamic range of the ADC, $V_{OCM}$ can be set to $V_{REF}$ / 2 by using a simple resistive divider.

The circuit in Figure 111 shows a single-ended to differential DAQ block optimized for low distortion and noise using the THS4551 and the ADS892xB. This front-end circuit configuration requires a single-ended bipolar signal at the input of the FDA and provides a fully-differential output to drive the ADC inputs. The common-mode voltage of the input signal provided to the ADC is set by the $V_{OCM}$ pin of the THS4551 (not shown in Figure 111). To use the complete dynamic range of the ADC, $V_{OCM}$ can be set to $V_{REF}$ / 2 by using a simple resistive divider.

### 8.2.5 Application Curves

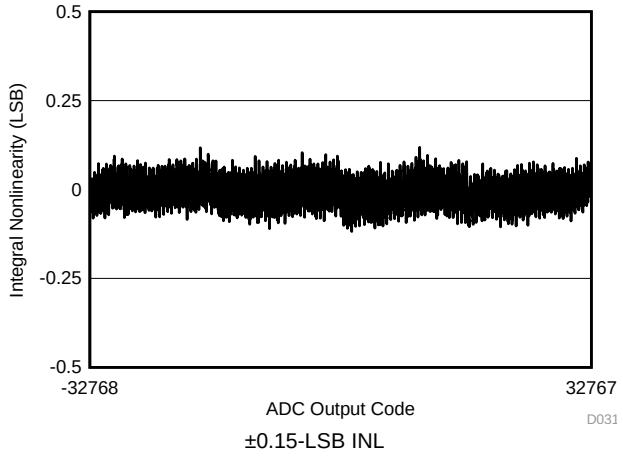



**Figure 112. Typical Linearity, Differential Input**

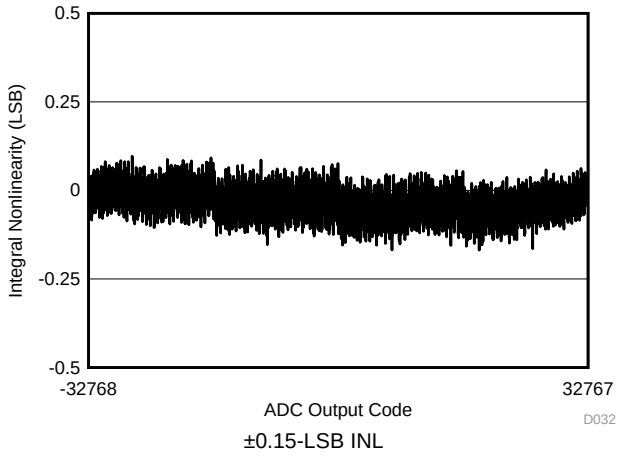
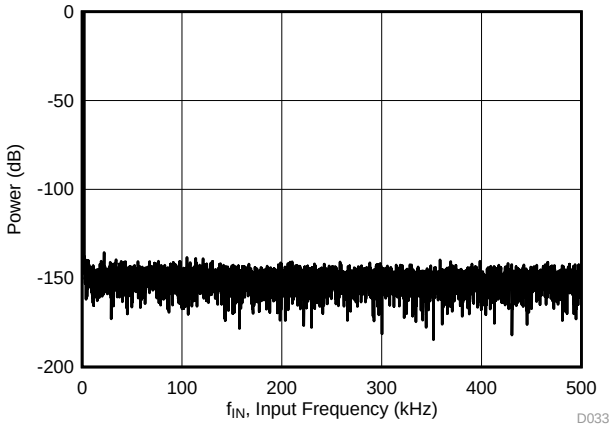


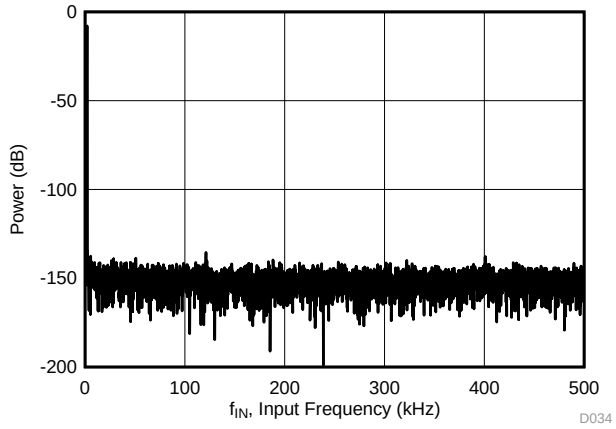

**Figure 113. Typical Linearity, Single-Ended Input**


Copyright © 2016–2017, Texas Instruments Incorporated



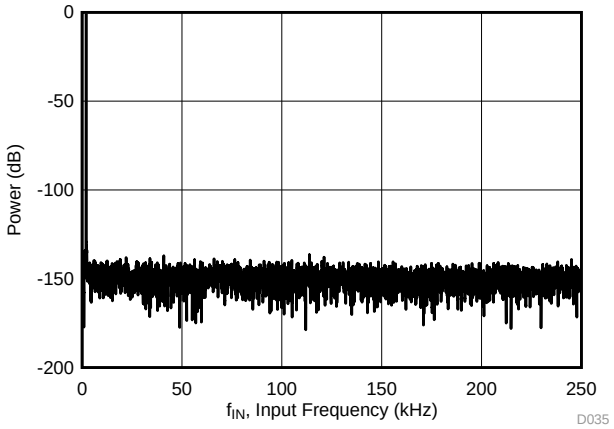

SNR = 96.1 dB, THD = –131.7 dB

**Figure 114. Noise-Performance FFT Plot: ADS8920B, Differential Input**



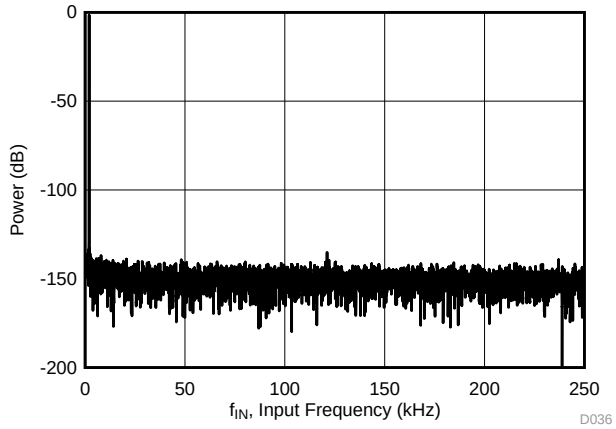

SNR = 95.9 dB, THD = –125.9 dB

**Figure 115. Noise-Performance FFT Plot: ADS8920B, Single-Ended Input**



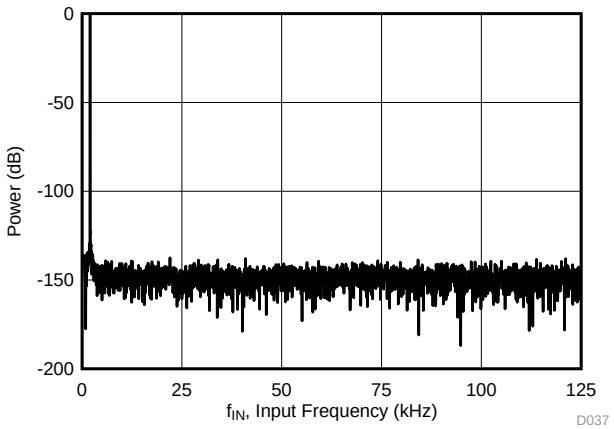

SNR = 96.2 dB, THD = –132 dB

**Figure 116. Noise-Performance FFT Plot: ADS8922B, Differential Input**



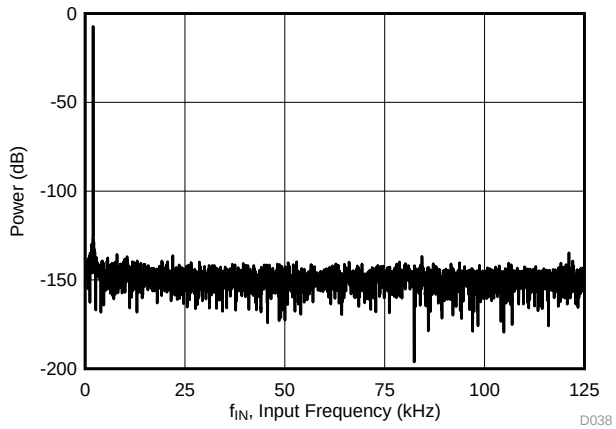

SNR = 96 dB, THD = –126 dB

**Figure 117. Noise-Performance FFT Plot: ADS8922B, Single-Ended Input**




SNR = 96.1 dB, THD = –131.5 dB

**Figure 118. Noise-Performance FFT Plot: ADS8924B, Differential Input**




SNR = 95.9 dB, THD = –125.6 dB

**Figure 119. Noise-Performance FFT Plot: ADS8924B, Single-Ended Input**

Copyright © 2016–2017, Texas Instruments Incorporated

## 9 Power-Supply Recommendations

The devices have two separate power supplies: $RV_{DD}$ and $DV_{DD}$. The internal reference buffer and the internal LDO operate on $RV_{DD}$. The ADC core operates on the LDO output (available on the DECAP pins). $DV_{DD}$ is used for the interface circuits. $RV_{DD}$ and $DV_{DD}$ can be independently set to any value within their permissible ranges.

The $RV_{DD}$ supply voltage value defines the permissible range for the external reference voltage $V_{REF}$ on REFIN pin as:

$$2.5\ V \le V_{REF} \le (RV_{DD} - 0.3)\ V \quad (19)$$

In other words, to use the external reference voltage of $V_{REF}$, set $RV_{DD}$ so that:

$$3\ V \le RV_{DD} \le (V_{REF} + 0.3)\ V \quad (20)$$

Place a 10-µF decoupling capacitor between the RVDD and GND pins, and between the DVDD and GND pins, as shown in Figure 120. Use a minimum 1-µF decoupling capacitor between the DECAP pins and the GND pin.

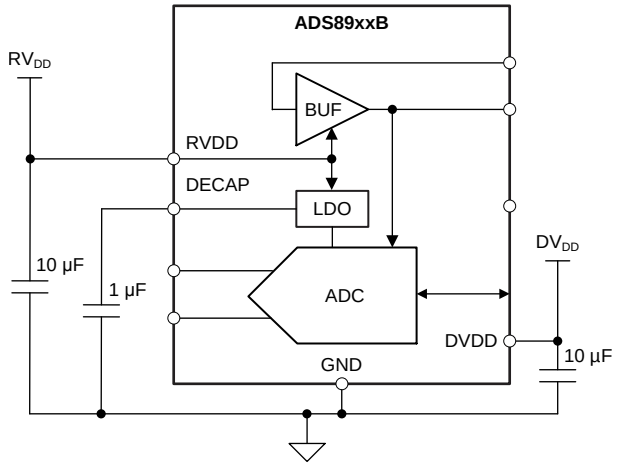



**Figure 120. Power-Supply Decoupling**


Copyright © 2016–2017, Texas Instruments Incorporated

# 10 Layout

## 10.1 Layout Guidelines

This section provides some layout guidelines for achieving optimum performance with the ADS892xB device family.

### 10.1.1 Signal Path

As illustrated in Figure 121, the analog input signals are routed in opposite directions to the digital connections. The reference decoupling components are kept away from the switching digital signals. This arrangement prevents noise generated by digital switching activity from coupling to sensitive analog signals.

### 10.1.2 Grounding and PCB Stack-Up

Low inductance grounding is critical for achieving optimum performance. Grounding inductance is kept below 1 nH with 15-mil grounding vias and a printed circuit board (PCB) layout design that has at least four layers. Place all critical components of the signal chain on the top layer with a solid analog ground from subsequent inner layers to minimize via length to ground.

For lowest inductance grounding, connect the GND pins of the ADS892xB (pin 11 and pin 15) directly to the device thermal pad and place at least four 8-mil grounding vias on the device thermal pad.

### 10.1.3 Decoupling of Power Supplies

Place the decoupling capacitors on $RV_{DD}$, the LDO output, and $DV_{DD}$ within 20 mil from the respective pins, and use a 15-mil via to ground from each capacitor. Avoid placing vias between any supply pin and the respective decoupling capacitor.

### 10.1.4 Reference Decoupling

Dynamic currents are also present at the REFBUFOUT and REFM pins during the conversion phase, and excellent decoupling is required to achieve optimum performance. Place a 10-μF, X7R-grade, ceramic capacitor with at least 10-V rating and an ESR of 1-Ω between the REFBUFOUT and the REFM pins, as illustrated in Figure 121. Select 0603- or 0805-size capacitors to keep equivalent series inductance (ESL) low. Connect the REFM pins to the decoupling capacitor before a ground via.

### 10.1.5 Differential Input Decoupling

Dynamic currents are also present at the differential analog inputs of the ADS892xB. Use C0G- or NPO-type capacitors to decouple these inputs because with these type of capacitors, capacitance stays almost constant over the full input voltage range. Lower-quality capacitors (such as X5R and X7R) have large capacitance changes over the full input-voltage range that may cause degradation in the performance of the device.

Copyright © 2016–2017, Texas Instruments Incorporated

## 10.2 Layout Example

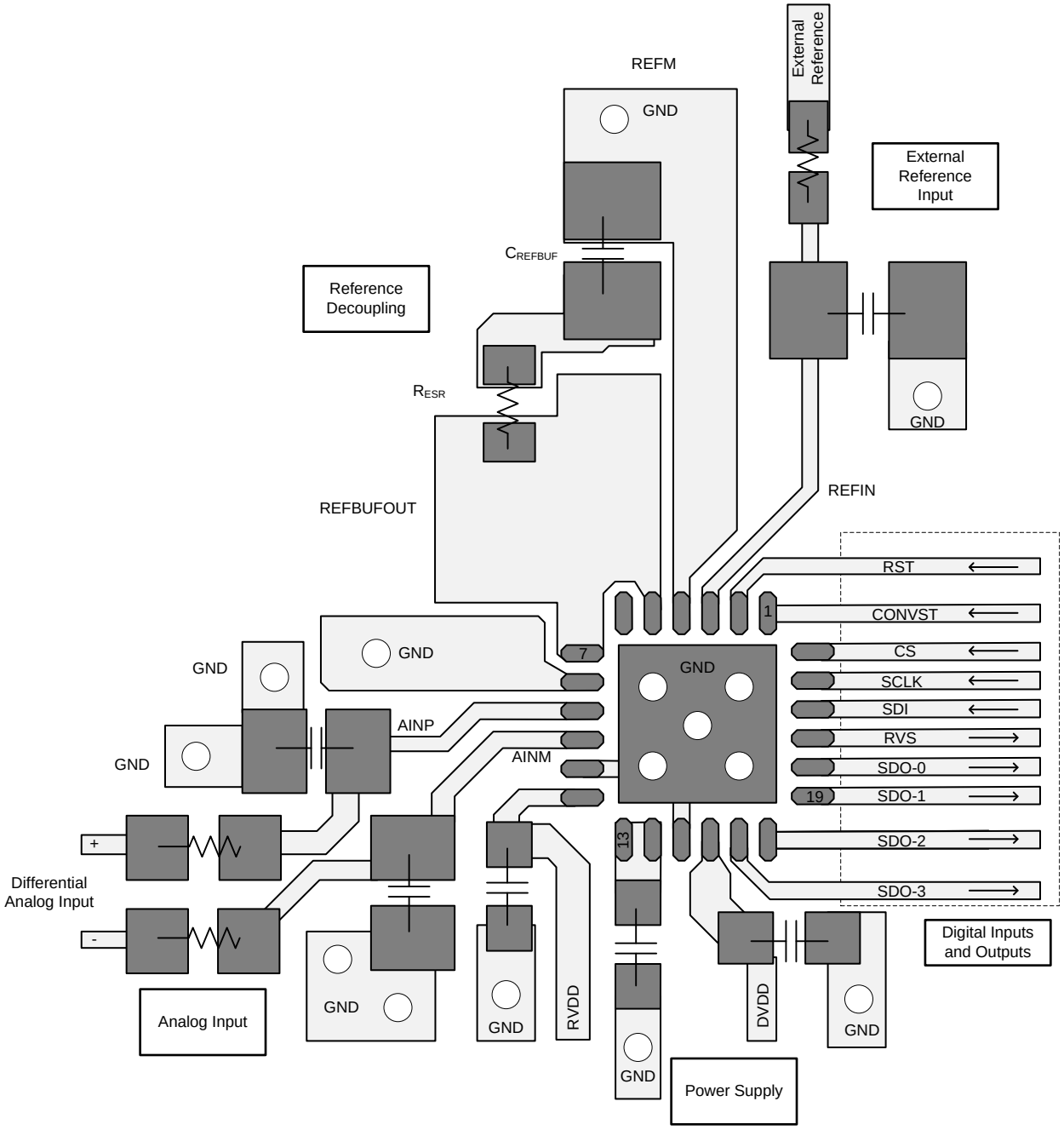



**Figure 121. Recommended Layout**


Copyright © 2016–2017, Texas Instruments Incorporated

# 11 Device and Documentation Support

## 11.1 Documentation Support

### 11.1.1 Related Documentation

For related documentation see the following:

- *ADS8920BEVM-PDK User's Guide* (SBAU270)
- *Enabling Faster, Smarter, and More Robust System Solutions for SAR ADCs With TI's multiSPI™ Digital Interface* (SBAY002)
- *Ultrasound CW Doppler Summing and 20-bit True Raw Data Conversion Reference Design* (TIDA-01351)
- *20-Bit, 1-MSPS, 4-Ch Small Form Factor Design for Test and Measurement Applications Reference Design* (TIDUBW7)
- *20-Bit, 1-MSPS Isolator Optimized Data Acquisition Reference Design Maximizing SNR and Sample Rate* (TIDA-01037)
- *A 20-bit,1 MSPS Isolated Data Acquisition (DAQ) Reference Design Optimizing Jitter for Maximum SNR and Sample Rate* (TIDA-01035)
- *OPAx625 High-Bandwidth, High-Precision, Low THD+N, 16-Bit and 18-Bit Analog-to-Digital Converter (ADC) Drivers Data Sheet* (SBOS688)
- *REF5050 Low-Noise, Very Low Drift, Precision Voltage Reference Data Sheet* (SBOS410)
- *THS4551 Low Noise, Precision, 150MHz, Fully Differential Amplifier* (SBOS778)

## 11.2 Related Links

The following table lists quick access links. Categories include technical documents, support and community resources, tools and software, and quick access to order now.

**Table 23. Related Links**

| PARTS | PRODUCT FOLDER | ORDER NOW | TECHNICAL DOCUMENTS | TOOLS & SOFTWARE | SUPPORT & COMMUNITY |
|---|---|---|---|---|---|
| ADS8920B | Click here | Click here | Click here | Click here | Click here |
| ADS8922B | Click here | Click here | Click here | Click here | Click here |
| ADS8924B | Click here | Click here | Click here | Click here | Click here |

## 11.3 Receiving Notification of Documentation Updates

To receive notification of documentation updates, navigate to the device product folder on ti.com. In the upper right corner, click on *Alert me* to register and receive a weekly digest of any product information that has changed. For change details, review the revision history included in any revised document.

## 11.4 Community Resources

The following links connect to TI community resources. Linked contents are provided "AS IS" by the respective contributors. They do not constitute TI specifications and do not necessarily reflect TI's views; see TI's Terms of Use.

**TI E2E™ Online Community** ***TI's Engineer-to-Engineer (E2E) Community.*** Created to foster collaboration among engineers. At e2e.ti.com, you can ask questions, share knowledge, explore ideas and help solve problems with fellow engineers.

**Design Support** ***TI's Design Support*** Quickly find helpful E2E forums along with design support tools and contact information for technical support.

Copyright © 2016–2017, Texas Instruments Incorporated

### 11.5 Trademarks

TINA-TI, E2E are trademarks of Texas Instruments.
All other trademarks are the property of their respective owners.

### 11.6 Electrostatic Discharge Caution



This integrated circuit can be damaged by ESD. Texas Instruments recommends that all integrated circuits be handled with appropriate precautions. Failure to observe proper handling and installation procedures can cause damage.

ESD damage can range from subtle performance degradation to complete device failure. Precision integrated circuits may be more susceptible to damage because very small parametric changes could cause the device not to meet its published specifications.

### 11.7 Glossary

SLYZ022 — *TI Glossary*.

This glossary lists and explains terms, acronyms, and definitions.

## 12 Mechanical, Packaging, and Orderable Information

The following pages include mechanical, packaging, and orderable information. This information is the most current data available for the designated devices. This data is subject to change without notice and revision of this document. For browser-based versions of this data sheet, refer to the left-hand navigation.


Copyright © 2016–2017, Texas Instruments Incorporated

## PACKAGING INFORMATION

| Orderable part number | Status (1) | Material type (2) | Package \| Pins | Package qty \| Carrier | RoHS (3) | Lead finish/ Ball material (4) | MSL rating/ Peak reflow (5) | Op temp (°C) | Part marking (6) |
|---|---|---|---|---|---|---|---|---|---|
| ADS8920BRGER | Active | Production | VQFN (RGE) \| 24 | 3000 \| LARGE T&R | Yes | NIPDAU | Level-2-260C-1 YEAR | -40 to 125 | 8920B |
| ADS8920BRGER.B | Active | Production | VQFN (RGE) \| 24 | 3000 \| LARGE T&R | Yes | NIPDAU | Level-2-260C-1 YEAR | -40 to 125 | 8920B |
| ADS8920BRGET | Active | Production | VQFN (RGE) \| 24 | 250 \| SMALL T&R | Yes | NIPDAU | Level-2-260C-1 YEAR | -40 to 125 | 8920B |
| ADS8920BRGET.B | Active | Production | VQFN (RGE) \| 24 | 250 \| SMALL T&R | Yes | NIPDAU | Level-2-260C-1 YEAR | -40 to 125 | 8920B |
| ADS8920BRGETG4 | Active | Production | VQFN (RGE) \| 24 | 250 \| SMALL T&R | Yes | NIPDAU | Level-2-260C-1 YEAR | -40 to 125 | 8920B |
| ADS8920BRGETG4.B | Active | Production | VQFN (RGE) \| 24 | 250 \| SMALL T&R | Yes | NIPDAU | Level-2-260C-1 YEAR | -40 to 125 | 8920B |
| ADS8922BRGER | Active | Production | VQFN (RGE) \| 24 | 3000 \| LARGE T&R | Yes | NIPDAU | Level-2-260C-1 YEAR | -40 to 125 | 8922B |
| ADS8922BRGER.B | Active | Production | VQFN (RGE) \| 24 | 3000 \| LARGE T&R | Yes | NIPDAU | Level-2-260C-1 YEAR | -40 to 125 | 8922B |
| ADS8922BRGET | Active | Production | VQFN (RGE) \| 24 | 250 \| SMALL T&R | Yes | NIPDAU | Level-2-260C-1 YEAR | -40 to 125 | 8922B |
| ADS8922BRGET.B | Active | Production | VQFN (RGE) \| 24 | 250 \| SMALL T&R | Yes | NIPDAU | Level-2-260C-1 YEAR | -40 to 125 | 8922B |
| ADS8924BRGER | Active | Production | VQFN (RGE) \| 24 | 3000 \| LARGE T&R | Yes | NIPDAU | Level-2-260C-1 YEAR | -40 to 125 | 8924B |
| ADS8924BRGER.B | Active | Production | VQFN (RGE) \| 24 | 3000 \| LARGE T&R | Yes | NIPDAU | Level-2-260C-1 YEAR | -40 to 125 | 8924B |
| ADS8924BRGET | Active | Production | VQFN (RGE) \| 24 | 250 \| SMALL T&R | Yes | NIPDAU | Level-2-260C-1 YEAR | -40 to 125 | 8924B |
| ADS8924BRGET.B | Active | Production | VQFN (RGE) \| 24 | 250 \| SMALL T&R | Yes | NIPDAU | Level-2-260C-1 YEAR | -40 to 125 | 8924B |

(1) **Status:** For more details on status, see our product life cycle.

(2) **Material type:** When designated, preproduction parts are prototypes/experimental devices, and are not yet approved or released for full production. Testing and final process, including without limitation quality assurance, reliability performance testing, and/or process qualification, may not yet be complete, and this item is subject to further changes or possible discontinuation. If available for ordering, purchases will be subject to an additional waiver at checkout, and are intended for early internal evaluation purposes only. These items are sold without warranties of any kind.

(3) **RoHS values:** Yes, No, RoHS Exempt. See the TI RoHS Statement for additional information and value definition.

(4) **Lead finish/Ball material:** Parts may have multiple material finish options. Finish options are separated by a vertical ruled line. Lead finish/Ball material values may wrap to two lines if the finish value exceeds the maximum column width.

(5) **MSL rating/Peak reflow:** The moisture sensitivity level ratings and peak solder (reflow) temperatures. In the event that a part has multiple moisture sensitivity ratings, only the lowest level per JEDEC standards is shown. Refer to the shipping label for the actual reflow temperature that will be used to mount the part to the printed circuit board.

(6) **Part marking:** There may be an additional marking, which relates to the logo, the lot trace code information, or the environmental category of the part.

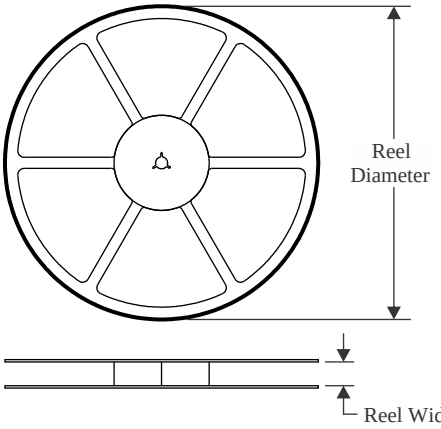
Multiple part markings will be inside parentheses. Only one part marking contained in parentheses and separated by a "~" will appear on a part. If a line is indented then it is a continuation of the previous line and the two combined represent the entire part marking for that device.

**Important Information and Disclaimer:**The information provided on this page represents TI's knowledge and belief as of the date that it is provided. TI bases its knowledge and belief on information provided by third parties, and makes no representation or warranty as to the accuracy of such information. Efforts are underway to better integrate information from third parties. TI has taken and continues to take reasonable steps to provide representative and accurate information but may not have conducted destructive testing or chemical analysis on incoming materials and chemicals. TI and TI suppliers consider certain information to be proprietary, and thus CAS numbers and other limited information may not be available for release.

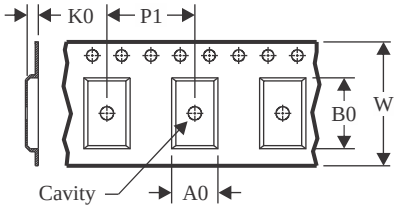
In no event shall TI's liability arising out of such information exceed the total purchase price of the TI part(s) at issue in this document sold by TI to Customer on an annual basis.

## TAPE AND REEL INFORMATION

**REEL DIMENSIONS**

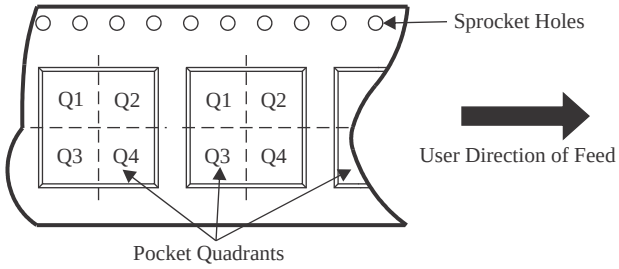



**TAPE DIMENSIONS**




| | |
|---|---|
| A0 | Dimension designed to accommodate the component width |
| B0 | Dimension designed to accommodate the component length |
| K0 | Dimension designed to accommodate the component thickness |
| W | Overall width of the carrier tape |
| P1 | Pitch between successive cavity centers |

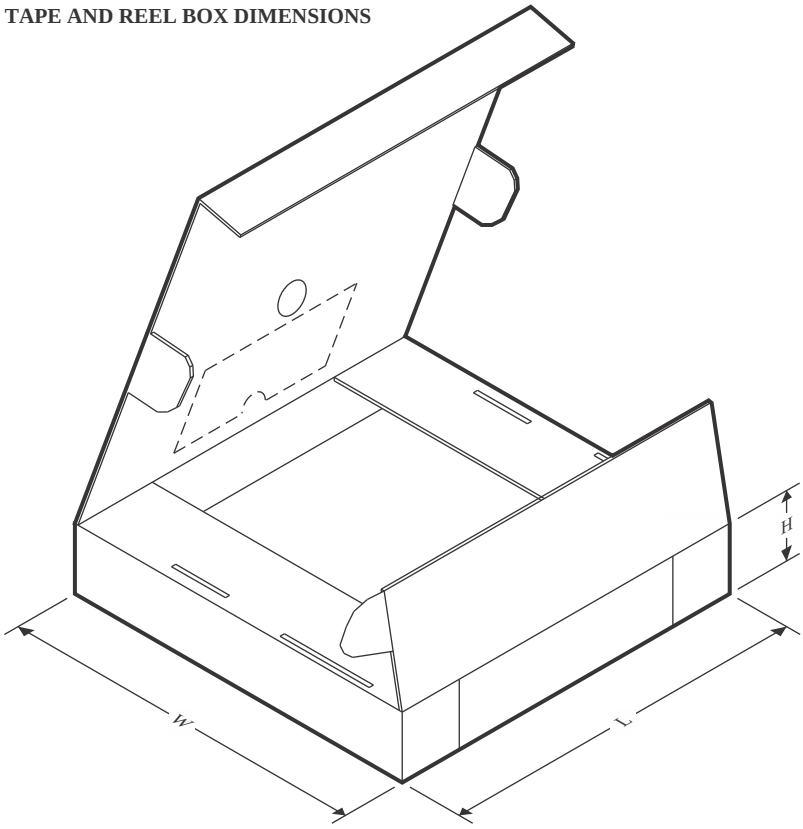
**QUADRANT ASSIGNMENTS FOR PIN 1 ORIENTATION IN TAPE**




*All dimensions are nominal

| Device | Package Type | Package Drawing | Pins | SPQ | Reel Diameter (mm) | Reel Width W1 (mm) | A0 (mm) | B0 (mm) | K0 (mm) | P1 (mm) | W (mm) | Pin1 Quadrant |
|---|---|---|---|---|---|---|---|---|---|---|---|---|
| ADS8920BRGER | VQFN | RGE | 24 | 3000 | 330.0 | 12.4 | 4.25 | 4.25 | 1.15 | 8.0 | 12.0 | Q2 |
| ADS8920BRGET | VQFN | RGE | 24 | 250 | 180.0 | 12.4 | 4.25 | 4.25 | 1.15 | 8.0 | 12.0 | Q2 |
| ADS8920BRGETG4 | VQFN | RGE | 24 | 250 | 180.0 | 12.4 | 4.25 | 4.25 | 1.15 | 8.0 | 12.0 | Q2 |
| ADS8922BRGER | VQFN | RGE | 24 | 3000 | 330.0 | 12.4 | 4.25 | 4.25 | 1.15 | 8.0 | 12.0 | Q2 |
| ADS8922BRGET | VQFN | RGE | 24 | 250 | 180.0 | 12.4 | 4.25 | 4.25 | 1.15 | 8.0 | 12.0 | Q2 |
| ADS8924BRGER | VQFN | RGE | 24 | 3000 | 330.0 | 12.4 | 4.25 | 4.25 | 1.15 | 8.0 | 12.0 | Q2 |
| ADS8924BRGET | VQFN | RGE | 24 | 250 | 180.0 | 12.4 | 4.25 | 4.25 | 1.15 | 8.0 | 12.0 | Q2 |

TAPE AND REEL BOX DIMENSIONS



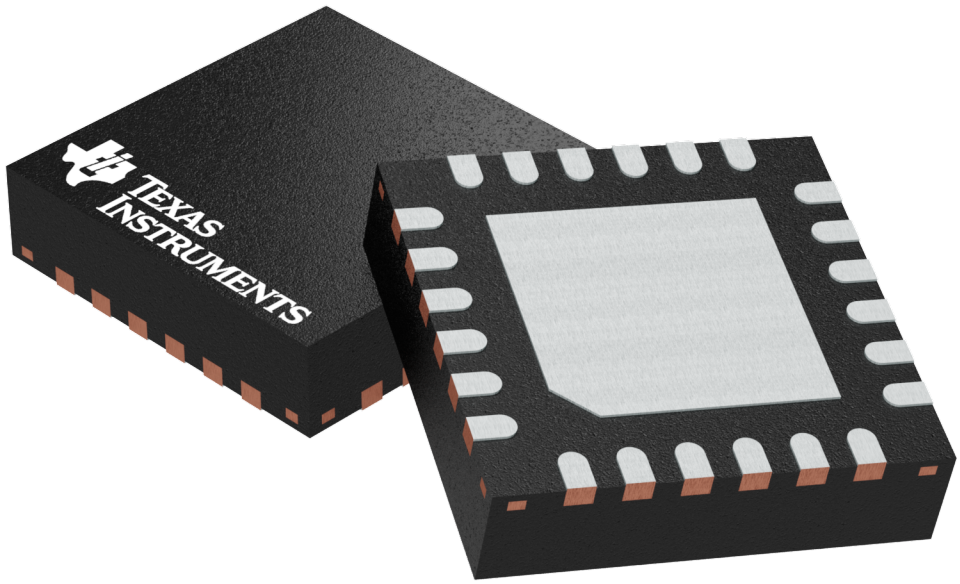

*All dimensions are nominal

| Device | Package Type | Package Drawing | Pins | SPQ | Length (mm) | Width (mm) | Height (mm) |
|---|---|---|---|---|---|---|---|
| ADS8920BRGER | VQFN | RGE | 24 | 3000 | 346.0 | 346.0 | 33.0 |
| ADS8920BRGET | VQFN | RGE | 24 | 250 | 210.0 | 185.0 | 35.0 |
| ADS8920BRGETG4 | VQFN | RGE | 24 | 250 | 210.0 | 185.0 | 35.0 |
| ADS8922BRGER | VQFN | RGE | 24 | 3000 | 346.0 | 346.0 | 33.0 |
| ADS8922BRGET | VQFN | RGE | 24 | 250 | 210.0 | 185.0 | 35.0 |
| ADS8924BRGER | VQFN | RGE | 24 | 3000 | 346.0 | 346.0 | 33.0 |
| ADS8924BRGET | VQFN | RGE | 24 | 250 | 210.0 | 185.0 | 35.0 |

# GENERIC PACKAGE VIEW

## RGE 24 VQFN - 1 mm max height

PLASTIC QUAD FLATPACK - NO LEAD




Images above are just a representation of the package family, actual package may vary.
Refer to the product data sheet for package details.

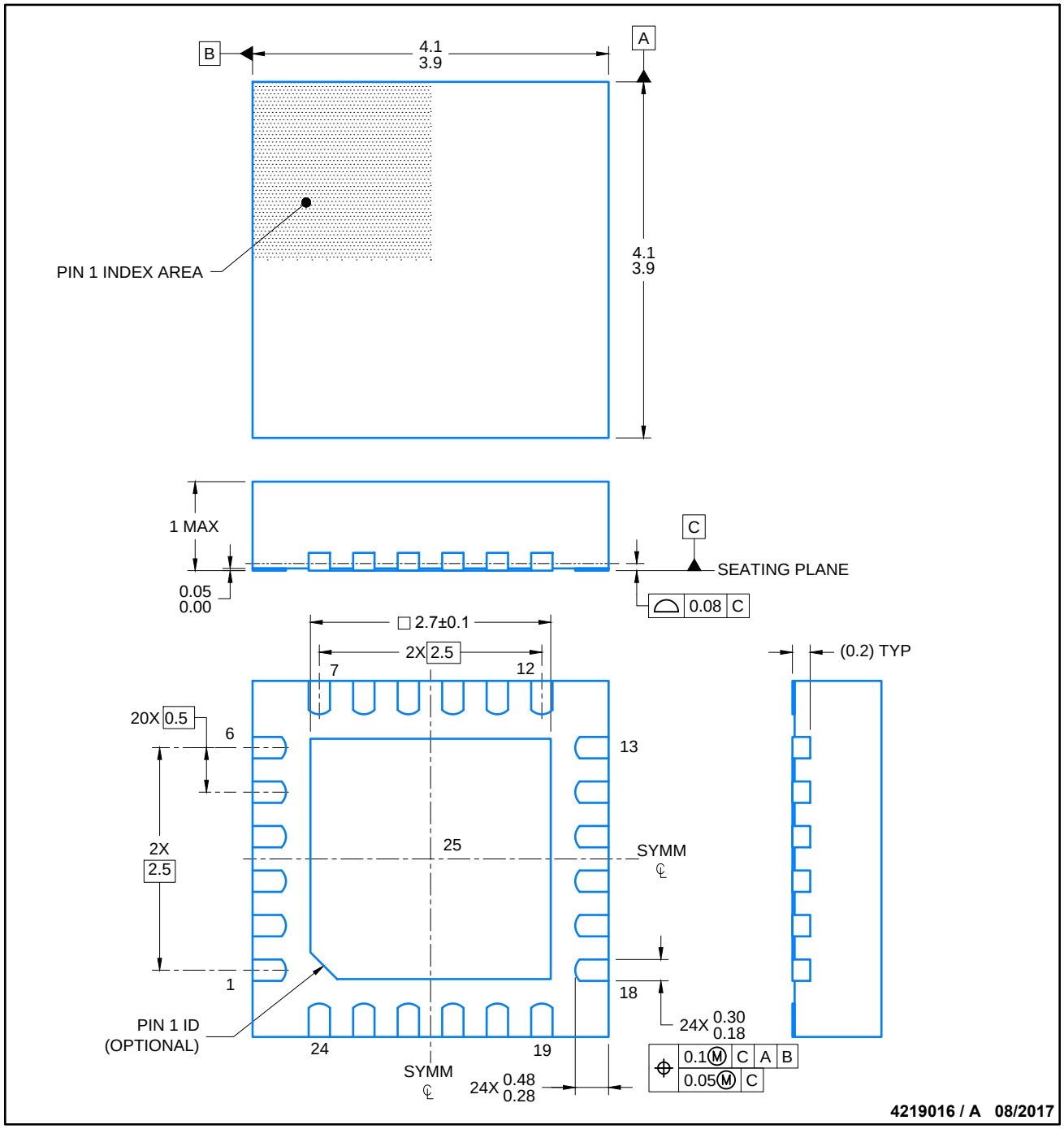
4204104/H

# PACKAGE OUTLINE

## RGE0024H

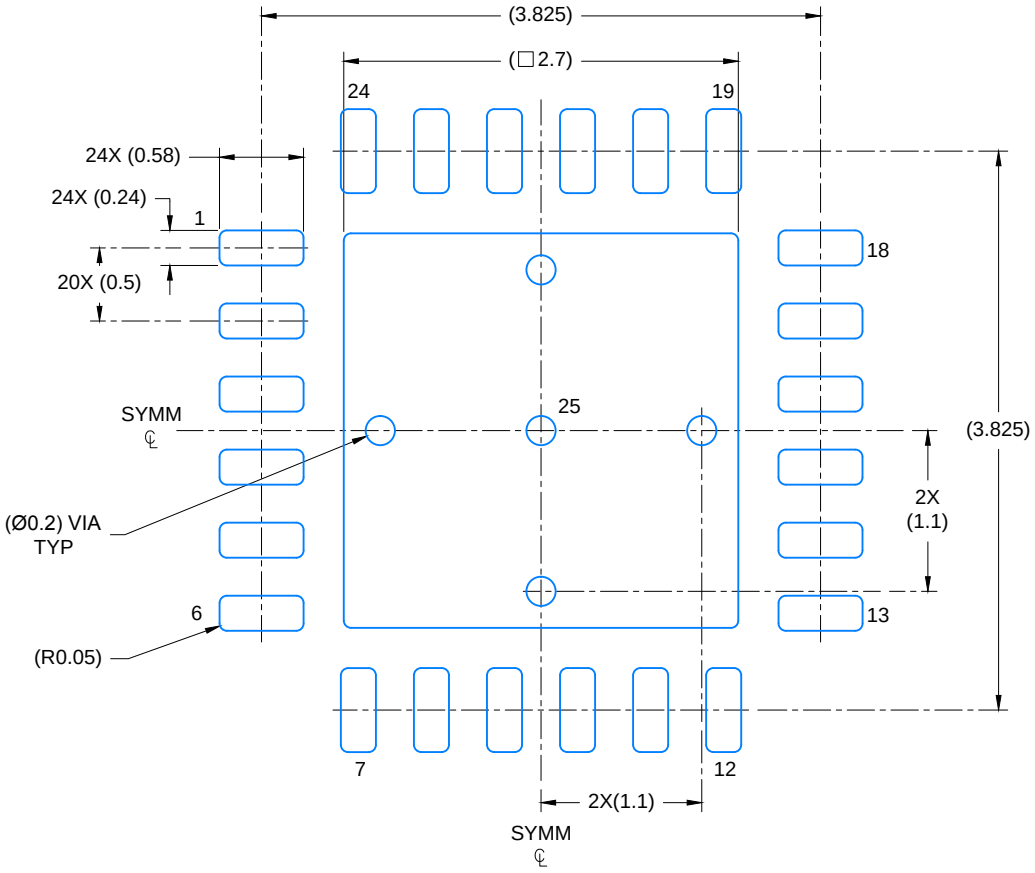
### VQFN - 1 mm max height

PLASTIC QUAD FLATPACK- NO LEAD



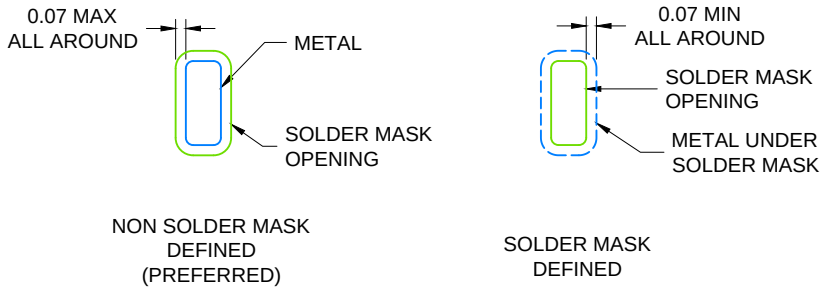

NOTES:

1. All linear dimensions are in millimeters. Any dimensions in parenthesis are for reference only. Dimensioning and tolerancing per ASME Y14.5M.
2. This drawing is subject to change without notice.
3. The package thermal pad must be soldered to the printed circuit board for thermal and mechanical performance.




LAND PATTERN EXAMPLE

SCALE: 20X

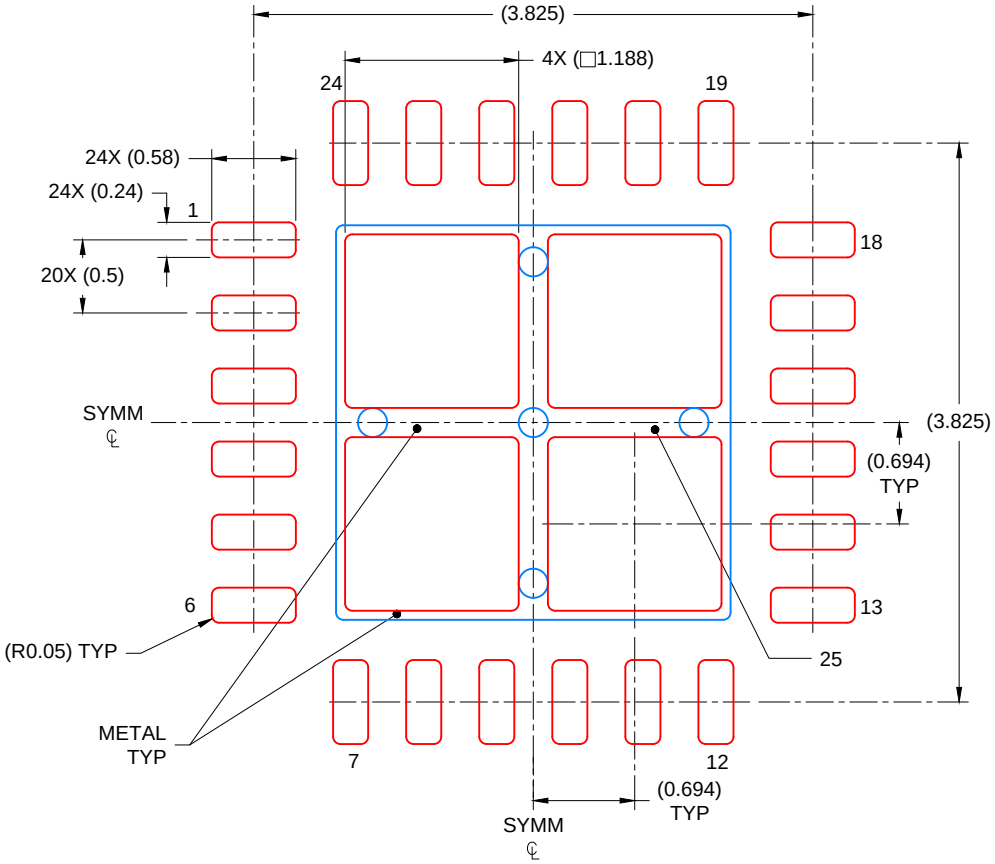



SOLDER MASK DETAILS

4219016 / A 08/2017

NOTES: (continued)

4. This package is designed to be soldered to a thermal pad on the board. For more information, see Texas Instruments literature number SLUA271 (www.ti.com/lit/slua271).
5. Solder mask tolerances between and around signal pads can vary based on board fabrication site.




SOLDER PASTE EXAMPLE
BASED ON 0.125 mm THICK STENCIL

EXPOSED PAD
78% PRINTED COVERAGE BY AREA
SCALE: 20X

4219016 / A 08/2017

NOTES: (continued)

6. Laser cutting apertures with trapezoidal walls and rounded corners may offer better paste release. IPC-7525 may have alternate design recommendations..

# IMPORTANT NOTICE AND DISCLAIMER

TI PROVIDES TECHNICAL AND RELIABILITY DATA (INCLUDING DATA SHEETS), DESIGN RESOURCES (INCLUDING REFERENCE DESIGNS), APPLICATION OR OTHER DESIGN ADVICE, WEB TOOLS, SAFETY INFORMATION, AND OTHER RESOURCES “AS IS” AND WITH ALL FAULTS, AND DISCLAIMS ALL WARRANTIES, EXPRESS AND IMPLIED, INCLUDING WITHOUT LIMITATION ANY IMPLIED WARRANTIES OF MERCHANTABILITY, FITNESS FOR A PARTICULAR PURPOSE OR NON-INFRINGEMENT OF THIRD PARTY INTELLECTUAL PROPERTY RIGHTS.

These resources are intended for skilled developers designing with TI products. You are solely responsible for (1) selecting the appropriate TI products for your application, (2) designing, validating and testing your application, and (3) ensuring your application meets applicable standards, and any other safety, security, regulatory or other requirements.

These resources are subject to change without notice. TI grants you permission to use these resources only for development of an application that uses the TI products described in the resource. Other reproduction and display of these resources is prohibited. No license is granted to any other TI intellectual property right or to any third party intellectual property right. TI disclaims responsibility for, and you will fully indemnify TI and its representatives against, any claims, damages, costs, losses, and liabilities arising out of your use of these resources.

TI’s products are provided subject to TI’s Terms of Sale or other applicable terms available either on ti.com or provided in conjunction with such TI products. TI’s provision of these resources does not expand or otherwise alter TI’s applicable warranties or warranty disclaimers for TI products.

TI objects to and rejects any additional or different terms you may have proposed.

Mailing Address: Texas Instruments, Post Office Box 655303, Dallas, Texas 75265
Copyright © 2025, Texas Instruments Incorporated